Departament de Teoria
del Senyal i Comunicacions

Contribution to Spectrum Management in Cognitive Radio Networks: A Cognitive Management Framework

Doctoral Dissertation

Faouzi Bouali

2013

UNIVERSITAT POLITÈCNICA
DE CATALUNYA
BARCELONATECH

Departament de Teoria del Senyal i Comunicacions
UNIVERSITAT POLITÈCNICA DE CATALUNYA

Contribution to Spectrum Management in Cognitive Radio Networks: A Cognitive Management Framework

By

Faouzi Bouali

A Thesis Submitted to the
Department of Signal Theory and Communications
of the Universitat Politècnica de Catalunya
in Partial Fulfillment of the Requirements for the Degree of

DOCTOR OF PHILOSOPHY

Barcelona, July, 2013

Thesis Advisor: Prof. Oriol Sallent
Mobile Communication Research Group (GRCM)
Department of Signal Theory and Communications (TSC)
Universitat Politècnica de Catalunya (UPC)

Contact information

✉ Faouzi Bouali
Mobile Communication Research Group (GRCM)
Dept. Signal Theory and Communications (TSC)
Universitat Politècnica de Catalunya (UPC)
Jordi Girona 1-3, Campus Nord UPC
Building D4 Office 11508034- Barcelona Spain
faouzi.bouali@tsc.upc.edu
fawez2507@yahoo.fr
http://grcm.tsc.upc.edu/es/faouzi

Text printed in Barcelona
First edition, July 2013

To my mother,
To the soul of my father
To my wife and daughter,
To all my beloved family,
for their unconditional love and support.

This page is intentionally left blank

Abstract

To overcome the current under-utilization of spectrum resources, the CR (Cognitive Radio) paradigm has gained an increasing interest to perform the so-called Dynamic Spectrum Access (DSA). In this respect, Cognitive Radio networks (CRNs) have been strengthened with cognitive management support to push forward their deployment and commercialization. This dissertation has assessed the relevance of exploiting several cognitive management functionalities in various scenarios and case studies.

Specifically, this dissertation has constructed a generic cognitive management framework, based on the fittingness factor concept, to support spectrum management in CRNs. Under this framework, the dissertation has addressed two of the most promising CR applications, namely an Opportunistic Spectrum Access (OSA) to licensed bands and open sharing of license-exempt bands. In the former application, several strategies that exploit temporal statistical dependence between primary activity/inactivity durations to perform a proactive spectrum selection have been discussed. A set of guidelines to select the most relevant strategy for a given environment have been provided. In the latter application, a fittingness factor-based spectrum selection strategy has been proposed to efficiency exploit the different bands. Several formulations of the fittingness factor have been compared, and their relevance have been assessed under different settings.

Drawing inspiration from these applications, a more general proactive strategy exploiting a characterization of spectrum resources at both the

time and frequency domains has been developed to jointly assist spectrum selection (SS) and spectrum mobility (SM) functionalities. Several variants of the proposed strategy, each combining different choices and options of implementation, have been compared to identify which of its components have the most significant impact on performance depending on the working conditions of the CRN. To assess rationality of the proposed strategy with respect to other strategies, a cost-benefit analysis has been conducted to confront the introduced gain in terms of user satisfaction level to the incurred cost in terms of signaling amount.

Finally, the dissertation has conducted an analysis of practicality aspects in terms of robustness to environment uncertainty and applicability to realistic environments. With respect to the former aspect, robustness has been assessed in front of two sources of uncertainty, namely imperfection of the acquisition process and non-stationarity of the environment, and additional functionalities have been developed, when needed, to improve robustness. With respect to the latter, the proposed framework has been applied to a Digital Home (DH) environment to validate the obtained key findings under realistic conditions.

Resumen

A fin de subir la eficiencia de uso del espectro, el paradigma de la radio cognitiva (CR[1]) ha ganado mucho interés para permitir un acceso dinámico al espectro (DSA[2]). En esta línea, las redes radio cognitivas (CRNs[3]) se han enriquecido de un soporte de gestión cognitiva para incitar su despliegue y comercialización. Esta tesis ha valorado la relevancia de explotar varias funcionalidades de gestión cognitiva en distintos escenarios y casos de estudio prácticos.

Específicamente, esta tesis ha construido un marco genérico de gestión cognitiva, basado en el concepto de fittigness factor, para soportar la gestión de los recursos radio en las CRNs. En este marco, dos de las aplicaciones más interesantes de las CRs, a saber el acceso oportunista al espectro (OSA[4]) de las bandas licenciadas y el reparto abierto de las bandas exentas de licencia. En lo que se refiere a la primera aplicación, se han propuesto y evaluado varias estrategias explotando la dependencia entre las duraciones de actividad e inactividad de los usuarios primarios para llevar a cabo una selección de espectro proactiva. También se han proporcionado una serie de directrices para escoger la estrategia más relevante para un cierto entorno. Con respecto a la segunda aplicación, se ha propuesto una estrategia de selección de espectro con el fin de proporcionar una utilización eficiente de las distintas bandas. Varias formulaciones del fittigness factor han sido propuestas y evaluadas y sus relevancias se han valorado para distintas configuraciones.

[1]Del inglés, *Cognitive Radio*.
[2]Del inglés, *Dynamic Spectrum Access*.
[3]Del inglés, *Cognitive Radio Networks*.
[4]Del inglés, *Opportunistic Spectrum Access*.

Inspirándose en estas aplicaciones, se ha propuesto una estrategia proactiva más general para soportar de manera conjunta las funcionalidades de selección de espectro (SS[5]) y movilidad de espectro (SM[6]) a base de una caracterización de los recursos de espectro en ambos dominios temporal y espectral. Se han comparado varias variantes de la dicha estrategia, cada una combinando distintas alternativas y opciones de implementación, para identificar cuáles de sus componentes tiene el mayor impacto sobre el rendimiento según las condiciones operativas del CRN. La racionalidad de la metodología propuesta con respecto a otras estrategias ha sido evaluada gracias a un análisis coste-beneficio, confrontando la ganancia en términos del nivel de satisfacción de los usuarios con el coste resultante en términos de señalización.

Finalmente, se han analizado los aspectos de practicidad en términos de robustez a la incertidumbre y aplicabilidad en entornos realistas. En lo que se refiere al primer aspecto, la robustez se ha evaluado frente a dos fuentes de incertidumbre, la imperfección del proceso de adquisición y la no estacionalidad del entorno, y se han propuesto funcionalidades de soporte para mejorar la robustez cuando sea necesario. En lo que concierne el segundo aspecto, el marco se ha aplicado al entorno hogar digital (DH[7]) para valorar la validez de los resultados obtenidos bajo condiciones más realistas.

[5] Del inglés, *Spectrum Selection*.
[6] Del inglés, *Spectrum Mobility*.
[7] Del inglés, *Digital Home*.

Acknowledgements

First and foremost, I am grateful to God for his guidance along my life in general, and my doctoral studies in particular. Without guidance of God, I would have never succeeded in anything.

I would like to thank my thesis advisor Dr. Oriol Sallent for his guidance along this research. I'm convinced that his directions, suggestions and unlimited support have been crucial for all the performed achievements. I am equally thankful to Dr. Jordi Pérez-Romero and Dr. Ramon Agustí for their valuable and helpful assistance.

I would like to extend my gratitude to all past and present colleagues at the Mobile Communication Research Group (GRCM) of the Dept. of Signal Theory and Communications (TSC) at the Technical University of Catalunya (UPC), for the good times we shared over the past four years.

Last, but not least, I am thankful to my family for their patience, support and unconditional encouragement.

thanks a lot,

Faouzi Bouali

July, 2013

Contents

List of Figures

List of Tables

List of Algorithms

Acronyms

ACO	Ant Colony Optimization
bps	bits per second
BS	Base Station
CA	Context Awareness
CDMA	Code Division Multiple Access
CR	Cognitive Radio
CRN	Cognitive Radio Network
CSI	Channel State Information
DC	Duty Cycle
DH	Digital Home
DOFDM	Differential Orthogonal Frequency Division Multiplexing
DSA	Dynamic Spectrum Access
Er	Erlang
FCC	Federal Communications Commission
FI	Future Internet
ICT	Information and Communication Technology

ISM Industrial, Scientific, and Medical

KD Knowledge Database

KM Knowledge Manager

KPI Key Performance Indicator

MNO Mobile Network Operator

MSC Message Sequence Chart

OFDM Orthogonal Frequency Division Multiplexing

ON Opportunistic Network

OSA Opportunistic Spectrum Access

PDF Probability Density Function

PRP Preemptive Resume Priority

PSD Power Spectral Density

PU Primary User

QoS Quality of Service

RAT Radio Access Technology

REM Radio Environment Map

RF Radio Frequency

RKRL Radio Knowledge Representation Language

RL Reinforcement Learning

RMSE Root Mean Squared Error

RT Reliability Tester

SDR Software Defined Radio

SpHO	Spectrum Hand-Over
SU	Secondary User
TVWS	TV White Space
UHF	Ultra High Frequency
UWB	Ultra-Wide Band
WMN	Wireless Mesh Network
WPAN	Wireless Personal Area Network

1. Introduction

1.1 State-of-the-art on cognitive radio networks

1.1.1 The myth of spectrum scarcity

The growth and deployment of radio communications has led to several radio systems all operating in the same electromagnetic spectrum. To rigorously protect these systems against interference, governments used to allocate to each radio system fixed portions of spectrum, separated by guard bands, over large geographical regions (e.g., whole countries), on a long-term basis (e.g., several years), and under exclusive exploitation licenses. This static process known as *command-and-control* allocation has gradually occupied significant parts of finite spectrum resources, and resulted in a common belief of "spectrum scarcity", that we are running out of usable radio frequencies. This belief together with the continuous need to deploy new wireless services raised serious concerns about the future of wireless communications.

Nevertheless, these concerns started to be appeased when the Federal Communications Commission (FCC) published in a report prepared by the Spectrum-Policy Task Force the astonishing fact that spectrum in the United States is vastly under-utilized during some periods of time in several geographical locations [1, 2]. Since then, many spectrum measurement campaigns performed in different regions all over the world have confirmed the high under-utilization of spectrum [3, 4], thus proving that the often called "spectrum scarcity" is artificial and is simply the result of the flawed *command-and-control* allocation.

1.1.2 Cognitive radios to enable dynamic spectrum access

Current spectrum under-utilization has called for a fundamental rethinking of the spectrum allocation process to avoid wasting valuable radio resources. In this context, the term Dynamic Spectrum Access (DSA) stands for the opposite of the static *command-and-control* spectrum management policy and covers any innovative solution meant to share spectrum among several radio systems with sake of increasing the overall spectrum utilization. One of the key concepts to enable the revolutionary DSA approach to access and share spectrum is the Cognitive Radio (CR) paradigm originally coined by Mitola and Maguire in their seminal paper [5] as a SDR (Software Defined Radio) extended with self-awareness to determine appropriate radio etiquettes. In this paper, they focused on developing the Radio Knowledge Representation Language (RKRL), and explained how CRs can enhance the flexibility of personal wireless services. After some time, the RRKL language was expanded in Mitola's doctoral dissertation with a particular focus on natural language processing and machine learning tasks [6].

Since then, the CR concept has been reconsidered by many subsequent papers, each trying to redefine it in particular scenarios. In the specific DSA context, the following definition proposed in [7] is one of the most cited ones:

"*Cognitive radio is an intelligent wireless communication system that is aware of its surrounding environment (i.e., outside world), and uses the methodology of understanding-by-building to learn from the environment and adapt its internal states to statistical variations in the incoming Radio Frequency (RF) stimuli by making corresponding changes in certain operating parameters (e.g., transmit-power, carrier-frequency and modulation strategy) in real-time, with two primary objectives in mind:*

- *Highly reliable communications whenever and wherever needed;*
- *Efficient utilization of the radio spectrum.*"

According to this definition, CRs should support six key capabilities, namely, awareness, intelligence, learning, adaptability, reliability, and efficiency. These capabilities need to be combined to perform the following key cognitive tasks [7]:

1. *Radio-scene analysis*, which consists in estimating interference conditions of the radio environment and identifying the set of available spectrum chunks, referred to as *spectrum holes* or *white spaces*.

2. *Channel identification*, which consists in estimating the channel-state information (CSI) and predicting the channel capacity.

3. *Transmit-power control and spectrum management*, which adjusts transmission parameters based on a feedback received from previous tasks.

Note that the first two tasks are usually performed on the receiver side, while the third one is executed on the transmitter side.

These cognitive tasks interact among themselves and with the external radio environment according to the CR basic cognition cycle described in Figure 1.1. In the beginning of the cycle, the receiver obtains from the radio environment a set of RF stimuli, from which it identifies the set of *spectrum holes*. For each of these *spectrum holes*, estimates of the CSI and available channel capacity are first determined, and then communicated to the transmitter together with a characterization of the radio environment in terms of advanced traffic and noise-floor statistics. At the end of the cycle, the transmit power control and spectrum management functionalities on the transmitter side exploit the provided data to adjust the transmitted signal. Note that a feedback about the perceived performance by the receiver is continuously sent to the transmitter to maintain harmony between both sides.

The described cognition cycle focuses on the main CR application, namely enabling a DSA-type access. Nevertheless, thanks to the spectacular advances that has been achieved in digital signal processing, networking, machine learning, computer software, and computer hardware, CR has evolved to cover a much broader paradigm, where many aspects of communication systems may be improved via cognition.

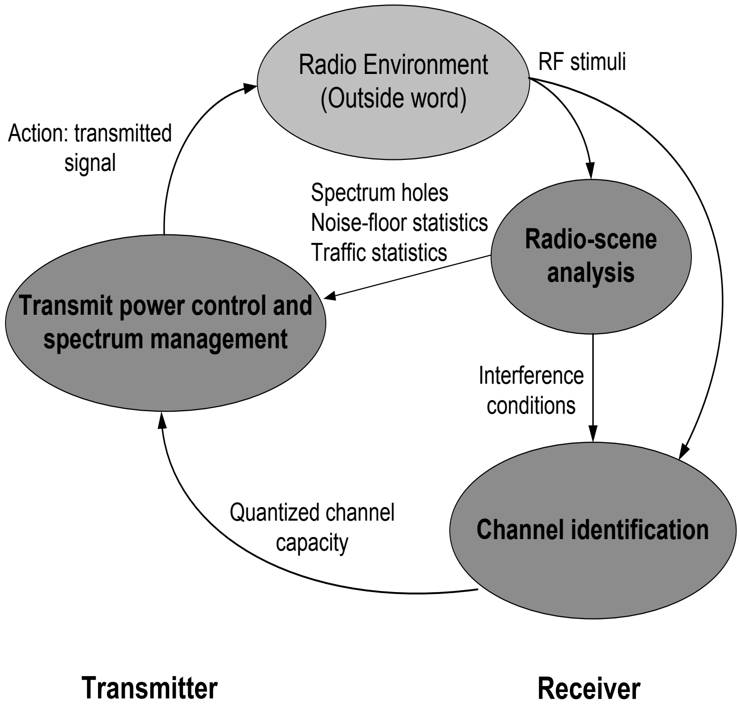

Figure 1.1: CR basic cognition cycle [7]

1.1.3 Dynamic spectrum access models

Several DSA models have been proposed to increase spectrum usage efficiency depending on the specificities of the environment. As described in Figure 1.2, DSA strategies can be in general classified into three different models [8]:

1.1.3.1 Dynamic exclusive use model

This model maintains the basic structure of the static *command-and-control* allocation policy. Spectrum bands are licensed to radio systems for exclusive use, but some flexibility is introduced to improve spectrum efficiency by using one of the following approaches:

- Spectrum property rights [9]. This approach allows licensees or spectrum owners to sell and trade parts of their spectrum resources, and to freely

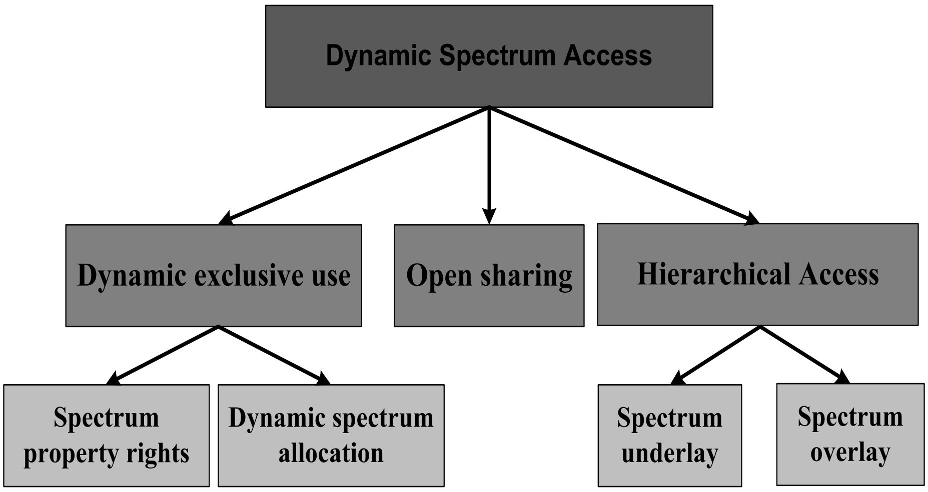

Figure 1.2: Classification of DSA models

choose technology. In this context, economy and market will play an important role in driving towards the most profitable use of sold/traded resources. Note that, in this case, licensees have the right to lease or share spectrum for profit without the intervention of regulators.

- Dynamic spectrum allocation [10, 11]. This approach was first brought forth by the European DRiVE (Dynamic Radio for IP-Services in Vehicular Environments) project. Spectrum efficiency is improved by a dynamic spectrum assignment based on the spatial and temporal traffic statistics of different services. Similarly to the traditional *command-and-control* allocation policy, spectrum is allocated to be exclusively used by each service in a given region and at a given time. This allocation, however, varies at a much faster scale than the traditional policy.

1.1.3.2 Open sharing model

Also referred to as spectrum commons [12, 13], this model employs open sharing among peer users as the basis for managing a spectral region. Drawing support from the success of wireless services operating in the unlicensed industrial, scientific, and medical (ISM) radio band (e.g., WiFi), both centralized [14, 15] and distributed [16, 17] strategies have been investigated to advocate the adoption of this model. However, this model is still far from reaching maturity. Its main limitation is the poor quality that may be obtained when the common good is over-exploited by too many users, which is known as the tragedy of commons [18, 19].

1.1.3.3 Hierarchical access model

This model introduces a hierarchical access structure that distinguishes between primary (licensed) and secondary (license-exempt) users. According to this model, Secondary Users (SUs) are allowed to access licensed spectrum and communicate provided that the interference amount perceived by Primary Users (PUs) remains limited. As shown in the illustrative example of Figure 1.3, SUs may communicate with a secondary Base Station (BS) and share spectrum with a primary network if none of primary nodes (a primary BS and a set of PUs) is disturbed by the secondary operation.

To meet the strict constraint of sharing spectrum on a non-interference basis between all PUs and SUs, two different approaches have been proposed:

1.1.3.3.1 Spectrum overlay

Also referred to as Opportunistic Spectrum Access (OSA) [20], the overlay approach exploits local and instantaneous spectrum availabilities. According to OSA, only spectrum chunks that are not occupied by PUs in both time and space, the so-named *spectrum holes*, are opened for secondary operation. Therefore, SUs should identify and exploit these opportunities in an opportunistic manner as illustrated in the example shown in Figure 1.4.

1.1.3.3.2 Spectrum underlay

Unlike OSA, the underlay approach allows SUs to co-exist with PUs provided that a strict protection requirement is met. Specifically, SUs are required to operate with transmission powers below the noise floor of PUs. This is usually performed by technologies that spread secondary signals over wide spectrum bands, such as Code Division Multiple Access (CDMA) or Ultra-Wide Band (UWB). Thanks to

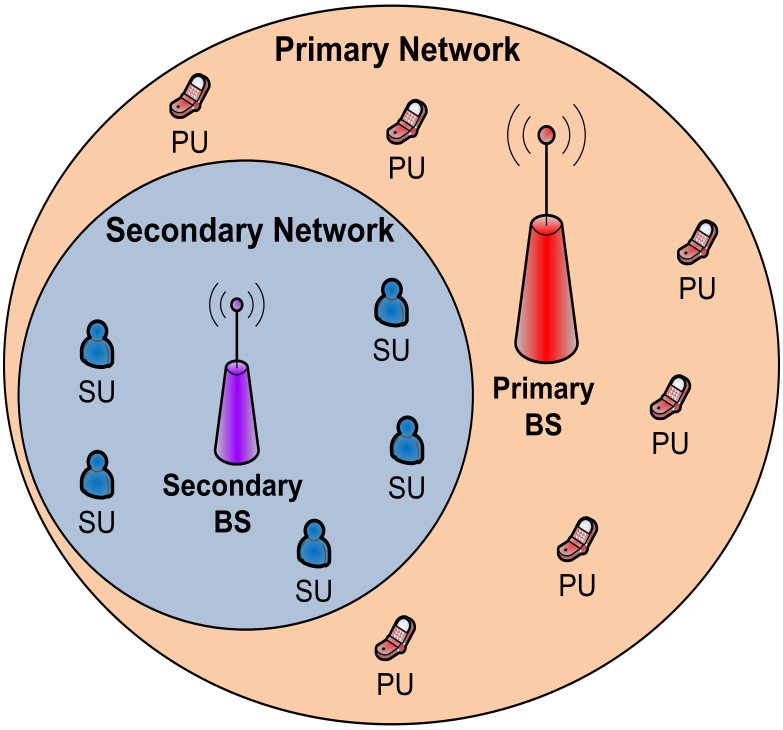

Figure 1.3: An illustrative example of the hierarchical access model

the unique features of these spread-spectrum techniques, SUs can achieve high data rates regardless of the activity of PUs. The main drawback of this approach is the need for extremely low SU transmission powers, which limits the applicability to short-range communication systems, such as Wireless Personal Area Networks (WPANs) [21].

1.1.4 Cognitive radio networks

With the advent of the CR paradigm, interconnection needs have rapidly raised and Cognitive Radio Networks (CRNs) have been proposed to connect a set of CRs operating according to one of the DSA models described in Section 1.1.3. For each of these models, the interconnection architecture may be built on the fly between different CRs (*ad-hoc mode*) or rely on some additional network nodes (*infrastructure mode*) [22].

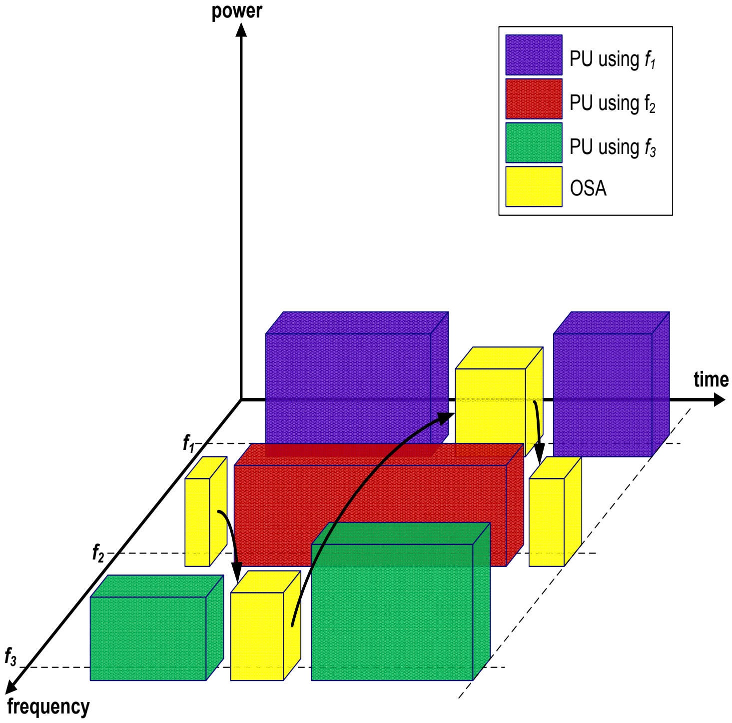

Figure 1.4: An illustrative example of OSA

The example shown in Figure 1.5 illustrates how both modes apply to access an unlicensed band and two licensed bands according to the open sharing and hierarchical access models, respectively. As can be observed, the different CRs may be connected either directly (*ad-hoc mode*, CRN_1) or indirectly through a secondary BS that provides a single-hop connection to each of the considered bands (*infrastructure mode*, CRN_2).

For both interconnection modes, CRNs are facing unique challenges in terms of coexistence with PUs and diverse Quality of Service (QoS) requirements associated with the various cognitive communications. In particular, the following issues should be tackled [22]:

- *Interference avoidance*: to operate while controlling the amount of interference perceived by primary networks.
- *QoS awareness*: to enable QoS-aware communications in dynamic and heterogeneous spectrum environments.

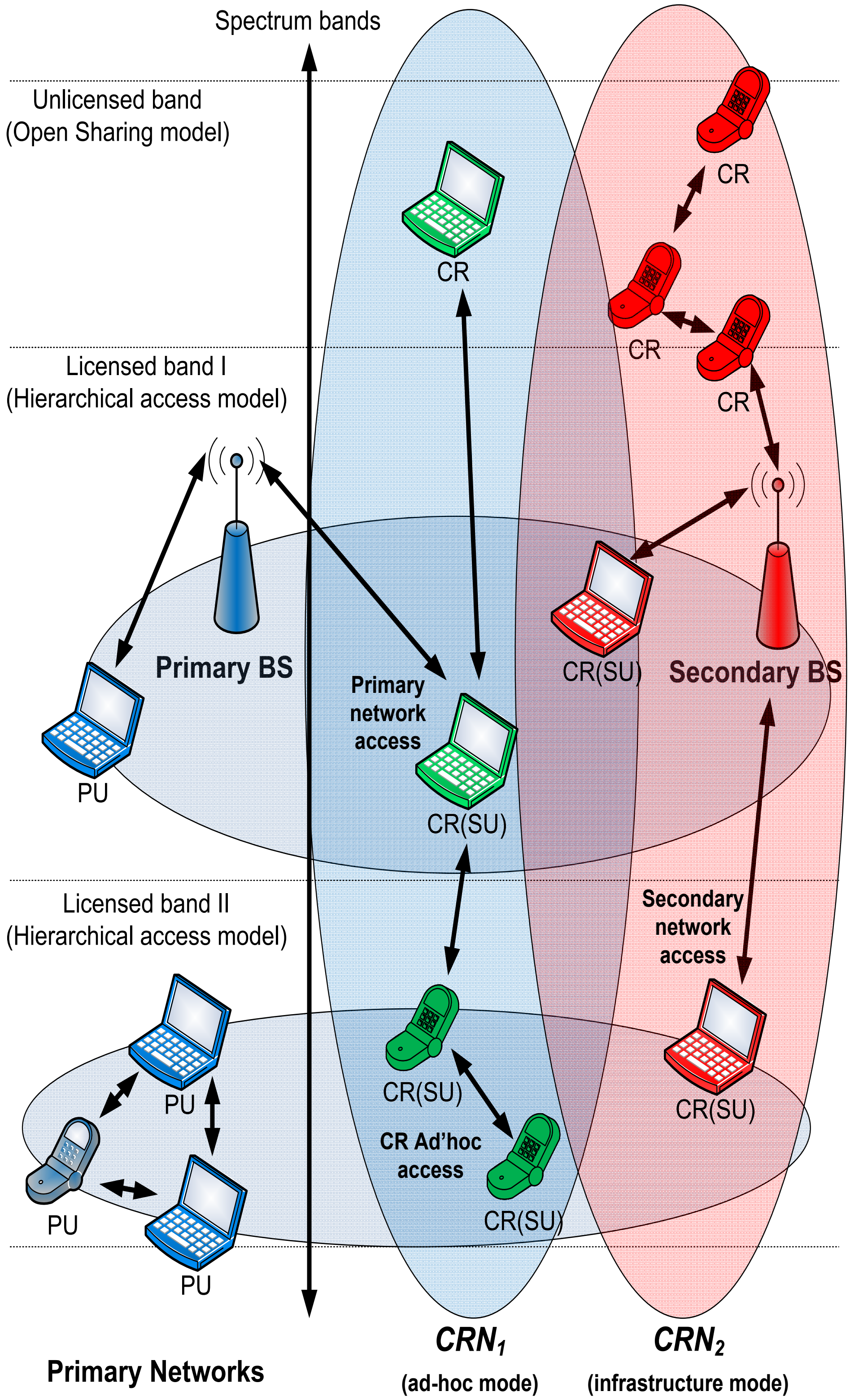

Figure 1.5: Possible architectures of CRNs

- *Seamless communication*: to provide seamless communications regardless of the activity of PUs

These unique features have called for a fundamental rethinking of the spectrum management process in CRNs compared to traditional wireless networks as will be explained in the next section.

1.1.4.1 Spectrum management functions

To address the unique challenges faced by CRNs, the spectrum management process has been structured to combine four major functions [22]:

- *Spectrum sensing*: When CRs are allowed to use only those unused portions of spectrum (e.g., spectrum overlay), CRNs should include a sensing mechanism that monitors available spectrum bands to identify potential *spectrum holes*.

- *Spectrum selection*: Based on identified *spectrum holes*, CRNs should allocate a proper channel to each of the various CR communications. This allocation depends not only on spectrum availability, but also on internal (and possibly external) CR policies.

- *Spectrum mobility*: CRs are not spectrum owners and do not have the exclusive right to use it. Therefore, whenever a PU requires a specific portion of spectrum in use by some CR, the corresponding CR communication must be switched to another vacant portion of the spectrum.

- *Spectrum sharing*: Access to spectrum should be coordinated among the different CRs to prevent any collision in the overlapping portions of spectrum.

Some of these short descriptions are cross-referenced, which means that the four spectrum management functions are somehow dependent. To better illustrate this dependency, Figure 1.6 maps each of these functions on the CR cognition cycle described in Figure 1.1.

It can be observed that all spectrum management functionalities are strongly interacting, and therefore they should be all designed within a single cross-layer

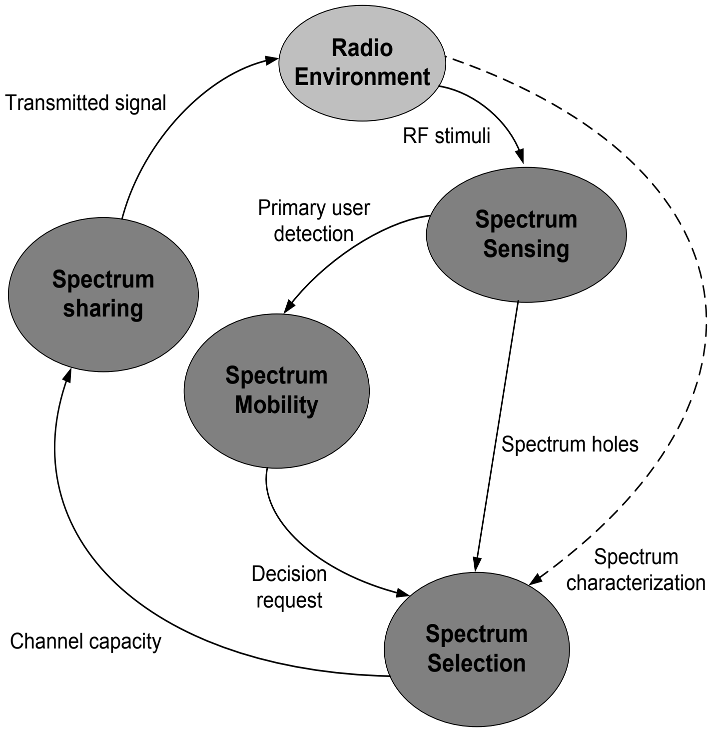

Figure 1.6: Interaction between CRN spectrum management functions

framework. Such framework should exploit all possible sources of information that may assist in the spectrum management decision-making process. To this end, CRNs have been strengthened with various forms of cognitive management support as will be explained in the following sub-sections.

1.1.4.2 Radio environment map support

To improve the accuracy and performance of cognitive operation, there has been a recent interest in identifying and exploiting additional and temporally consistent (i.e., long-term) knowledge of the environment to reduce the level of uncertainty that CRs may face. The exploited information may be stored locally or globally in a database-like system, commonly called Radio Environment Map (REM). The REM information should capture the most relevant specificities of the radio environment from the perspective of CRs, such as the "typical" behavior of spectrum users and experienced radio propagation conditions. The REM support can be envisioned

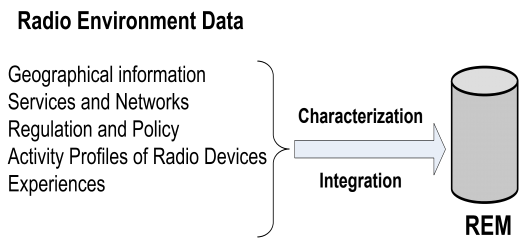

Figure 1.7: Network support and prior knowledge provided by the REM [26]

as a large-scale navigator for CRs by providing useful awareness about external networks, such as non-cognitive legacy systems together with a cognitive support to the associated internal networks. Therefore, the key principles to design a powerful REM are to decide what type of information must be stored and how to make such information available to the various CRs.

To meet these requirements, the REM may cover, among others, multi-domain environmental information, such as geographical features, available services, spectral regulations, location of the various entities of interest (e.g., radios, reflectors, and obstacles), radio-equipment capability profiles, relevant policies and past experiences (Figure 1.7). This information can be updated based on observations made by distributed CR nodes, and then disseminated within the CRN [23–25]. The most popular approaches to perform such dissemination are (a) using a dedicated control channel and (b) sharing a traffic channel.

In general, REM architectures could be classified into global or local REMs, depending on the origin, extent and scope of the stored information. A global REM is usually implemented at least partially as a network back-end system, whereas a local REM typically resides within the network of CRs. Both local and global REMs may be integrated into a common framework and exchange data periodically to keep the stored information up-to-date (Figure 1.8). Obviously, CRNs would benefit the most from an integrated architecture including both global and local REMs, i.e., by combining information from these two databases. The global REM, could be used to store larger amounts of data as well as to carry out more intensive computations especially if implemented in back-end, whereas local REMs would improve responsiveness and decrease latency. These benefits are better illustrated in the following case studies:

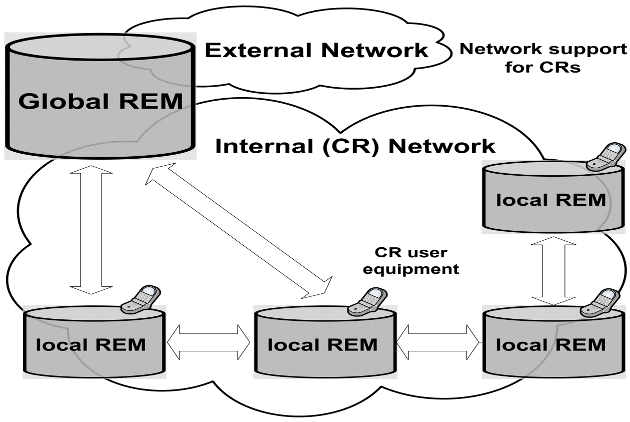

Figure 1.8: Local and global REMs [23]

- The interference range of CRs is often larger than their sensing range. Thus, the global REM could be used by CRs to "see" far beyond their sensing range, and improve environmental characterization. In this respect, the work of [27] showed that a global REM characterization of possible PU positions improves CR performance by about 2-10 *dB* compared to the case that uses only a local REM.

- Local REMs would be better restricted to limited time-scale measurements in comparison with global REMs that might contain measurements for larger time scales (e.g., days, weeks, months). This multi-scale recording of activities could be used by CRs to predict the behavior of PUs in the near and far future.

- The information stored in local REMs by various CR nodes could be combined by the global REM to infer future changes in the environment.

1.1.4.3 Optimizing end-to-end performance

As CRNs are gradually deployed, the path connecting two CRs may involve several intermediate nodes, which may hurt the end-to-end performance perceived by each of the communicating parties. Nevertheless, the individual CR cognitive capabilities described in Section 1.1.2 focus on the individual CR performance, and thus cannot control end-to-end performance. Therefore, CRNs should be strengthened with additional cognitive functionalities to optimize the operation from the network perspective. In particular, the following capabilities may be introduced [28]:

1. *End-to-end performance*, which determines, for each networking communication, an end-to-end performance target that would strike a balance between the heterogeneous requirements of all nodes present along the communication path and available network resources and policies.

2. *Cognitive ability*, which improves awareness by gathering useful information from different domains, such as the wireless, network, user, and policy domains.

3. *Autonomous decision-making*, which exploits the gathered information to autonomously optimize end-to-end performance.

4. *Adaptive reconfiguration ability*, which adjusts and reconfigures network operation parameters, such as network working modes and topologies, system protocols, and radio parameters following the optimization decisions made by the *autonomous decision-making* module.

These network-level capabilities are interacting according to optimization process described in Figure 1.9. The CRN gathers multi-domain network information, analyzes it, and makes a set of decisions to optimize end-to-end performance. Based on these decisions, the CRN may reconfigure some of its parameters. Note that all CRN tasks are performed to achieve the performance target previously determined by the *end-to-end performance* module.

1.1.4.4 Towards real cognitive management architectures

The expected benefits of exploiting cognitive management support that have been established in many studies [29–31] together with the shown usefulness of such support in strengthening both the awareness level and end-to-end performance of CRNs have persuaded to exploit more advanced cognitive management tools to optimize the whole CRN operation.

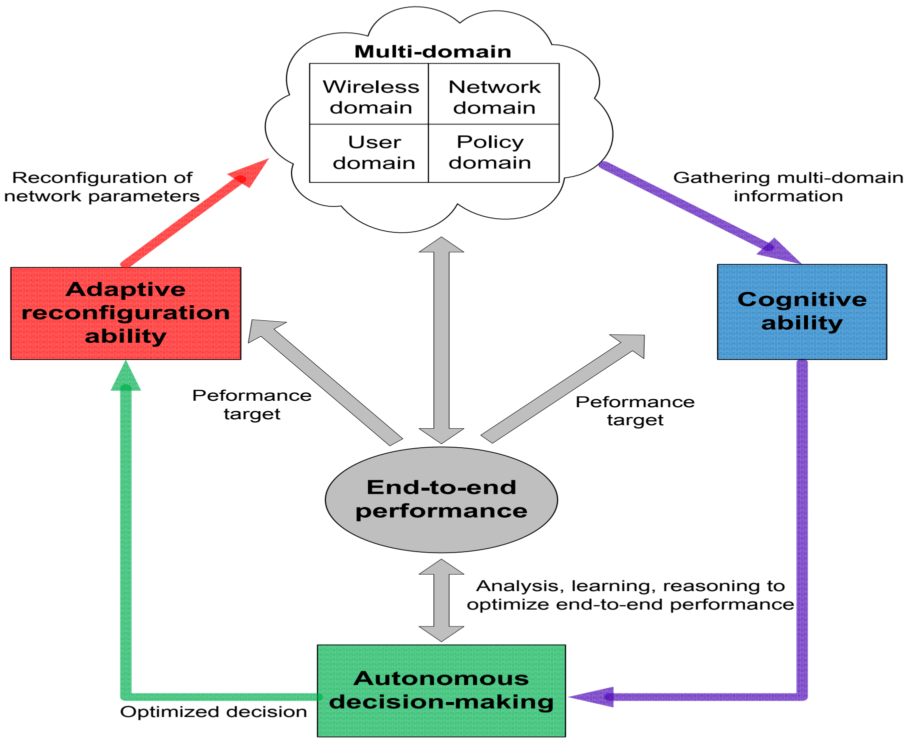

Figure 1.9: Optimization process of end-to-end performance [28]

In this respect, several cognitive management architectures have been constructed to guide the CRN operation in some specific scenarios. For instance, the work in [32] proposes to introduce cognitive management tools into the Future Internet (FI) to support operators in managing their infrastructure and services. Based on a joint analysis of infrastructure capabilities, application- and business-driven requirements, authors argue that cognitive management systems represent a viable solution to strengthen FI with additional "self-management" and "learning" features. In [33], a cognitive framework is proposed to perform an autonomous optimization of resource usage in next-generation home networks. The proposed framework relies on a home cognitive resource manager to dynamically optimize performance of network nodes according to the goals, restrictions and policy regulations formulated by network stake-holders. The work of [34] proposes a cognitive device management system to dynamically select and adapt the most appropriate technology in a multi-Radio Access Technology (RAT) context. The proposed system first acquires useful knowledge through an advanced learning scheme based on Bayesian statistics, and then exploits the acquired knowledge to select the optimal device configuration. In [35], cognitive management tools are applied to enhance efficiency of medical applications. In particular, a novel cognitive architecture named *Co-health* is proposed to exploit available knowledge and previous experience to support electronic healthcare, especially in emergency situations.

Apart from these scenario-specific architectures, there has been an increasing trend towards constructing generic cognitive management frameworks, in which advanced cognitive functionalities can be developed for different scenarios and environments. For instance, the authors of [36] introduce a cross-layer reconfiguration framework that optimizes all CRN parameters to jointly meet user requirements, realize interoperability between heterogeneous networks and improve adaptability to dynamic environments. The proposed framework integrates several functional entities that exploit advanced Ant Colony Optimization (ACO) techniques to perform an autonomous reconfiguration of the decision-making process with respect to a multitude of complex objectives. The work of [37] focuses on optimizing the CRN topology to perform an optimal routing. The problem is first formulated as a multi-objective optimization problem, and then tackled using an advanced ACO solver.

The shown usefulness of cognitive capabilities has stimulated the initiation of many research projects (e.g., [38–40]) and standardization activities (e.g., [41, 42]) to further strengthen and promote the use of cognitive management systems.

1.2 Recent progress on spectrum management in cognitive radio networks

This section makes a state-of-the-art analysis of the spectrum management functionalities described in Section 1.1.4.1. The analysis focuses particularly on *spectrum selection* and *spectrum mobility*, the two other functionalities (*spectrum sensing* and *spectrum sharing*) being out of the scope of this dissertation.

1.2.1 Spectrum selection

The spectrum selection (SS) functionality aims at selecting the most adequate spectrum portions to carry out cognitive transmissions subject to not interfering all surrounding PUs. To succeed in making such critical decisions, SS should take into account all the relevant information related to a given scenario, such as CR requirements, achievable channel capacities, and the maximum tolerable interference by PUs.

In this respect, most of early proposals dealt with specific issues related to this problem. For instance, the effect of various PUs on the CR channel selection policy is analyzed in [43]. Specifically, successful CR transmission time is analyzed in the presence of heterogeneous PUs in terms of activity statistics and protection requirements. The work in [44] focuses on SS-related issues in a multi-channel radio network. Considering a general setting with un-slotted PUs, an optimal SS policy is developed and assessed. Authors of [45] consider the problem of bandwidth selection in a multi-band context. An optimal bandwidth selection schemes is developed to maximize the CR throughput subject to some band switching costs for both the single- and multi-CR cases. In [46], the channel aggregation feature is studied in a Differential Orthogonal Frequency Division Multiplexing (DOFDM) context. In this respect, an aggregation-aware SS scheme that performs a maximum span of available channels is developed and assessed.

The aforementioned proposals were shown to efficiently deal with various SS-related issues. Nevertheless, they all rely on a strong knowledge about PUs that may not be available in practice. To overcome this limitation, there has been an increasing interest in exploiting advanced learning tools. In particular, many Reinforcement Learning (RL)-based solutions have been developed to train CRs in front of the uncertainty of the environment. For instance, an RL framework is constructed in [47] to detect available spectrum opportunities in an Orthogonal Frequency Division Multiplexing (OFDM) network. The proposed framework enables to dynamically reconfigure each cognitive communication by one of three possible actions, namely to keep transmission in the current band, perform a detection phase in a different band while keeping transmission in the current band, or switch transmission to a different band. In [48], a more general setting with heterogeneous channels in terms of transmission range, packet error rate and primary utilization is considered. In this respect, an RL-based SS scheme is developed to strike a balance between the achievable CR throughput and incurred channel switching cost. In [49], spectrum is modeled as an auction market, where CRs may compete for available channels. A Q-learning-based bidding strategy is proposed to improve CR performance in terms of both the packet loss and transmission rate. In [50], a self-evaluating RL-based strategy is proposed to assist spectrum management in cognitive ad'hoc networks. The proposed strategy continuously monitors rewards received by CRs to detect disruptive changes in the environment.

Most of these RL-based proposals do not require any a-priori knowledge about PUs, but simply adapt cognitive operation based on direct observations from the environment. While these pure learning approaches overcome the problem of practicality of early proposals, they may be too conservative in scenarios where some useful knowledge about PUs can be easily obtained. Therefore, there has been a recent shift towards an intermediate approach that neither assumes perfect knowledge about primary systems, nor ignores useful information that may be available, but exploits all possible sources of information.

In this respect, many recent SS proposals have attempted to identify and exploit the most relevant primary activity features in a given environment. For instance, the work in [51] proposes to assist the SS decision-making process by an external database that provides information about the most probably un-occupied channels. The results show that exploiting database queries together with spectrum sensing reports enables to significantly improve performance with respect to a pure random search, particularly for high traffic loads. In [52], multi-time scale predictive primary statistical models are built at different time scales based on sensing reports. Based on these models, "bad channels" are eliminated through a usability filter, and a pro-active SS scheme that maximizes spectrum utilization subject to minimizing disturbance of PUs is proposed and assessed. In [53], a statistical model that predicts lengths of *spectrum holes* is developed. Based on this model, a prediction-based SS strategy is developed to better satisfy CR requirements. In [54], a set of primary randomness levels are introduced. In this respect, a simple classification method is applied to qualify primary traffic as periodic or stochastic. For both randomness levels, specific procedures to estimate the remaining idle time of each channel are developed. The proposed classification-based approach is shown to significantly reduce the amount of collisions with PUs compared to a system operating without classification. In [55], deterministic patterns are proposed to characterize the activity of PUs in some standardized channels. A proposed SS mechanism that exploits these patterns is developed to minimize channel selection or equivalently increase the system throughput.

1.2.2 Spectrum mobility

The spectrum mobility (SM) functionality refers to the situation when an ongoing cognitive communication needs to be transferred to another channel due to e.g., unavailability of the current channel. This procedure so-called Spectrum Hand-Over (SpHO) is a unique characteristic of CRNs that has to reach maturity before DSA could really prosper.

However, the SM functionality has not been intensively investigated compared to the other spectrum management functionalities, and only few fundamental SM studies can be found in the literature [56]. Instead, most of proposals have developed proactive SS strategies to minimize the number of subsequent SpHOs at the time of making SS decisions. For instance, the work in [57] introduces a proactive *spectrum hole* reservation scheme that reserves an additional channel for each of the expected-to-be-switched CR communications. The proposed scheme is shown to reduce the number of SpHO failures at the cost of a higher blocking rate for incoming requests. This work is later extended in [58] to reserve some channels, not only to the likely-to-be-switched communications, but to all CR communications. In this respect, a fractional bandwidth is reserved for the reassignments performed following the SpHO procedure, thus giving them higher priority compared to the initial assignments performed at session establishment. In [59], long-term observation outcomes are exploited to determine a target channel sequence for each SpHO that may be performed in the future. Specifically, a Preemptive Resume Priority

(PRP) M/G/1 queuing network model is used to find the optimal channel sequence that jointly minimizes the total service time for multiple SpHOs.

All the above-mentioned proactive schemes exploit a proper characterization of spectrum resources to minimize the risk of subsequent SpHOs before CR communications are established. Nevertheless, such knowledge may not be available in some scenarios and the decision about possible reconfigurations cannot be then anticipated. In this respect, some proposals have followed a reactive approach to determine target channels on an on-demand basis after the SpHO request is made. For instance, the work in [60] develops a set of recovery schemes to reallocate available resources to the failed flows due to activity of PUs in a Wireless Mesh Network (WMN). In [61], an analytical framework is constructed to evaluate the impact of reactive SpHOs on channel utilization and latency performance. The proposed framework combines a PRP M/G/1 queueing network and a state diagram to quantify channel utilization and data delivery time under various traffic arrival rates, service time distributions and SpHO processing times. In [62], both proactive and reactive strategies are compared when various PU bandwidths are used. The results show that the former strategies have better performance in terms of the total transmission data rate and number of disruptions by primary users, while the latter enjoy less channel switches and a higher channel utilization rate.

Apart from studying proactive and reactive channel selection strategies, other proposals have focused on optimizing the SpHO procedure for some particular architectures. For instance, the work in [63] considers a distributed architecture where only incomplete and vague information may be available to CRs. To cope with uncertainty, a fuzzy-based approach is proposed to properly initiate SpHOs to guarantee quick decisions and real-time operation. In [64], a strategy is developed to minimize the service disruption caused by SpHO failures in a cellular architecture. The proposed approach exploits differences in propagation losses between the serving and target channels for each SpHO, and triggers, when needed, SpHOs to avoid CR communication interruption.

1.3 Motivations and scope

The DSA/CR concept has emerged as the most promising solution to pursue higher efficiency in spectrum usage. Embedding CRNs with an advanced cognitive management support has been thought of as a powerful option to improve their performance and push forward their massive deployment and commercialization. In this context, this dissertation proposes to assess the relevance of several cognitive management functionalities in various scenarios and case studies. Specifically, the dissertation constructs a novel cognitive management framework to enable a more reliable characterization of the radio environment, and consequently a more efficient utilization of available spectrum resources. While most of existing solutions are relying on some form of cognitive management support customized for very specific scenarios, the proposed framework offers the possibility of developing standalone cognitive management functionalities that can be instantiated differently depending on specificities of different environments.

Managing several cognitive management capabilities within a single framework enables to eliminate any inter-redundancy and avoid potential conflict between them. Therefore, independent cognitive management functionalities can be developed to strengthen CRNs with additional capabilities and features. For instance, the CRN awareness level can be strengthened by statistical patterns that characterize the activity of the diverse users sharing the spectrum and the CRN reactivity to changes can be improved by additional learning and adaptability capabilities. Thanks to this support, spectrum management can be assisted to increase the level of CR satisfaction without interfering any of the incumbent spectrum users. Therefore, the proposed framework enables to exploit all possible sources of information and develop advanced cognitive management functionalities to assist the spectrum management decision-making process to perform the most efficient usage of available spectrum resources.

1.4 Thesis contributions

This dissertation aims at constructing a cognitive management framework for assisting spectrum management in CRNs. While this problem may be tackled directly, the multitude of incumbent spectrum users and possible DSA strategies suggests that a set of preliminary studies would be better initially conducted to gain insight into the problem, and devise the main principles to determine the most relevant cognitive functionalities for different scenarios. In this respect, a set of algorithmic solutions are proposed to assist two of the most promising CR applications, namely OSA to licensed bands and open sharing of license-exempt bands. As a result of these studies, which constitute the first of the three parts of this dissertation, a set of supporting contributions (SCs) are performed with respect to each of the considered case studies. Drawing inspiration from these studies, the functional architecture of the proposed framework is constructed and a general strategy to assist spectrum management is developed in the second part of this dissertation. Based on an exhaustive assessment of the proposed solution, a set of core contributions (CCs) are performed. An analysis of practicality aspects in terms of robustness to environment uncertainty and applicability to realistic environments is conducted in the third part of the dissertation, thus leading to a set of practicality contributions (PCs). Finally, the key conclusions about performed contributions are provided together with some possible future directions.

The main contributions of this dissertation are the following:

[SC.1] *Exploitation of cognitive management functionalities to support OSA to licensed bands*. Different strategies to support an OSA-type access with a proper temporal characterization of incumbent spectrum users are proposed. A set of key principles are developed to capture the main dependencies between relevance of each of these strategies and specificities of the environment (e.g., dynamism of the radio environment, incumbent user types and secondary traffic loads). These principles enable a generic SS strategy to properly adjust the decision criterion for different configurations and settings.

[SC.2] *Exploitation of cognitive management functionalities to support open sharing of license-exempt bands*. A SS strategy that exploits a new fittingness factor concept is proposed to support open sharing of license-exempt bands. The frequency domain characterization in terms of fittingness factor enables to track the suitability of the different bands to support the heterogeneous requirements of CR applications, which results in significant performance gains with respect to other strategies.

[CC.1] *Construction of a cognitive management functional architecture for optimizing spectrum management in CRNs.* Drawing inspiration from [SC.1] and [SC.2], the proposed architecture introduces a standalone knowledge management domain to store and manage the most relevant knowledge about the radio environment out of the decision-making domain. This domain separation enables to develop generic cognitive management functionalities independently from the decision-making process. Then, these functionalities are properly instantiated in different scenarios to provide the most relevant support to each task performed by the decision-making process.

[CC.2] *Development of a generic strategy to assist spectrum management.* A generic spectrum management strategy that captures both the temporal and spectral variability of spectrum pools is proposed to assist spectrum management. The generic aspect of the proposed strategy is guaranteed by a functional description of each of its components (e.g., decision criterion, fittingness factor function and context awareness strategy) with several possibilities of implementation. Each of these components introduces a degree of freedom that can be set differently for different environments and configurations.

[CC.3] *Reduction of degrees of freedom.* Degrees of freedom of the proposed strategy are reduced by properly implementing some of its components to support a multitude of possible configurations. In this respect, different variants of the proposed strategy, each combining different choices and options of implementation, are compared and the best variant is selected.

[CC.4] *Assessment of rationality of the proposed strategy.* This study contributes to assess rationality of exploiting cognitive management functionalities to support spectrum management. Performance of the best variant selected in [CC.3] is assessed from both the gain and cost perspectives with respect to other strategies.

[PC.1] *Enhancement of robustness to uncertainty.* The implicit assumption that acquired knowledge about the environment is reliable is called into question by introducing two sources of uncertainty, namely imperfection of the CRN acquisition process and non-stationarity of the environment. Robustness to both types of uncertainty is assessed, and the proposed framework is extended, when needed, to improve robustness.

[PC.2] *Applicability to realistic environments.* The proposed framework is applied to efficiently exploit the heterogeneous sources of spectrum that may be available in a Digital Home environment. The richness of the considered environment and the diverse radio and interference conditions that may be experienced within it enables to assess effectiveness of the proposed framework under realistic conditions.

1.4.1 Related publications

The above-listed contributions have been published in several journal articles (JAs) and international conference articles (CAs). These dissemination activities are listed in the following:

1.4.1.1 Journals (published/in press)

[JA.1] **F. Bouali**, O. Sallent, J. Pérez-Romero, and R. Agustí, "A Fittingness Factor-based Spectrum Management Framework for Cognitive Radio Networks," Wireless Personal Communications pp. 1–15, 2013. [Online]. Available: http://dx.doi.org/10.1007/s11277-013-1128-6 [CC.1][CC.2][CC.3].

[JA.2] **F. Bouali**, O. Sallent, J. Pérez-Romero, and R. Agustí, "A Cognitive Management Framework for Spectrum Selection," Computer Networks Journal, 2013. [Online]. Available: http://dx.doi.org/10.1016/j.comnet.2013.06.008 [CC.4].

1.4.1.2 Journals (submitted)

[JA.3] **F. Bouali**, O. Sallent, J. Pérez-Romero, and R. Agustí, "Exploiting Knowledge Management for Supporting Multi-Band Spectrum Selection in Non-Stationary Environments," IEEE Transactions on Wireless Communications, submitted 2013 (under second review) [PC.1] [PC.2].

1.4.1.3 International conferences

[CA.1] **F. Bouali**, O. Sallent, J. Pérez-Romero, and R. Agustí, "Strengthening radio environment maps with primary-user statistical patterns for enhancing cognitive radio operation," Sixth International ICST Conference on Cognitive Radio Oriented Wireless Networks and Communications (CROWNCOM), 2011, June 2011, pp. 256 –260 [SC.1][PC.1].

[CA.2] **F. Bouali**, O. Sallent, J. Pérez-Romero, and R. Agustí, "A Novel Spectrum Selection Strategy for Matching Multi-Service Secondary Traffic to Heterogeneous Primary Spectrum Opportunities," in Personal Indoor and Mobile Radio Communications (PIMRC), 2011 [SC.1].

[CA.3] **F. Bouali**, O. Sallent, J. Pérez-Romero, and R. Agustí, "A framework based on a fittingness factor to enable efficient exploitation of spectrum opportunities in cognitive radio networks", 14th International Symposium on Wireless Personal Multimedia Communications (WPMC), Oct. 2011, pp. 1–5 [SC.2].

[CA.4] **F. Bouali**, O. Sallent, J. Pérez-Romero, and R. Agustí, "Exploiting Knowledge Management for Supporting Spectrum Selection in Cognitive Radio Networks," in Cognitive Radio Oriented Wireless Networks and Communications (CROWNCOM), 2012 [CC.1][CC.2].

[CA.5] J. Pérez-Romero, O. Sallent, **F. Bouali**, H. Sarvanko, M. Mustonen, M. Matinmikko, Haeyoung Lee, S. Vahid, K. Moessner, "A spectrum selection framework for Opportunistic Networks," Future Network & Mobile Summit (FutureNetw), 2012 , vol., no., pp.1-9, 4-6 July 2012 [CC.4].

[CA.6] **F. Bouali**, O. Sallent, and J. Pérez-Romero, "Knowledge Management Framework for Robust Cognitive Radio Operation in Non-Stationary Environments," in Personal Indoor and Mobile Radio Communications (PIMRC), 2013 [PC.1].

1.4.2 Project involvement

The work carried out during the doctoral research period has been linked to the following research projects funded by both Spanish and European Union entities:

- FARAMIR: "Flexible and spectrum-Aware Radio Access through Measurements and modeling In cognitive Radio systems", funded by the European Union in the Seventh Framework Programme (FP7), Information and Communication Technology (ICT), Small or Medium Scale Focused Research Project (STREP), Ref. ICT-248351.

- OneFIT: "Opportunistic Networks and Cognitive Management Systems for Efficient Application Provision in the Future Internet", funded by the European Union in the Seventh Framework Programme (FP7).

This project involvement has offered a unique opportunity to present the work to various project partners, from both industry and academia, receive useful comments and share ideas and experiences. The resulting research diversity has helped a lot in improving the quality of the work. Contributions by the author towards each of these projects are summarized in the following:

- FARAMIR: The author contributed to support an OSA-type access to licensed bands by strengthening REMs with a set of advanced statistics that capture hidden dependence structures potentially exhibited by primary activity/inactivity durations. In addition, an SS strategy was proposed to efficiently exploit these patterns in a multi-application context.

- OneFIT: The author contributed to assist spectrum management of Opportunistic Networks (ONs) with a cognitive management framework based on a new fittingness factor concept. Based on the proposed framework, a proactive spectrum management strategy was proposed to jointly assist SS and SM functionalities. In addition, the proposed framework was extended to support two constraints that may face the formation of ONs, namely the heterogeneous operator preferences in using the different bands and the non-stationarity of the environment.

The outcome of this project involvement is reflected not only in the aforementioned journal and conference publications, but also in several contributions towards project deliverables (PDs), chronologically listed hereafter:

Project Deliverables

[PD.1] J. Pérez-Romero (Editor), "Conceptual Framework for enabling Measurement-based Mechanisms," FARAMIR project, Deliverable D5.1, February, 2011.

[PD.2] M. Bourdellès, S. Pega (Editors), "Formulation, implementation considerations, and first performance evaluation of algorithmic solutions," OneFit Project, Deliverable D4.1, May 2011.

[PD.3] J. Pérez-Romero (Editor), "Evaluation of Selected Measurement-based Techniques," FARAMIR Project, Deliverable D5.2, February 2012.

[PD.4] J. Pérez-Romero (Editor), "Performance assessment and synergic operation of algorithmic solutions enabling opportunistic networks," OneFit Project, Deliverable D4.2, June 2012.

[PD.5] J. Vahid (Editor), " Performance evaluation of synergic operation of algorithms enabling opportunistic networks," OneFit Project, Deliverable D4.3, December 2012.

1.5 Thesis outline

The work presented in this PhD dissertation can be structured in three main parts as illustrated in Figure 1.10. The first part conducts a set of preliminary studies to get insight into exploiting cognitive management to optimize cognitive operation in different case studies. The second part presents and evaluates the proposed framework and algorithmic solution from a cost-benefit perspective, while the third part analyses and extends it for better practicality. Enlightened by the results obtained in these parts, the key conclusions of the dissertation together with some possible future directions are provided in the last part of the dissertation (Chapter 8). Note that Chapter 2 that belongs to the second part is presented first for better readability.

The first part considers to benchmark the usefulness of exploiting cognitive management techniques to drive two of the most popular CR applications. The first application, which is covered by Chapter 3, proposes to exploit the temporal behavior of PUs to guide an OSA-type access to licensed bands. Specifically, a set of advanced statistics that capture dependence structures potentially exhibited by primary activity/inactivity durations are proposed and exploited by a proactive spectrum management strategy assuming the operating bucket configuration determined in Annex A and the duration patterns described in Annex B. The second application, which is covered by Chapter 4, proposes to exploit a new fittingness factor concept to assist open sharing of license-exempt bands. The suitability of these bands to meet the heterogeneous requirements of CR applications is assessed and exploited by a fittingness-factor based SS.

Drawing inspiration from these studies, the second part constructs a cognitive management framework to support spectrum management in CRNs. Specifically, Chapter 2 constructs the functional architecture of the proposed framework. The proposed architecture relies on a Knowledge Manager that monitors the suitability of existing spectral resources to support the spectrum management decision-making process. The Knowledge Manager monitoring is based on information retrieved from a Knowledge Database that stores a set of relevant statistics about the environment. Chapter 5 develops a generic spectrum management strategy that exploits the Knowledge Manager support to jointly optimize the SS and SM functionalities. Several variants of the proposed strategy, each combining different choices and options of implementation, are compared. Based on this comparison, the best variant is firstly determined, and secondly assessed from both the cost and benefit perspectives to assess its rationality.

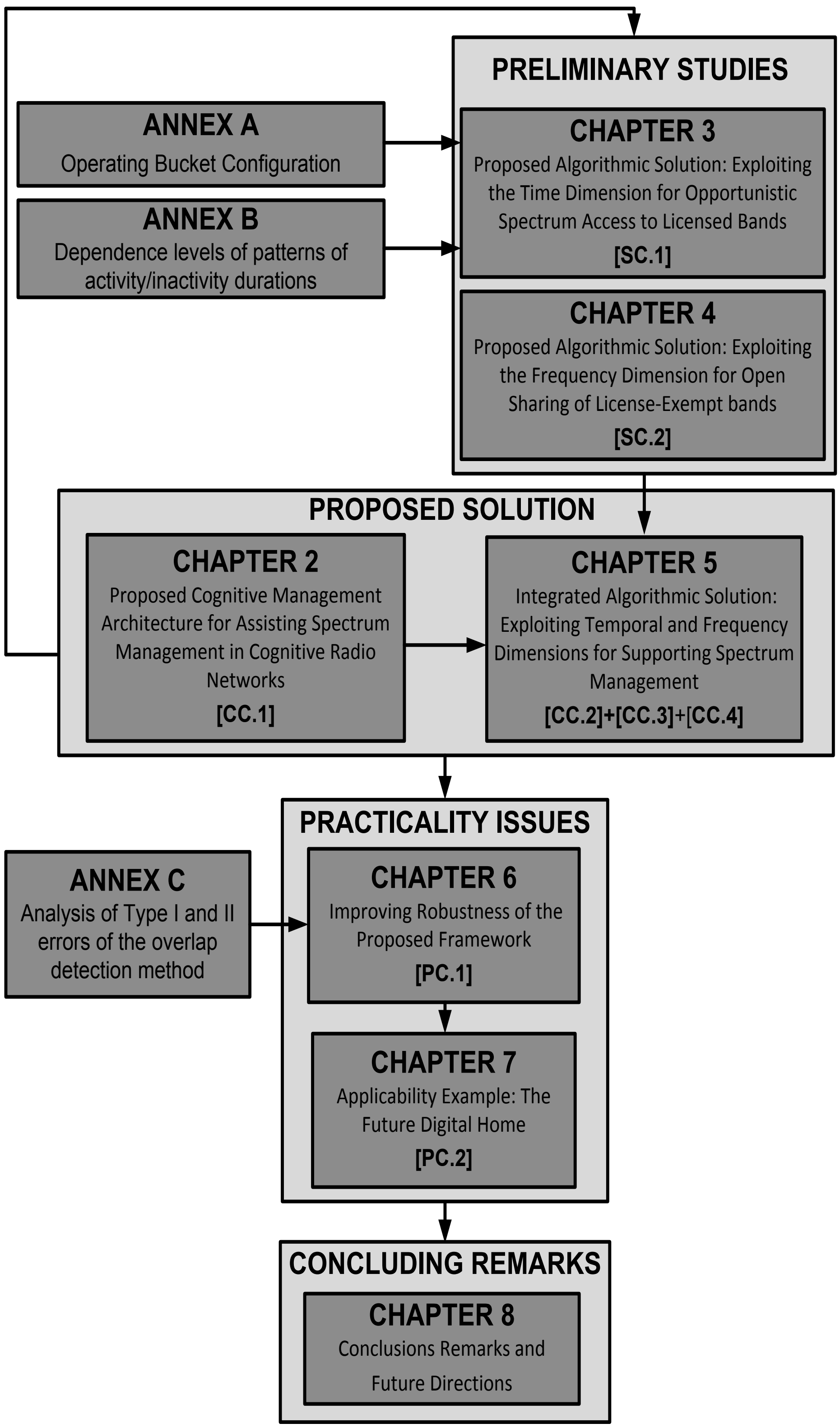

Figure 1.10: Outline of the PhD dissertation

The third part deals with various aspects related to practicality of the proposed solution. The main objective is to determine the extent to which the obtained key findings based on simulations remain valid under realistic settings. In this respect, Chapter 6 assesses robustness to two sources of uncertainty in the data stored in the Knowledge Database, namely imperfection of the acquisition process and non-stationarity of the environment. In the former case, performance is assessed for different levels of convergence achieved in the acquired data. In the latter, the proposed architecture is extended with a Reliability Tester that detects, based on the detection method described in Annex C, relevant changes in the environment, and updates the content of the Knowledge Database accordingly. Chapter 7 applies the extended framework to a realistic Digital Home environment. The richness of the considered environment allows to associate the concepts and assumptions of previous chapters (e.g., interference conditions and model of non-stationarity) with real world phenomena observed within the Digital Home, thus showing practicality of the proposed solution.

Short biography

Faouzi Bouali received his telecommunication engineering degree (2004) and his master's degree in networks (2006) all with distinction from the Higher Communication School of Tunis (SUP'COM), Tunisia. From 2005 to 2009, he worked as radio optimization engineer within the Tunisian National Phone company (Tunisie Telecom) where he was involved in many optimization projects of GSM/GPRS/W-CDMA networks. Since October 2009, he has been pursuing his PhD degree within the Mobile Communication Research Group (GRCM) of the Dept. of Signal Theory and Communications (TSC) at the Technical University of Catalunya (UPC) in Barcelona. His current research interests span the field of mobile radio-communication systems with a specific focus on efficient Radio Resource Management algorithms, quality of service provisioning, and networking solutions for DSA networks.

2. Proposed Cognitive Management Architecture for Assisting Spectrum Management in Cognitive Radio Networks

The problem considered here is the selection of the spectrum to be assigned to a set of L radio links that need to be established between pairs of terminals and/or network infrastructure nodes. The purpose of the l-th radio link is to support the communication flow generated by a given application (e.g., voice, web browsing, or video call) whose requirements are expressed in terms of a required bit rate $R_{req,l}$ and mean holding time $T_{req,l}$. As shown in the example of Figure 2.1, the established radio links may connect a terminal node to a network infrastructure (links $\#1$ and $\#2$) or two terminal nodes (links $\#3$ and $\#4$). To meet the heterogeneous requirements from diverse applications, it is assumed that the network infrastructure is responsible for assigning the suitable spectrum resources to each radio link. In this respect, the spectrum is modeled as a set of P blocks (denoted as "pools" in this dissertation), each of bandwidth BW_p. The SS decisions made on the network infrastructure side are indicated to mobile terminals through suitable control channels (denoted in Figure 2.1 as dashed lines in case there is no data connection with the network infrastructure).

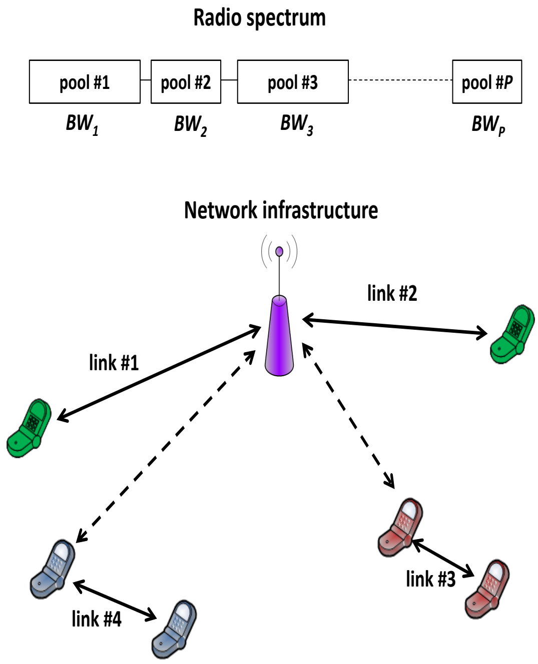

Figure 2.1: Example of established radio links

2.1 Functional architecture

To exploit cognitive management functionalities to meet the heterogeneous requirements of CR applications, the functional architecture depicted in Figure 2.2 is proposed. Inspired by the ETSI-RRS architecture [65, 66], two cognitive management entities are introduced on both the terminal and network infrastructure sides to manage relevant knowledge about the environment. According to this architecture, most of the cognitive management functionalities are executed in a centralized manner on the network infrastructure side with support from the terminal side. Specifically, as illustrated in Figure 2.2, the execution involves the following entities:

1. The knowledge management entity, which is responsible for storing and managing the relevant knowledge obtained from the radio environment that will be used by the decision-making entity. It is composed of a knowledge manager (KM) that monitors the suitability of existing spectral resources to support the set of heterogeneous application requirements. The KM mon-

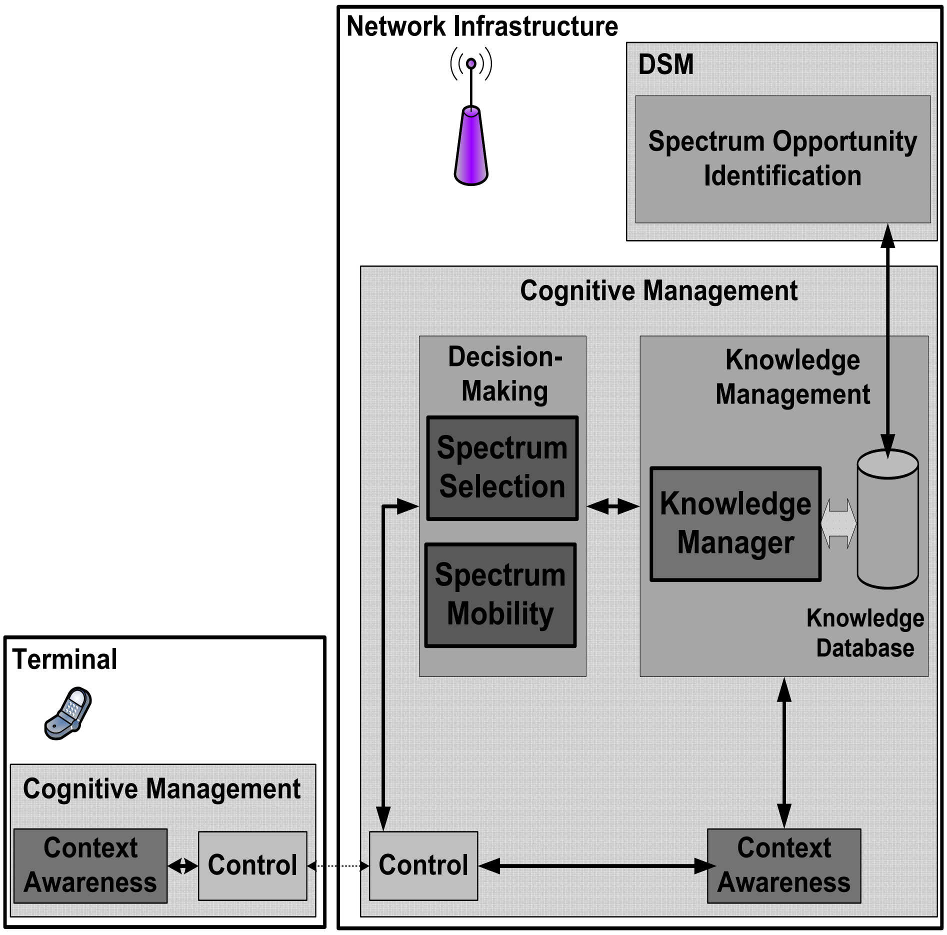

Figure 2.2: Functional architecture of the proposed cognitive management framework for spectrum management

itoring is based on information retrieved from a knowledge database (KD) that stores a set of relevant statistics about the environment and the list of available spectrum pools (*Av_Pools*).

2. The decision-making entity, which is responsible for assigning the appropriate pools to established radio links. For that purpose, it interacts with the KM that will provide the relevant information for the decisions to be made. Decision-making is split into two functional entities: the SS functionality, which will pick up a up a suitable pool for each communication whenever a new request for establishing a given link arrives, and the SM functionality,

which will perform the reconfiguration of assigned pools whenever changes occur in the environment and better pools can be found for some links.

3. The context awareness (CA) entity, which is responsible for taking measurements on both the terminal and network infrastructure sides. Actual measurements of performance achieved in a given link when using a certain spectrum pool are exploited by the KM to support future SS decisions.

Finally, the control modules depicted in Figure 2.2 illustrate the need for control message exchange between the terminal and network infrastructure to support the diverse cognitive management mechanisms and procedures (e.g., the establishment/release of radio links and measurement reporting). The interested reader is referred to [67, 68] for details on possible implementation options of this exchange of control messages through the use of a cognitive control channel.

It is worth mentioning that the considered centralized setting mainly targets local environments (e.g., Digital Home) where access to a central point can be relatively easy. Nevertheless, the proposed framework also accepts decentralized or hybrid (e.g., centralized database for TV whitespace and decentralized for ISM band) architectures. In such scenarios, decision making functionalities (i.e., SS and SM) would be executed at each terminal based the support provided by a local knowledge management domain. More details about how to build such local knowledge management domains are given at the end of Section 2.2.

2.2 Knowledge management

2.2.1 Knowledge database

The KD stores the most relevant information about the environment to support DSA. In particular, two separate characterizations of spectral resources in the time and frequency domains are retained in the KD to support some of the DSA models proposed in Section 1.1.3. For a more general DSA setting, a set of statistical metrics exploiting both domains are proposed in Section 2.2.1.3.

2.2.1.1 Time domain

Assuming the OSA model described in Section 1.1.3.3.1, it is proposed to retain in the KD a set statistics to characterize the temporal variability of spectral resources due to the activity of PUs. These statistics can be classified into first-order metrics, such as means or conditional probabilities or higher-order metrics, such as variances or correlation functions. For each pool $p \in \{1,...,P\}$, the two discrete random sequences ON_p and OFF_p are introduced to denote the sequences of primary activity (ON) and inactivity (OFF) durations, respectively. At a given discrete time index j, $ON_p(j)$ and $OFF_p(j)$ correspond to the j-th successive ON and OFF durations, respectively. It is assumed for the sake of simplicity that primary activity time series are independent across pools.

To offer a high scalability, it is proposed to make most of statistics characterizing primary ON/OFF durations structured in buckets. A bucket contains all ON (alternatively OFF) durations falling in a given interval. Buckets for ON durations are numbered as $a \in \{1,...,|B_p^{ON}|\}$ so that $B_p^a \in B_p^{ON}$ denotes the $a-th$ bucket, B_p^{ON} the set of buckets and $|.|$ denotes the cardinality. The same would be for OFF durations numbered as $b \in \{1,...,|B_p^{OFF}|\}$, $B_p^b \in B_p^{OFF}$ denoting the $b-th$ bucket and B_p^{OFF} the set of buckets. Bucket length is assumed to be a fraction τ of the average value of the corresponding distribution. This means that, considering for instance OFF_p distributions, $\forall b \in \{1,...,|B_p^{OFF}|-1\}$, the bucket B_p^b is defined as

$$B_p^b = [(b-1) \cdot \tau \cdot E(OFF_p), b \cdot \tau \cdot E(OFF_p)[\tag{2.1}$$

where $E(OFF_p)$ denotes the average value of OFF_p. The last bucket $B_p^{|B_p^{OFF}|}$ is assumed to be infinite of the form $[(|B_p^{OFF}| - 1) \cdot \tau \cdot E(OFF_p), \infty[$.

Based on the above considerations, a wide range of possible statistics of interest could be retained in the KD. For example, for each $p \in \{1, \ldots, P\}$, the following metrics can be extracted during a given acquisition time (acq_{time}):

- Average value of ON and OFF durations, $E(ON_p)$ and $E(OFF_p)$. The corresponding DC (Duty Cycle) can be therefore estimated as:

$$DC_p = \frac{E(ON_p)}{E(ON_p) + E(OFF_p)} \tag{2.2}$$

- Variances of ON and OFF durations, $VAR(ON_p)$ and $VAR(OFF_p)$.
- The empirical probability density function (PDF) of ON_p:

$$pdf_{ON}^{p}(B_p^a) = Prob\left[ON_p(j){\in}B_p^a\right], \forall a{\in}\{1,\ldots,|B_p^{ON}|\} \tag{2.3}$$

- The empirical PDF of OFF_p:

$$pdf_{OFF}^{p}(B_p^b) = Prob\left[OFF_p(j){\in}B_p^b\right], \forall b{\in}\{1,\ldots,|B_p^{OFF}|\} \tag{2.4}$$

- The conditional probability of observing certain OFF duration given that certain ON duration was observed. Specifically, $CP_{OFF,ON}^{p}(B_p^b, B_p^a)$ is defined as the conditional probability of observing OFF_p in $B_p^b{\in}B_p^{OFF}$ given that the last outcome of ON_p was observed in $B_p^a{\in}B_p^{ON}$:

$$CP_{OFF,ON}^{p}(B_p^b, B_p^a){=}Prob\left[OFF_p(j){\in}B_p^b/ON_p(j){\in}B_p^a\right] \tag{2.5}$$

- A proposed measure of dependence level between successive ON/OFF durations defined as

$$DEP_p{=}\frac{1}{|B_p^{ON}|}\sum_{B_p^a{\in}B_p^{ON}}\max_{B_p^b{\in}B_p^{OFF}}\left(\delta_{a,b}{\cdot}CP_{OFF,ON}^{p}(B_p^b, B_p^a)\right) \tag{2.6}$$

where $\forall a{\in}\{1,\ldots,|B_p^{ON}|\}$ and $\forall b{\in}\{1,\ldots,|B_p^{OFF}|\}$, $\delta_{a,b}$ is a dependence indicator between B_p^a and B_p^b defined as

$$\delta_{a,b} = \begin{cases} 1 & \text{if } CP_{OFF,ON}^{p}(B_p^b, B_p^a) > pdf_{OFF}^{p}(B_p^b), \\ 0 & \text{otherwise.} \end{cases} \tag{2.7}$$

Note that only those buckets B_p^a such that $pdf_{ON}^{p}(B_p^a){\neq}0$ are considered in B_p^{ON} when calculating DEP_p in (2.6). The value of DEP_p will range from 0, corresponding to the case where ON and OFF durations are independent, to 1, corresponding to the case in which the OFF duration is totally known from preceding ON duration.

- The conditional mean of OFF_p given the last outcome of ON_p was observed in bucket $B_p^a \in B_p^{ON}$ defined as follows

$$E(OFF_p/ON_p \in B_p^a) = \sum_{B_p^b \in B_p^{OFF}} \hat{B}_p^b \cdot CP^p_{OFF,ON}(B_p^b, B_p^a) \tag{2.8}$$

where $\hat{B}_p^b$ is the center value of bucket B_p^b which is given by $\hat{B}_p^b = (b - 0.5) \cdot \tau \cdot E(OFF_p)$.

Depending on primary activity characteristics, useful knowledge about PUs can be inferred thanks to some of the above metrics. For instance, in case $VAR(OFF_p) = 0$ is observed, a deterministic primary inactivity pattern can be inferred, and e.g., $E(OFF_p)$ would provide full estimation of primary OFF durations. In the more general case, $E(OFF_p)$ may not be the best choice for characterizing OFF durations if there are some patterns involving ON/OFF durations (e.g., dependencies between consecutive ON/OFF durations or between two successively observed OFF durations). In this respect, DEP_p can be for instance used to evaluate how dependent consecutive ON/OFF durations are. The observation of a high DEP_p value indicates that $E(OFF_p/ON_p \in B_p^a)$ would provide a much better estimator of actual OFF durations.

2.2.1.2 Frequency domain

To assess the suitability of spectral resources to meet the requirements of the different applications, the so-called "fittingness factor" ($F_{l,p}$) was introduced in [69] as a metric capturing how suitable each p-th spectrum pool is for the application supported by the l-th radio link. $F_{l,p}$ assesses the suitability in terms of the bit rate that can be achieved while operating in the spectrum pool p (denoted as $R(l,p)$) versus the bit rate required by the corresponding application ($R_{req,l}$).

From a general perspective, the fittingness factor can be formulated as a function of the utility $U_{l,p}$ that the l-th link can obtain from the p-th pool, where the utility is defined as [70]:

$$U_{l,p} = \frac{\left(\frac{R(l,p)}{R_{req,l}}\right)^{\xi}}{1 + \left(\frac{R(l,p)}{R_{req,l}}\right)^{\xi}} \tag{2.9}$$

where ξ is a shaping parameter that allows the function to capture different degrees of elasticity of the application with respect to the required bit rate. The achievable bit rate by link l using pool p ($R(l,p)$) will depend on the total noise and interference power spectral density (PSD) I_p experienced in each pool p.

Based on the above concept, two different fittingness factor functions are defined:

- Fittingness factor function #1: It is the utility itself, that is:

$$F_{l,p}=f_1(U_{l,p})=U_{l,p} \tag{2.10}$$

  Let us note that $f_1(U_{l,p})$ is a monotonically increasing function of the ratio $R(l,p)/R_{req,l}$.

- Fittingness factor function #2: It is defined as:

$$F_{l,p}=f_2(U_{l,p})=\frac{1-e^{-\frac{K\cdot U_{l,p}}{\frac{R(l,p)}{R_{req,l}}}}}{\lambda} \tag{2.11}$$

  where K is a shaping parameter and λ is a factor that normalizes the maximum of the fittingness factor to one that is given by:

$$\lambda = 1-e^{-\frac{K}{(\xi-1)^{\frac{1}{\xi}}+(\xi-1)^{\frac{1-\xi}{\xi}}}} \tag{2.12}$$

To illustrate the behavior of the proposed fittingness factor functions, Figure 2.3 plots both $f_1(U_{l,p})$ and $f_2(U_{l,p})$ functions for ξ=5 and K=1. While $f_1(U_{l,p})$ monotonically increases with the bit rate $R(l,p)$, $f_2(U_{l,p})$ increases up to the maximum at $R(l,p)=\sqrt[\xi]{\xi-1}\cdot R_{req,l}$, and then decreases. This behavior of $f_2(U_{l,p})$ reduces the value of the fittingness factor whenever the available bit rate is much higher than the required one, thus resulting in a more efficient usage of spectral resources than just considering $f_1(U_{l,p})$.

In order to characterize the suitability of a given pool p to a given link l based on the history of using this pool, it is proposed to retain in the KD observed $F_{l,p}$ values based on measurements extracted from the radio environment. In particular, the measurement of $R(l,p)$ of active link/pool pairs will be obtained, from which the current value of $F_{l,p}$ will be computed according to (2.10) or (2.11), and stored in the database together with a timer indicating elapsed time since the measurement was obtained ($\Delta k_{l,p}$).

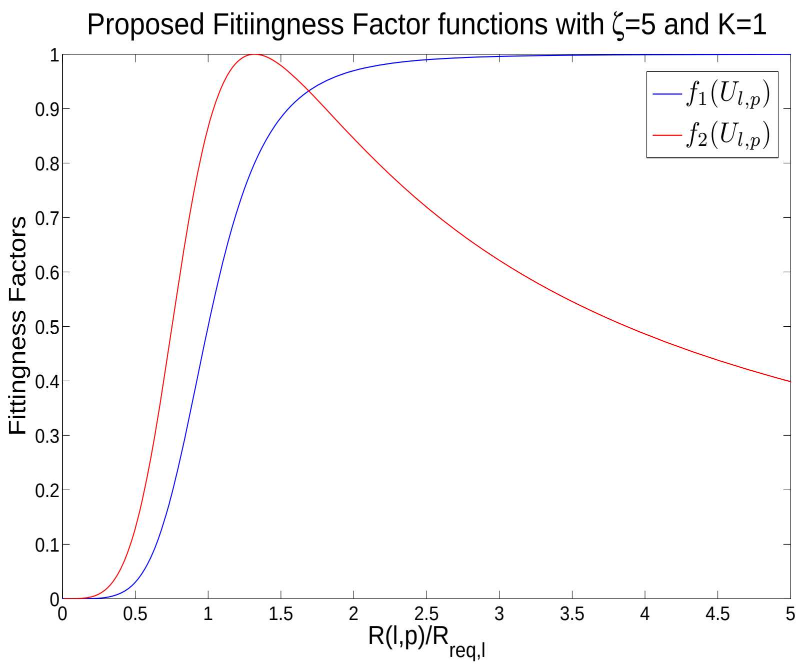

Figure 2.3: Behavior of fittingness factor functions with ξ=5 and K=1.

2.2.1.3 Combined time and frequency domains

In order to jointly capture temporal and spectral variability of spectrum pools, it is proposed to retain in the KD a set of statistics characterizing the fittingness factor behavior observed during acq_{time}. It is assumed that $F_{l,p}$ values may jump between two states, LOW ($<\delta_{l,p}$) or HIGH ($\geq\delta_{l,p}$), due to changes in radio and interference conditions. Depending on the considered DSA model, these changes may be the result of e.g., activity of some external interferers or PUs for the open sharing and OSA models described in Section 1.1.3, respectively. Assuming a stationary behavior of the different pools during system operation, the following statistics are generated and stored in the KD based on the previously obtained measurements of $R(l,p)$ and $F_{l,p}$:

- The probability $P_L^{l,p}(\delta_{l,p})$ of observing a LOW fittingness factor:

$$P_L^{l,p}(\delta_{l,p}){=}Prob\left[F_{l,p}{<}\delta_{l,p}\right] \tag{2.13}$$

- The probability $P_H^{l,p}(\delta_{l,p})$ of observing a HIGH fittingness factor is then given by:

$$P_H^{l,p}(\delta_{l,p}){=}1{-}P_L^{l,p}(\delta_{l,p}) \tag{2.14}$$

- The average of observed LOW fittingness factor values:

$$\overline{F_L^{l,p}}{=}E\left(F_{l,p}|F_{l,p}{<}\delta_{l,p}\right) \tag{2.15}$$

where $E(X)$ denotes the expected value of random variable X.

- The average of observed HIGH fittingness factor values:

$$\overline{F_H^{l,p}}{=}E\left(F_{l,p}|F_{l,p}{\geq}\delta_{l,p}\right) \tag{2.16}$$

Furthermore, to monitor fittingness factor variability, the following statistical metrics are considered to determine the extent to which the state of the fittingness factor is likely to remain constant for a certain time n:

- Given $F_{l,p}$ is LOW at a given time instant k, the probability that $F_{l,p}$ will be LOW at each time instant up to time $k{+}n; n{\in}\mathbb{N}$ defined as follows:

$$P_{L,L}^{l,p}(n,\delta_{l,p}){=}Prob\left[F_{l,p}(k+j){<}\delta_{l,p},\forall j{\in}\{1,\ldots,n\}|F_{l,p}(k){<}\delta_{l,p}\right] \tag{2.17}$$

where $F_{l,p}(k)$ denotes the observed $F_{l,p}$ value at time k.

- Given $F_{l,p}$ is HIGH at a given time instant k, the probability that $F_{l,p}$ will be HIGH at each time instant up to time $k{+}n; n{\in}\mathbb{N}$ defined as follows:

$$P_{H,H}^{l,p}(n,\delta_{l,p}){=}Prob\left[F_{l,p}(k+j){\geq}\delta_{l,p},\forall j{\in}\{1,\ldots,n\}|F_{l,p}(k){\geq}\delta_{l,p}\right] \tag{2.18}$$

2.2.2 Knowledge manager

The KM plays a key role between the knowledge management and decision-making domains of the proposed architecture. It manages the information retained in the KD to determine which information about the environment is most relevant to the decision-making entity in both the temporal and spectral domains.

2.2.2.1 Time domain

In the time domain, the KM keeps, an estimate of remaining OFF duration for each idle pool p based on different subsets of KD statistics. In this respect, a first estimator subtracts the so-far observed OFF duration (denoted as Obs_OFF^p) from an estimation of actual OFF duration ignoring all dependence effects as follows:

$$Rem\_OFF_1^p = E(OFF_p) - Obs\_OFF^p \tag{2.19}$$

Next, assuming that last ON_p duration falls in bucket B_p^a , a second estimator subtracts so-far observed OFF duration from an estimation of actual OFF duration given last observed ON duration as follows:

$$Rem\_OFF_2^p = E(OFF_p / ON_p \in B_p^a) - Obs\_OFF^p \tag{2.20}$$

2.2.2.2 Frequency domain

In the frequency domain, the KM keeps an estimation of $F_{l,p}$ values based on available statistics at the KD. These estimated values, denoted as $\hat{F}_{l,p}$, are obtained following Algorithm 2.1, and are provided upon request to the decision-making module. The estimate $\hat{F}_{l,p}$ is determined based on whether the state of the $F_{l,p}$ stored in the KD is likely to be the same that was obtained $\Delta k_{l,p}$ time units before (this criterion is checked on lines 5 and 11 with respect to the significance thresholds Thr_LOW and Thr_HIGH, respectively). In such case, $\hat{F}_{l,p}$ is set to the last measured $F_{l,p}$ value (lines 6 and 12). Otherwise, $\hat{F}_{l,p}$ is randomly set to either $\overline{F_L^{l,p}}$ or $\overline{F_H^{l,p}}$, i.e., the average $F_{l,p}$ values in the LOW and HIGH states, respectively, with probabilities $P_L^{l,p}(\delta_{l,p})$ and $1 - P_L^{l,p}(\delta_{l,p})$ (lines 8 and 14). Once all link/pool pairs have been explored, the list of all estimated fittingness factor values ($\{\hat{F}_{l,p}\}_{1 \le l \le L, 1 \le p \le P}$) is returned back to the decision-making entity (line 19).

The KM also captures relevant changes in these estimated values and informs the decision-making module for its consideration.

The knowledge management domain may also be applied to decentralized architectures. For such scenarios, a local KD can be constructed at each of the terminals. The local KD would retain the last observed ON_p and $F_{l,p}$ values together with

Algorithm 2.1 Knowledge Manager

Knowledge Manager
for l=1 $\rightarrow L$ **do**
    for p=1 $\rightarrow P$ **do**
        if $F_{l,p}$ is LOW **then**
            if $P^{l,p}_{L,L}(\Delta k_{l,p}, \delta_{l,p}) \geq Thr\_LOW$ **then**
                $\hat{F}_{l,p} \leftarrow F_{l,p}$;
            else
                Estimate $F_{l,p}$ as follows:

$$\hat{F}_{l,p} = \begin{cases} \overline{F^{l,p}_{L}} & \text{with probability } P^{l,p}_{L}(\delta_{l,p}), \\ \overline{F^{l,p}_{H}} & \text{with probability } 1\text{-}P^{l,p}_{L}(\delta_{l,p}). \end{cases}$$

            end if
        else
            if $P^{l,p}_{H,H}(\Delta k_{l,p}, \delta_{l,p}) \geq Thr\_HIGH$ **then**
                $\hat{F}_{l,p} \leftarrow F_{l,p}$;
            else
                Estimate $F_{l,p}$ as follows:

$$\hat{F}_{l,p} = \begin{cases} \overline{F^{l,p}_{L}} & \text{with probability } P^{l,p}_{L}(\delta_{l,p}), \\ \overline{F^{l,p}_{H}} & \text{with probability } 1\text{-}P^{l,p}_{L}(\delta_{l,p}). \end{cases}$$

            end if
        end if
    end for
end for
return $(\{\hat{F}_{l,p}\}_{1 \leq l \leq L, 1 \leq p \leq P})$;

the list of statistics defined in Sections 2.2.1.1 and 2.2.1.3 obtained based on local observations made by each terminal. For small neighborhoods with homogeneous interference conditions, each terminal may cooperate with its neighbors via context awareness modules to get the most recent ON_p and $F_{l,p}$ values observed in the neighborhood together with the timer $\Delta k_{l,p}$. Then, the KM can be executed at each of these terminals to determine local $Rem\_OFF^p_1$, $Rem\_OFF^p_2$ and $\hat{F}_{l,p}$ estimates based on local KD statistics.

2.3 Decision making

2.3.1 Spectrum selection

The SS functionality will be executed every time the start of a new application requires the establishment of a radio link to support communication. Figure 2.4 presents the Message Sequence Chart (MSC) associated with the execution of this functionality at the establishment of link l. The control module on the terminal side sends a link establishment request (*LinkEst_REQ(link l)*) to its counterpart on the network infrastructure side. The latter asks the SS entity to provide a suitable pool for that link (*SpPool_REQ(link l)*). Then, the SS entity asks the KM for a relevant information about all pools by sending the *INFO_REQ(link l, all pools)* message. The response is carried in the *INFO_RSP(Info)* message, where *Info* may contain an estimation of remaining primary OFF durations ($\{Rem\_OFF_1^p\}_{1\leq p\leq P}$ and $\{Rem\_OFF_2^p\}_{1\leq p\leq P}$) or fittingness factor values ($\{\hat{F}_{l,p}\}_{1\leq p\leq P}$). Based on provided information, the SS algorithm is executed. The SS process is completed when the selected pool $p^*(l)$ is communicated to the control module on the network infrastructure side (*SpPool_RSP(pool* $p^*(l)$*)*), and then forwarded to its counterpart on the terminal side (*LinkEst_RSP(pool* $p^*(l)$*)*).

2.3.2 Spectrum mobility

The SM functionality attempts to ensure highly efficient allocation of available spectrum pools to each of the established radio links. Therefore, whenever an event that might have influence on the SS decision-making process occurs, the SM will be executed. Such events include (1) a spectrum pool being released due to finalization of the corresponding application, or (2) a change in the suitability of used spectrum pools being detected caused by e.g., appearance of some external source of interference or PU for the open sharing and OSA models described in Section 1.1.3, respectively.

As an example, Figure 2.5 describes the process involving SM due to radio link release. Upon the release of a given link l, the control module on the terminal side

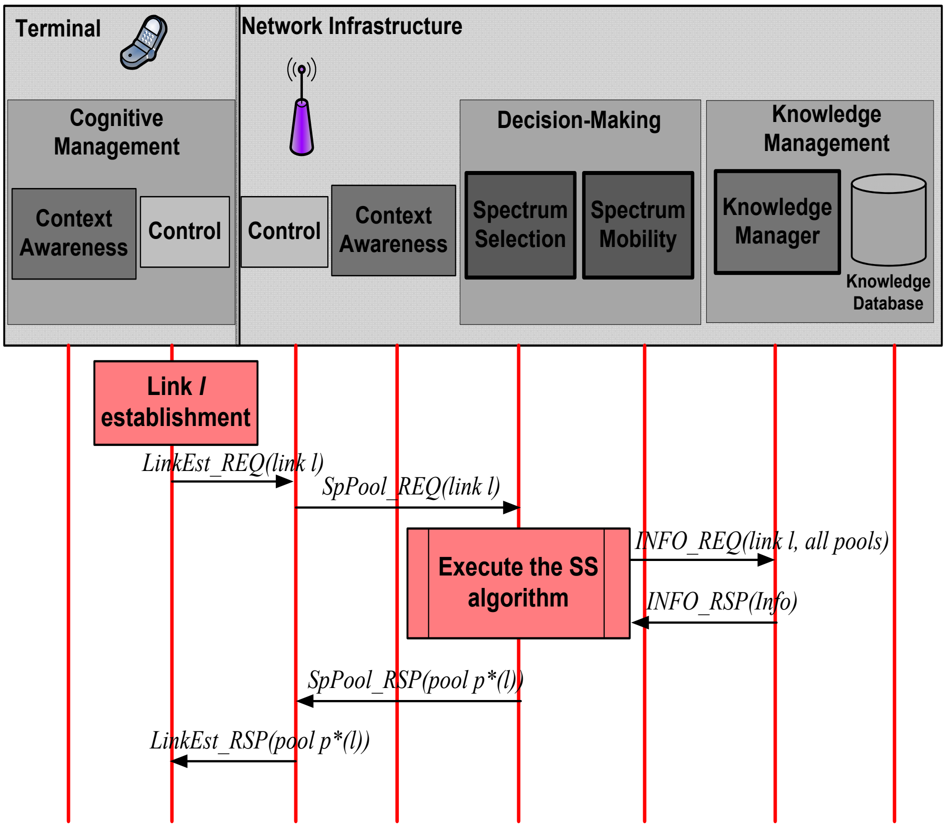

Figure 2.4: MSC for SS at the establishment of radio link l

informs its counterparts on the network infrastructure side (*LinkRelease_REQ(link l)*). In turn, the latter asks the SS entity to release the corresponding pool (*SpPool_REL(link l, pool* $p^*(l)$)) and informs its counterpart on the terminal side once complete (*LinkRelease_RSP(link l)*). If better pools can be found for some links, the SS entity asks the SM entity to perform a spectrum reconfiguration (*Trigger*). To achieve that, the SM entity consults the KM to obtain a relevant information about all links/pools (*INFO_REQ(all links, all pools)*). The response is carried in the *INFO_RSP(Info)* message, where *Info* may contain an estimation of remaining primary OFF durations ($\{Rem\_OFF_1^p\}_{1\leq p\leq P}$ and $\{Rem\_OFF_2^p\}_{1\leq p\leq P}$) or fittingness factor values ($\{\hat{F}_{l,p}\}_{1\leq l\leq L,1\leq p\leq P}$). Based on provided information, the SM algorithm is executed and links/pools to be reconfigured are indicated to the control module on the network infrastructure side (*SpPool_Reconfig(link* l^**, pool* p^*)). For each of these link/pool pairs, the control module on the terminal side is asked

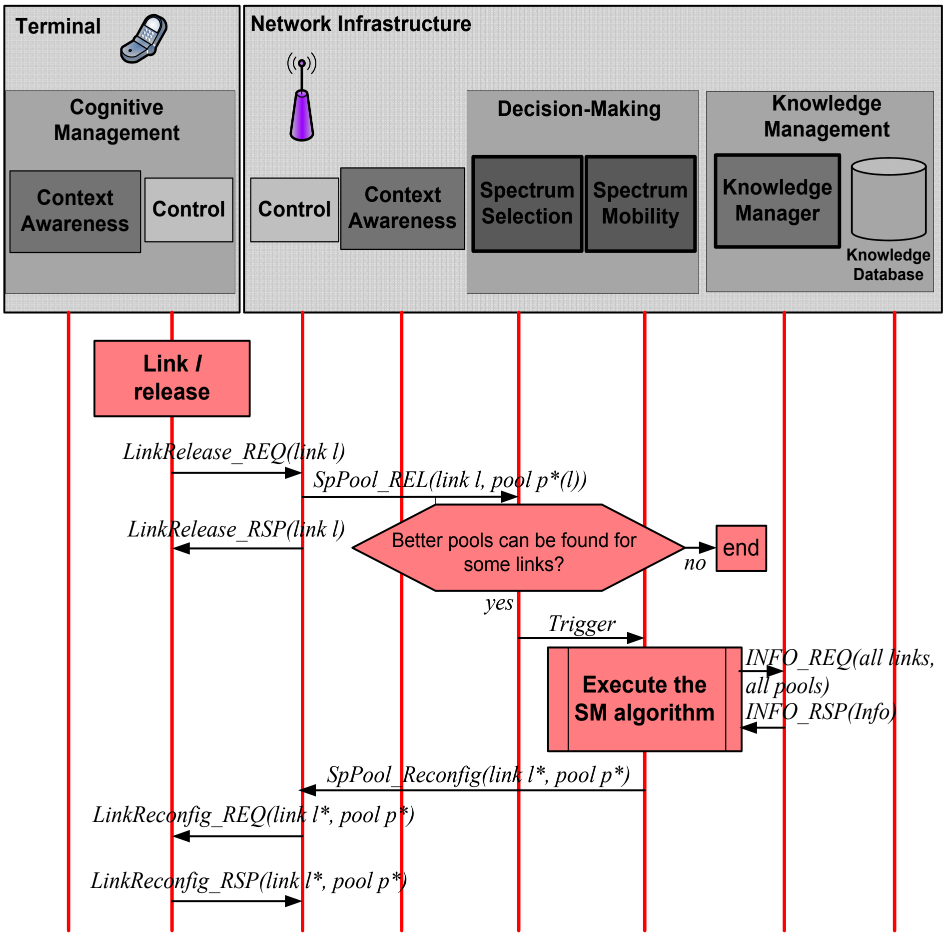

Figure 2.5: MSC for SM due to the release of radio link l

to execute the reconfiguration decision (*LinkReconfig_REQ(link* l^**, pool* p^**)*). Once this decision is made, an acknowledgment is sent back to the counterpart on the network infrastructure side (*LinkReconfig_RSP(link* l^**, pool* p^**)*).

2.4 Context awareness

The CA functional entity is of major importance to enable the network infrastructure domain to assess the actual conditions experienced by the different applications over the established radio links. This assessment ability enables the cognitive cycle to be closed and the decision-making processes on the infrastructure side (e.g., SM) to react to any change, thus allowing for a highly efficient allocation of radio

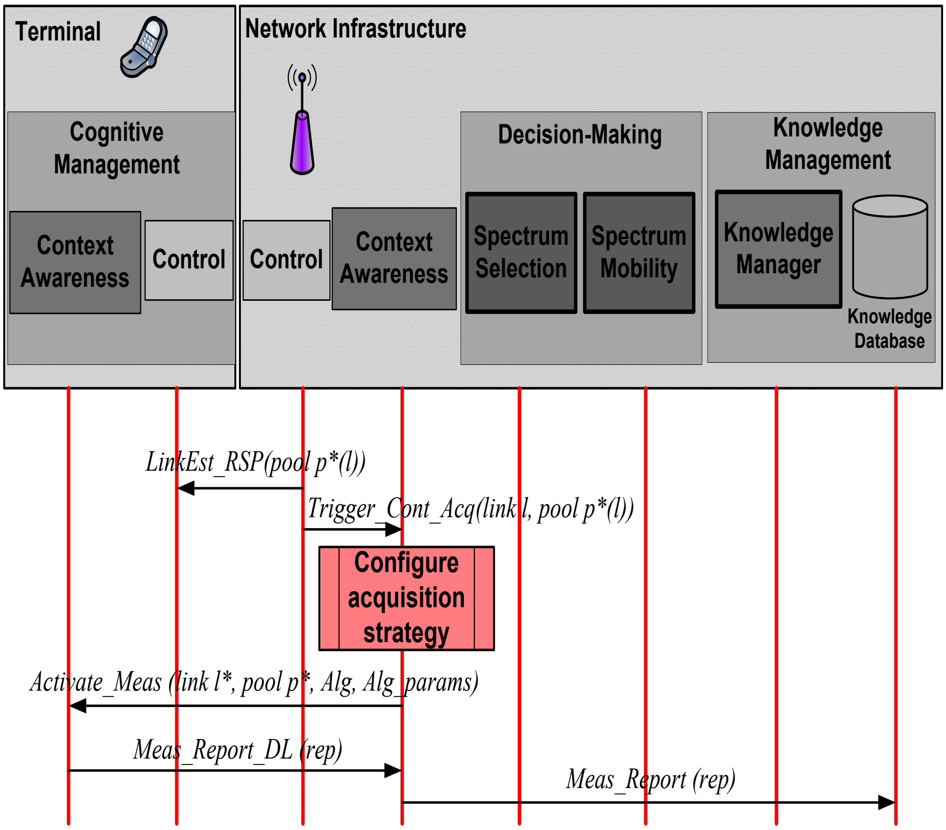

Figure 2.6: MSC for the configuration of measurements at link establishment

resources.

In particular, at link establishment, the network infrastructure side decides an acquisition strategy depending on the dynamics of the radio environment. As shown in Figure 2.6, after communicating the selected pool $p^*(l)$ to its counterpart on the terminal side (*LinkEst_RSP(pool* $p^*(l)$*)*), the control module on the network infrastructure side asks its associated CA module to trigger a context acquisition strategy (*Trigger_Cont_Acq(link l, pool* $p^*(l)$*)*). The latter configures the acquisition strategy, and asks its counterpart on the terminal side to activate a set of measurements according to the configured strategy (*Activate_Meas(link* l^**, pool* p^**, Alg, Alg_params)*), where *Alg* and *Alg_params* denote the considered acquisition strategy algorithm and its optional set of parameters, respectively. These measurements are later reported by the CA module on the terminal side (*Meas_-Report_DL(rep)*), where *rep* may contain last observed primary ON_p durations or

$F_{l,p}$ values, and then combined with the measurements performed on the network infrastructure side before being sent to the KD (*Meas_Report(rep)*).

2.5 Chapter summary

A cognitive management framework has been constructed to support spectrum management in CRNs. The proposed framework relies on a standalone knowledge management domain that stores and manages a characterization of spectrum pools at both the time and frequency dimensions out of the decision-making domain. It is composed of a KM that monitors the suitability of existing spectral resources to support a set of heterogeneous CR applications. The KM monitoring is based on information retrieved from a KD that stores a set of relevant statistics about the environment. At the time dimension, the KM determines two dependence-based and dependence-free estimates of remaining OFF durations based on a set of statistical patterns stored in the KD to capture dependence structures between primary ON/OFF durations. At the frequency dimension, the KM determines an estimate of fittingness factor values based on a set of advanced statistics stored in the KD. To enable the applicability of the proposed framework to various scenarios and case studies, the required signaling messages between the knowledge management and decision making domains have been described in a generic way through a set of MSCs.

3. Proposed Algorithmic Solution: Exploiting the Time Dimension for Opportunistic Spectrum Access to Licensed Bands

This chapter proposes to exploit the time domain spectrum characterization provided by the KM to support an OSA-type access to licensed bands. In particular, the aim is to determine a proper SS criterion to pick up the best spectrum pool for SUs subject to not causing any harmful interference for PUs. While this problem accepts some mathematical formulation, the dynamism in the radio environment, the heterogeneity in PU types as well as SU traffic types and the fact that previous SS decisions condition future selections suggest, on the one side, that a heuristic approximation can be initially suitable in order to gain insight into the problem and devise the main principles to follow. On the other side, one can anticipate that the formulation of a comprehensive and general SS strategy is complex, since there will not be a single SS criterion that will result suitable in the wide range of different scenarios and configurations that may arise in practice. Therefore, the methodology followed in this chapter is two-step: firstly, a set of SS criteria are proposed in Section 3.1 and the main principles to drive SS are assessed in Section 3.2.3 to derive their main dependencies with other system parameters. Based on this assessment, the proposed SS criteria are compared in Section 3.2.4, and a generic SS strategy combining them is formulated in Section 3.2.5.

3.1 Proposed SS criteria

The estimates of remaining OFF durations provided by the KM will be considered in the SS decision-making process. One can expect that this knowledge can be beneficial with respect to a first reference SS criterion (*Rand*) where a random selection among idle pools is simply performed. The option *Rand* would be a reasonable criterion in case that there would not be a KD supporting the cognitive system and providing knowledge about PUs.

Apart from the reference random selection, two SS criteria exploiting differently the KM support are proposed in the following.

3.1.1 Blind proactive

To minimize disturbance caused by primary activity, a pro-active approach defining the best pool as the one that results in the least-likelihood for the appearance of a PU is proposed. In this respect, a criterion that maximizes estimated remaining OFF duration ignoring all dependence effects is defined as follows ($Crit_1$):

$$p^*_{Crit_1}(l) = \arg\max_{p \in Av\_Pools} (Rem\_OFF^p_1) \tag{3.1}$$

where $p^*(l)$ denotes the selected pool for link l.

Next, a dependence-based SS criterion that selects the pool whose estimated remaining OFF duration is maximized given last observed ON duration is proposed as follows ($Crit_2$):

$$p^*_{Crit_2}(l) = \arg\max_{p \in Av\_Pools} (Rem\_OFF^p_2) \tag{3.2}$$

For both criteria, in the very specific case of multiple pools fulfilling the maximization, the pool with the lowest DC_p is selected.

3.1.2 Proactive matching of application requirements to spectral resources

The SS criteria proposed in Section 3.1.1 blindly maximize remaining OFF duration for each established radio link regardless of the corresponding application. Nevertheless, it may be of interest to match selected spectrum pools to the requirements of CR applications. In this respect, two SS criteria selecting the pool whose remaining OFF duration estimate fits better application duration ($T_{req,l}$) are proposed as follows:

$$p^*_{Crit_3}(l) = \arg \min_{p \in Av\_Pools} |Rem\_OFF^p_1 - T_{req,l}| \tag{3.3}$$

$$p^*_{Crit_4}(l) = \arg \min_{p \in Av\_Pools} |Rem\_OFF^p_2 - T_{req,l}| \tag{3.4}$$

While $Crit_3$ estimates remaining OFF duration regardless of dependence effects, $Crit_4$ estimates it given last observed ON duration.

Note that unlike the blind proactive criteria proposed in Section 3.1.1 ($Crit_1$ and $Crit_2$), both $Crit_3$ and $Crit_4$ take into account characteristics of CR applications to choose a spectrum pool whose remaining OFF duration fits with $T_{req,l}$. This proactive matching aims at preventing that some CR applications use those pools that might be more suitable for others.

3.2 Evaluation study

To validate the proposed methodology, a controllable primary traffic pattern is proposed to characterize the activity of PUs. The main principles for estimating primary OFF durations are assessed for different instances of the proposed pattern. Based on this assessment, performances of the proposed SS criteria are compared for various combinations of primary traffic patterns and secondary configurations. Enlightened by this comparative study, an integrated strategy is developed.

3.2.1 Assumptions

In order to model primary traffic, λ_p^P and μ_p^P respectively denote the primary arrival and departure rates in each pool $p\in\{1,...,P\}$. As for secondary operation, the mean holding time of the l-th application ($T_{req,l}$) will be kept constant while varying the corresponding arrival rate (denoted as λ_l^L). To focus on the impact of temporal variability of spectrum resources, it is assumed that the bandwidth BW_p of all pools $p\in\{1,...,P\}$ is enough to meet all link requirements $R_{req,l}$. The status of pools is obtained based on a periodic sensing performed each $\Delta S[s]$. For the sake of simplicity, sensing is assumed to be free of miss-detections and false alarms. In the case a PU shows up in any of the opportunistically-accessed pools, the involved link will be handed-over to another pool if there is any, or will be dropped if there is no pool available. The effect of bucket configuration is studied in Annex A, where an operating configuration that strikes a balance between statistics accuracy and computational complexity is determined. It corresponds to $N_B^{opr}=|B_p^{ON}|=|B_p^{OFF}|=31$ and $\tau^{opr}=0.1$.

3.2.2 Primary activity time series

To assess relevance of the time domain characterization provided by the KM and evaluate the resulting SS performance, a controllable primary traffic time series is introduced for each pool $p\in\{1,...,P\}$ for different levels of randomness variability. Specifically, the sequence $\{ON_p\}_{1\leq p\leq P}$ is assumed to be $unif([ON_p^{min}, ON_p^{max}])$ or $expo(ON_p^{mean})$, where $unif[a,b]$ and $expo(x)$ denote random sequences uniformly distributed in the range $[a,b]$ and exponentially distributed with mean x, respectively. Then, at a given time index j, OFF duration is generated based on preceding ON duration $ON_p(j)$ as follows:

$$OFF_p(j) = \begin{cases} q\cdot f(ON_p(j))+(1-q)\cdot unif([OFF_p^{min}, OFF_p^{max}]) & \text{(uniform)} \\ q\cdot f(ON_p(j))+(1-q)\cdot expo(OFF_p^{mean}) & \text{(exponential)} \end{cases} \tag{3.5}$$

where $0{\leq}q{\leq}1$ is a probability that controls how dependent successive ON/OFF durations are, and the function f is defined as:

$$f(x) = \begin{cases} OFF_p^{min} + \frac{(x - ON_p^{min})\cdot(OFF_p^{max} - OFF_p^{min})}{ON_p^{max} - ON_p^{min}} & \text{(uniform)} \\ x \cdot \frac{OFF_p^{mean}}{ON_p^{mean}} & \text{(exponential)} \end{cases} \quad (3.6)$$

With these definitions, the sequence $\{OFF_p\}_{1\leq p\leq P}$ is equally distributed regardless of q, and $DEP_p{=}q$ for all $p{\in}\{1,\ldots,P\}$ (See proof in Annex B).

In what follows, it is assumed that KD statistics have achieved a good level of convergence. The reader is referred to Section 6.1.1 for a detailed analysis of the convergence times needed for the different KD statistics.

3.2.3 Assessment of principles for estimating primary OFF durations

This section aims at analyzing the key factors influencing estimation reliability of primary OFF durations.

At a given moment of secondary operation, Act_OFF^p is introduced to denote actual remaining OFF duration of a given pool $p{\in}\{1,\ldots,P\}$. The relative estimation error is defined as the difference between the dependence-based estimate of remaining OFF duration ($Rem\_OFF_2^p$) and actual duration (Act_OFF^p) relative to average OFF duration ($\frac{1}{\lambda_p^P}$):

$$error_{estim}^p{=}\lambda_p^P\cdot(Rem\_OFF_2^p{-}Act\_OFF^p) \quad (3.7)$$

Considering for instance a given pool with $\frac{1}{\lambda_p^P}{=}30\,s$ and $DC_p{=}0.5$, Figure 3.1 plots the histogram of $error_{estim}^p$ for different PU traffic patterns, characterized by the parameter q in the generation process described in Section 3.2.2. It is worth pointing that, for $q{=}0$, $E(OFF_p){=}E(OFF_p/ON_p{\in}B_p^a)$ and $Rem\_OFF_1^p{=}Rem\_OFF_2^p$, while for $q{=}1$, $Rem\_OFF_2^p$ becomes much more accurate than $Rem\_OFF_1^p$ because $E(OFF_p/ON_p{\in}B_p^a)$ gives actual OFF_p duration. This is clearly reflected in Figure 3.1, where for $q{=}0$, the rough estimation of remaining OFF durations results in an absolute value of the estimation error above

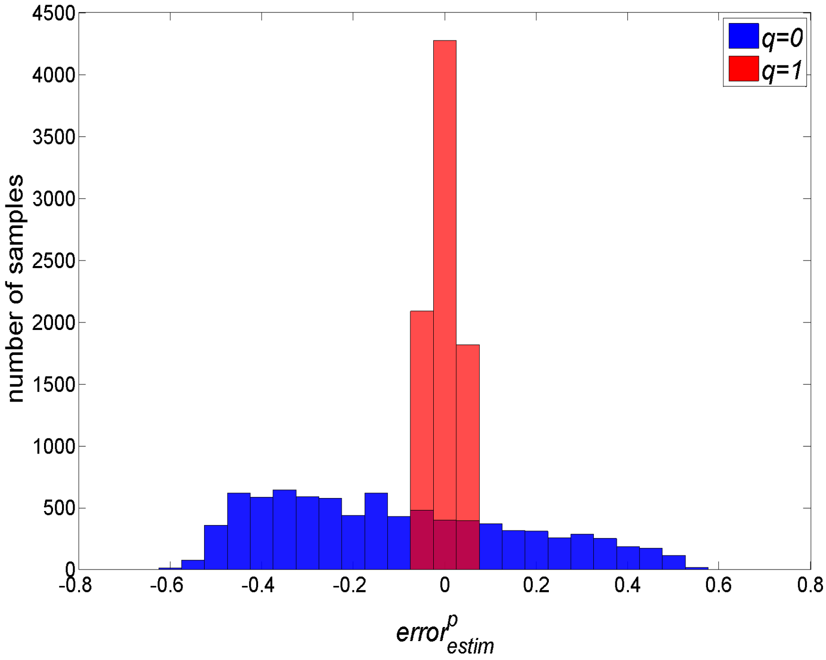

Figure 3.1: Estimation reliability of OFF periods, $\frac{1}{\lambda_p^P}$=30 s

0.3 about 50% of the time. On the contrary, for primary traffic sources exhibiting stronger dependence levels (i.e., q=1), the observed estimation error histogram concentrates to the origin because $E(OFF_p/ON_p{\in}B_p^a)$ exploits dependence between successive ON and OFF durations, thus making estimation much more accurate. Note that the fact that $error_{estim}^{P}{\neq}0$ for q=1 is due to the resolution of buckets. As a matter of fact, $error_{estim}^{P}$ tends to zero as buckets get squeezed (i.e., as τ gets smaller).

Given that estimation accuracy depends on the dependence level between ON/OFF durations and it can be different for each pool, it is proposed to introduce a compensation factor η_p in the dependence-based estimates of (3.2) and (3.4) so that the SS decision is not biased by the estimation error:

$$p^*_{Crit_2}(l){=}\arg \max_{p\in Av\_Pools} (\eta_p{\cdot}Rem\_OFF_2^p) \tag{3.8}$$

$$p^*_{Crit_4}(l){=}\arg \min_{p\in Av\_Pools} |\eta_p{\cdot}Rem\_OFF_2^p{-}T_{req,l}| \tag{3.9}$$

Table 3.1: Case study 1

	P	p	$\frac{1}{\mu_p^P}(s)$	$\frac{1}{\lambda_p^P}(s)$
PUs' parameters	16	1-4	15	60,27.8,15
		5-8	30	120,55.7,30
		9-12	60	240,111,60
		13-16	120	480,222.8,120
SUs' parameters	L	$\triangle S(s)$	$T_{req,l}(s)$	$\frac{1}{\lambda_l^L}(s)$
	1	0.1	6,24	6

3.2.4 Performance evaluation of spectrum selection criteria

This section discusses possible strategies to perform a proactive SS. In this respect, a comparative study between the proposed criteria is conducted for both the single- and multi-application contexts.

3.2.4.1 Single-application context

This section analyses the impact of KD statistics on the proposed SS criteria for the single-application context (L=1). The analysis considers only the blind proactive criteria proposed in Section 3.1.1 ($Crit_1$ and $Crit_2$) because there is no need to perform a matching for one single application. It is initially assumed for the sake of simplicity that η_p=1.

Performance is evaluated in terms of the number of SpHOs per secondary call because both $Crit_1$ and $Crit_2$ are pro-active in terms of SpHO events. The absolute performance gain of both criteria is defined as the percentage of reduction in the number of SpHOs with respect to *Rand*. Performance is analyzed for acq_{time}=15 h, where convergence has been achieved in most of the cases.

Considering the simulation parameters specified in Table 3.1 and a common duty cycle (DC_p=$DC, \forall p \in \{1, \ldots, P\}$) for the sake of simplicity, Figure 3.2 illustrates performances of all SS criteria with different primary/secondary traffic conditions for both fully-random (i.e., q=0) and fully-dependent (i.e., q=1) primary activity time series. As far as fully-random data are concerned, it is observed that

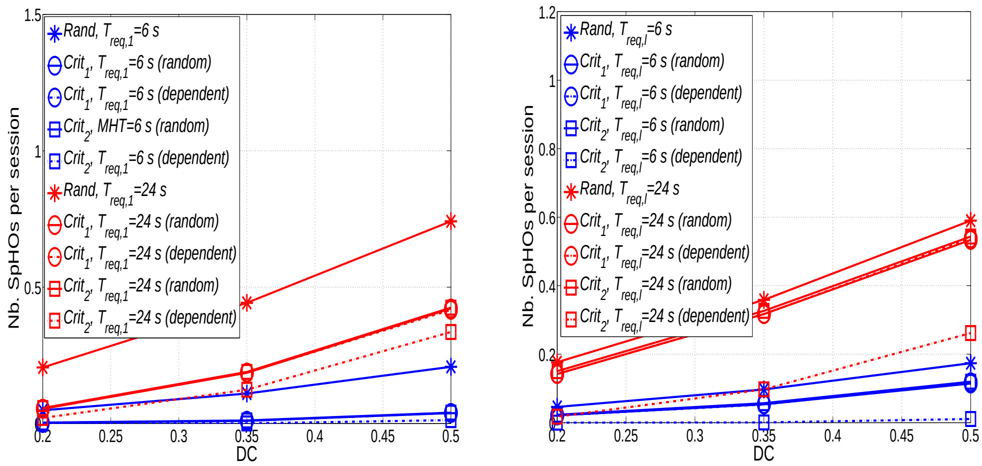

(a) (b)

Figure 3.2: Performance evaluation of SS criteria, single-application context with acq_{time}=15 h for (a) uniform occupancy time series and (b) exponential occupancy time series

both proactive criteria ($Crit_1$ and $Crit_2$) outperform the random selection (*Rand*) with equal gains. While $Crit_1$ outperforms *Rand* thanks to exploiting an estimation of remaining OFF durations, $Crit_2$ cannot further improve estimation accuracy because primary ON/OFF durations do not exhibit any useful dependence. As a matter of fact, free of any dependence $E(OFF_p){=}E(OFF_p/ON_p{\in}B_p^a)$ and $Rem\_OFF_1^p{=}Rem\_OFF_2^p$, so both $Crit_1$ and $Crit_2$ turn out to be the same.

Note that the introduced gains have different orders of magnitude depending on the considered distribution. While they range from 50% to 100% for uniform distributions (Figure 3.2(a)), they are between 10% and 50% for exponential distributions (Figure 3.2(b)). This is justified by the lower variability of uniform distributions, which makes both $E(OFF_p)$ and $E(OFF_p/ON_p{\in}B_p^a)$ reliable estimators of actual OFF durations as they do not deviate much from their means.

Considering next fully-dependent primary activity time series, it is observed that both *Rand* and $Crit_1$ are performing equally to the previous case, while $Crit_2$ succeeds in exploiting the increased dependence level to significantly outperform $Crit_1$. The absolute gain $Crit_2$ is introducing with respect to *Rand* ranges from 50% to 100% and is distributed differently for each of the considered distributions.

Table 3.2: Case study 2

	Parameter	Definition	Value
PUs	P	Number of pools	16
	$\frac{1}{\lambda_p^P}$	Average OFF period of pool p	15 s, $1 \leq p \leq 4$ 60 s, $5 \leq p \leq 16$
	$DC_p, \forall p \in \{1,..,P\}$	Duty Cycle	0.2
SUs	L	Number of links	2
	$T_{req,1}$	Mean holding time of link $\#1$	15 s
	$T_{req,2}$	Mean holding time of link $\#2$	60 s
	$\triangle S$	Sensing period	0.1 s

Specifically, the gain of $Crit_2$ with respect to $Crit_1$ is up to 15% of the absolute gain of $Crit_2$ (Figure 3.2(a)) for uniform distributions, while it reaches 70% for exponential data (Figure 3.2(b)).

3.2.4.2 Multi-application context

This section aims at getting an insight into the relevance of the proposed SS criteria as far as a multi-application secondary SS is concerned (i.e., L=2). Enlightened by the conducted analysis in Section 3.2.4.1, only the SS criteria based on the dependence-based estimate $Rem\_OFF_2^p$ are considered (i.e., $Crit_2$ and $Crit_4$). Considering the case study described in Table 3.2, performance of the proposed criteria is evaluated for different primary traffic patterns. Since the considered criteria are pro-active in terms of subsequent SpHO events, it is proposed to evaluate SS performance in terms of the overall SpHO rate (i.e. total number of SpHO/s). Note that even though the compensation factor η_p is in general a function of DEP_p, it is assumed for the sake of simplicity that η_p=0.95.

Figure 3.3 plots performances of $Crit_2$ and $Crit_4$ for the whole range of possible values of q for various secondary traffic mixes. For improved visualization, the figure is split into two sub-figures depending on the traffic load of each link l in Erlang (Er) defined as

$$L_l = \lambda_l^L \cdot T_{req,l} \tag{3.10}$$

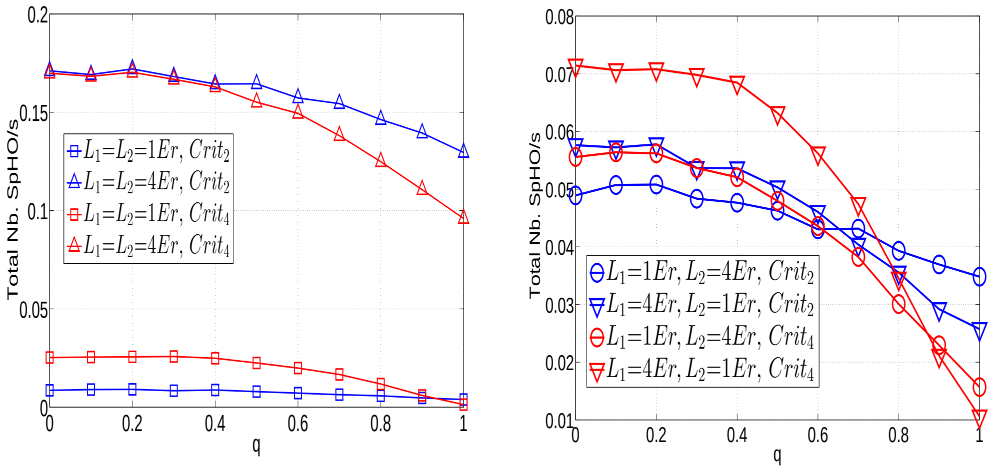

(a) (b)

Figure 3.3: Performance evaluation of SS criteria, multi-application context with (a) Extreme traffic loads and (b) Intermediate traffic loads

Specifically, Figure 3.3(a) and Figure 3.3(b) plot performances for extreme traffic loads (i.e. either low or high loads of both applications) and intermediate traffic loads, respectively. The corresponding performance of *Rand* is separately given by Table 3.3 because it is independent of q.

The first observation is that for all considered traffic loads, gains of $Crit_2$ and $Crit_4$ with respect to *Rand* are significant. Gains around 70% are observed for independent ON/OFF durations (i.e., q=0). As q increases, the accuracy of $E(OFF_p/ON_p \in B_p^a)$ in estimating OFF durations gets improved and gains increase up to 100%. Next, a comparison between $Crit_2$ and $Crit_4$ performances is performed.

3.2.4.2.1 Low traffic loads

The results show that for, low traffic loads of both applications (L_1=L_2=1 *Er*) (Figure 3.3(a)), $Crit_2$ is outperforming $Crit_4$ regardless of the dependence level at hand (q). This better performance is due to the fact that, at such low load conditions, there are often some available pools whose remaining OFF durations are longer than application duration $T_{req,l}$. The assignment of the largest $Rem\_OFF_2^p$

Table 3.3: SS performance of $Rand$

	$L_1(Er)$	$L_2(Er)$	Nb. SpHO/s
Extreme loads	1	1	0.66
	4	4	0.63
Intermediate loads	1	4	1.05
	4	1	0.51

estimate (i.e., $Crit_2$) selects the most available among these pools meaning that no subsequent SpHO will be experienced. On the contrary, assigning a pool whose $Rem\_OFF_2^p$ estimate fits $T_{req,l}$ (i.e., $Crit_4$) can result in more SpHOs if the reliability of OFF duration estimation in low. Specifically, as it has been observed in Section 3.2.3, for low dependence levels, $E(OFF_p/ON_p{\in}B_p^a)$ is just providing a rough estimation of actual OFF durations. This means that $Crit_4$ can assign link $\#1$ requests to pools whose remaining OFF duration were over-estimated and were wrongly supposed to tightly fit $T_{req,1}$. This increases the number of unnecessary SpHOs compared to $Crit_2$. As the dependence level q increases, the estimation reliability is improved, the number of unnecessary SpHOs performed by $Crit_4$ is reduced, and performances of $Crit_2$ and $Crit_4$ get closer.

3.2.4.2.2 High traffic loads

As far as high traffic loads are considered (L_1=L_2=4 *Er*) (Figure 3.3(a)), it is observed that $Crit_4$ outperforms $Crit_2$ for all dependence levels (q). At such high loads, it is less likely to find a pool whose remaining OFF duration fits $T_{req,l}$, which makes assigning pools to be switched-off in the future inevitable. This means that the wrong “fit” that may be performed by $Crit_4$ due to estimation inaccuracy is not likely to result in unnecessary SpHOs compared to $Crit_2$. On the contrary, the “fit” performed by $Crit_4$ tends to assign pools $\#1$-$\#4$ to link $\#1$ and pools $\#5$-$\#16$ to link $\#2$, which results in a better assignment.

3.2.4.2.3 Intermediate traffic loads

For intermediate traffic loads and mixes (Figure 3.3(b)), it is observed that relative performances of $Crit_2$ and $Crit_4$ strongly depend on the dependence level

Algorithm 3.1 Combined SS Strategy

1: $\{Rem\_OFF_2^p\}_{p\in\{1,\ldots,P\}} \longleftarrow \{0,\ldots,0\}$;
2: $Candidates \longleftarrow \emptyset$;
3: **for** $l{=}1 \rightarrow 2$ **do**
4: Send *INFO_REQ(link l, all pools)* to the KM;
5: Get *INFO_RSP(*$\{Rem\_OFF_2^p\}_{1\leq p\leq P}$*)* from the KM;
6: **if** $DEP{<}h(L_1, L_2)$ **then**
7: $Candidates \leftarrow \{p{\in}Av\_Pools/p{=}p^*_{Crit_2}(l)\}$;
8: **else**
9: $Candidates \leftarrow \{p{\in}Av\_Pools/p{=}p^*_{Crit_4}(l)\}$;
10: **end if**
11: $p^*_{strategy}(l) \leftarrow \arg\min_{p\in Candidates}(DC_p)$;
12: **end for**

q at hand. Specifically, for low dependence levels, $Crit_2$ is performing better, while $Crit_4$ is preferable for high dependence levels. This means that there is a threshold at which relative performances are reversed, and this threshold depends on the traffic load. Considering for instance $L_1{=}4$ *Er* and $L_2{=}1$ *Er*, $Crit_2$ is better up to $q{\approx}0.8$.

3.2.5 Combined SS strategy

Enlightened by the results obtained in Section 3.2.4.2, which indicate that the most suitable SS criterion depends on a number of aspects, such as the composition and characteristics of PUs, level of dependence exhibited by primary traffic, secondary application mix, this section develops a combined SS strategy for better exploiting statistical metrics provided by the KD. Inputs of the considered strategy are, on the one hand, the KM the statistical characterization of the different pools in terms of $E(OFF_p/ON_p{\in}B_p^a)$ and the dependence level DEP_p stored in the KD. It is assumed for the sake of simplicity that all pools have the same dependence level $DEP_p{=}DEP, \forall p{\in}\{1,\ldots,P\}$. The algorithm uses, on the other hand, as inputs traffic loads of CR applications as well as their characterizations in terms of $T_{req,l}$.

As detailed by the pseudo-code of Algorithm 3.1, it is assumed that radio links are established in the increasing order of their indices (loop in line 3). For a given link l, the decision-making entity gets current $Rem\_OFF_2^p$ estimates

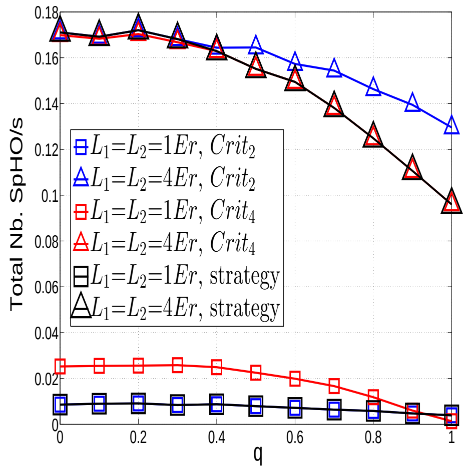

(a)

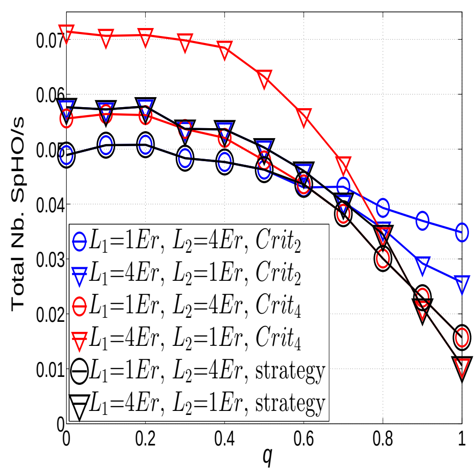

(b)

Figure 3.4: Performance evaluation of the combined SS strategy with (a) Extreme traffic loads and (b) Intermediate traffic loads

from the KM through the exchange of *INFO_REQ(link l, all pools)* and *INFO_-RSP(*$\{Rem\_OFF_2^p\}_{1\leq p\leq P}$*)* messages shown in Figure 2.4 (lines 4 and 5). Then, the list of potential pools for assignments to link l (*Candidates*) is built differently depending on the dependence level provided by the KD. Specifically, if DEP is below a given threshold DEP_{thr}, *Candidates* is built using $Crit_2$ (i.e., picking pools that maximize $Rem\_OFF_2^p$) (line 7). Otherwise, *Candidates* is constructed using $Crit_4$ (i.e., by pools that best fit $T_{req,l}$) (line 9). As it has been identified in Section 3.2.4.2, the threshold DEP_{thr} for deciding about the significance of the dependence level is a function (denoted as h) of traffic loads of both CR applications to capture the fact that each of the considered criteria may be convenient for some traffic mixes. Finally, in the very specific case of multiple pools in *Candidates*, the pool with the lowest DC_p is selected for the application request at hand (line 11).

Considering once again the case study described in Table 3.2, the function h defining the dependence threshold DEP_{thr} has been fit based on previous simulations using a polynomial regression model with an overall Root Mean Squared Error (RMSE) of 0.1. Based on this model, Figure 3.4 makes a comparison between performances of $Crit_2$, $Crit_4$ and the combined strategy for the whole range of possible values of q for various secondary traffic mixes. As pointed out previously, performance is measured in terms of the overall SpHO rate. It can be seen that the combined strategy efficiently switches between $Crit_2$ and $Crit_4$. As a result, it achieves approximately the best performance among them for all the considered combinations of primary dependence levels and secondary traffic mixes.

3.3 Chapter summary

This chapter has addressed the particular case study of an OSA-type access to licensed bands. The results have indicated that exploiting dependence structures between primary ON/OFF durations is always beneficial to improve reliability of estimating remaining OFF durations: for high dependence levels, a dependence-based estimate is much more reliable than a dependence-free estimate, while for low dependence levels, both estimates perform equally.

The same behavior has been observed for two SS strategies exploiting each of these estimates. For low dependence levels, both dependence-based and dependence-free SS strategies equally outperform a random selection scheme (*Rand*) with a gain that depends on the variability level of primary traffic: for low variability levels (i.e., uniform distributions), gains range from 50% to 100%, while for higher variability levels (i.e., exponential distributions), gains range from 10% to 50% due to worse reliability in estimating OFF durations. For high dependence levels, the dependence-based SS strategy performs much better due to better reliability in estimating OFF durations. The introduced gain with respect to *Rand* ranges from 50% to 100% and is independent of the considered distribution.

Therefore, two possible SS strategies exploiting the dependence-based estimate have been developed to minimize CR service interruption, namely a blind proactive strategy that selects pools with maximum estimated remaining OFF duration and a proactive matching strategy that selects pools whose remaining OFF durations fit better durations of CR applications. An evaluation of the observed performance in terms of the number of SpHOs/s has indicated that, for low CR traffic loads, the blind proactive selection performs better especially for low primary dependence levels. For high CR traffic loads, the proactive matching selection performs better especially for high primary dependence levels. For intermediate CR traffic loads, each of the considered strategies may perform better depending on the primary dependence level at hand. Therefore, a general strategy has been developed to capture these dependencies and achieve approximately the best performance for different combinations of primary dependence levels and CR traffic loads.

4. Proposed Algorithmic Solution: Exploiting the Frequency Dimension for Open Sharing of License-exempt bands

This chapter proposes to exploit the frequency domain spectrum characterization provided by the KM to guide open sharing of license-exempt bands. In this context, a fittingness factor–based SS criterion is proposed to efficiency exploit these bands depending on requirements of the applications to be supported. The intrinsic capability of the fittingness factor to track changes in interference levels is firstly analyzed, and the corresponding impact of SS performance is secondly evaluated.

4.1 Proposed SS criterion

To efficiently exploit license-exempt bands by active applications, a greedy criterion selecting the pool with the largest fittingness factor among the set of available pools (Av_Pools) is proposed:

$$p^*_{greedy}(l) = \arg \max_{p \in Av\_Pools} \left(\hat{F}_{l,p} \right) \tag{4.1}$$

Note that no knowledge about the actual radio conditions experienced in the different pools is required at link establishment because the selection decision is based solely on the KM estimation of $F_{l,p}$ values ($\hat{F}_{l,p}$).

4.2 Evaluation study

4.2.1 Simulation model

The considered scenario assumes a set of P=4 spectrum pools. The corresponding bands are BW_1=BW_2=400 *Khz* and BW_3=BW_4=1.2 *Mhz*. Each pool is assumed to experience a different noise and interference PSD $I(p)$, following the daily temporal patterns described by Figure 4.1. Note that a constant PSD I_1=I_2=3·10^{-13} *W/Hz* is considered for pools #1 and #2, while a two-level PSD that alternates between $I_{3,min}$=$I_{4,min}$=3·10^{-13} *W/Hz* and $I_{3,max}$=$I_{4,max}$=70·10^{-13} *W/Hz* is considered for pools #3 and #4. With these interference levels, the corresponding achievable bit rates are $R(l,1)$=$R(l,2)$=512 *Kbps*, $R(l,3)$=$R(l,4)$=1536 *Kbps* for low interference levels, and $R(l,3)$=$R(l,4)$=96 *Kbps* for high interference levels.

L=2 radio links are considered. Link #1 is associated with low-data-rate sessions ($R_{req,1}$=64 *Kbps* and $T_{req,1}$=2 *min*) while link #2 is associated with high-data-rate sessions ($R_{req,2}$=1 *Mbps* and $T_{req,2}$=20 *min*). Independent traffic loads are considered for each link, λ_l^L being the arrival rate over the l-th link that is varied during the simulations. As far as SS is concerned, the criterion proposed in Section 4.1 is considered. For the sake of simplicity, the focus is only on the initial spectrum assignments performed at link establishment, so no SpHO is performed even if the quality perceived by the application in the in use pool is not satisfactory. Instead, a dissatisfaction level is collected to benchmark attained performance. It is measured as the probability of experiencing a bit rate $R(l,p)$ below the requirement $R_{req,l}$.

Performance is obtained with a system-level simulator during a simulation time of 2 days operating in steps of 0.01 *s* with ξ=5 and K=1.

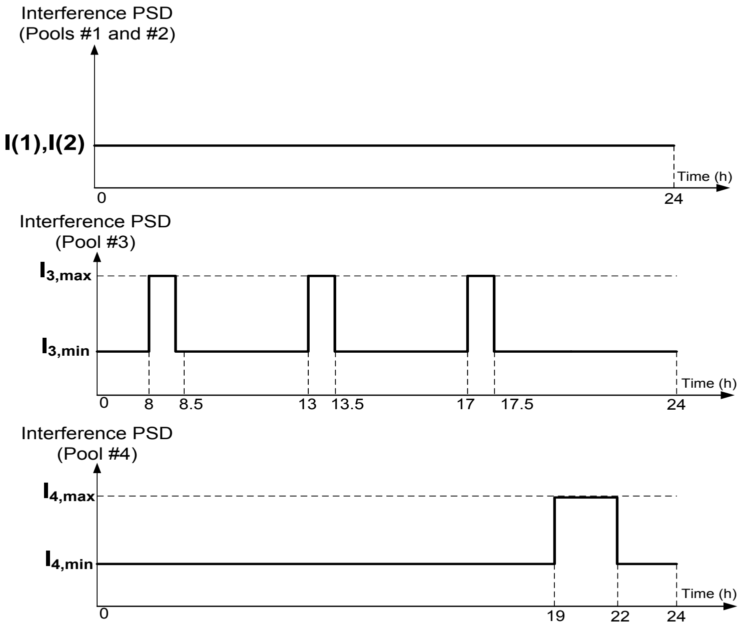

Figure 4.1: Daily pool interference patterns

4.2.2 Evaluation of fittingness factor capability to track changes

An analysis of the capability of fittingness factors to track changes in interference levels is carried out using the first function of (2.10) in which the fittingness factor equals the utility.

Figure 4.2 and Figure 4.3 illustrate, under different traffic loads, the time evolution of fittingness factors of the different pools for links $\#1$ and $\#2$, respectively. Discontinuous black lines represent the instants at which interference conditions change for pools $\#3$ and $\#4$.

For high load conditions -Figure 4.2(a) and Figure 4.3(a)- it is observed that fittingness factors of both links react fast to changes in interference levels. The reason for this fast reaction is that, once interference level increases for one pool (e.g., at t=8 h for pool $\#3$), there is always an active link on that pool due to the high traffic load, which forces the corresponding $F_{l,p}$ to be quickly reduced to a LOW value. Then, once the interference burst is over, (e.g., at t=8.5 h for pool $\#3$), the pool would initially keep the low value of $F_{l,p}$ associated with the case when interference was present (i.e., $F_{1,3}$=0.88 for link $\#1$ and $F_{2,3}$=0 for link $\#2$), and

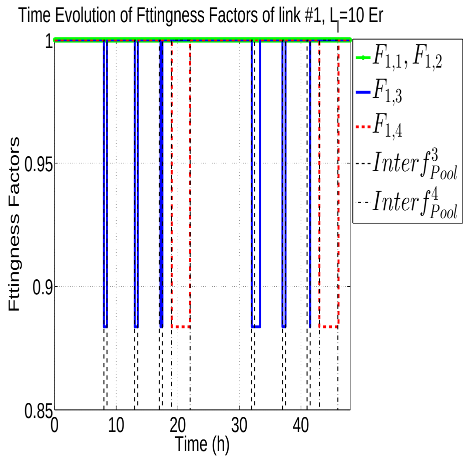

(a)

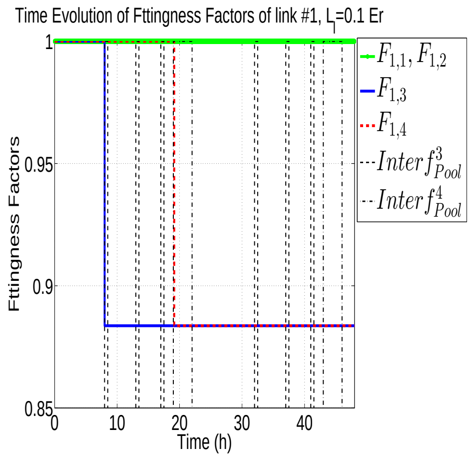

(b)

Figure 4.2: Time evolution of fittingness factors of link $\#1$ for (a) High Traffic load (L_1=10 *Er*) and (b) Low Traffic load (L_1=0.1 *Er*)

correspondingly it will be excluded by the SS in future assignments. Nevertheless, due to the considered high traffic load, in a future spectrum decision, it will happen that all pools with HIGH fittingness factor values will be occupied and a pool with a LOW $F_{l,p}$ value will be eventually assigned again to some link session. When this happens, the measured quality over this link session will reveal that this pool is again providing good performance and, correspondingly, its $F_{l,p}$ will be increased to a HIGH value. Note that some interference change events of pool $\#3$ are missed by link $\#2$ meaning that they occur without any change in fittingness factor values (see e.g., Figure 4.3(a) during the interference change at t=13 h).

In turn, Figure 4.2(b) and Figure 4.3(b) illustrate the case of low traffic loads. The main observation is that, once interference level increases for the first time in an occupied pool, the fittingness factor associated with the corresponding active link is reduced, and then kept unchanged during remaining simulation time. The reason for this behavior is that, under such low traffic loads, the greedy SS algorithm is preventing accessing again the pool whose fittingness factor has been reduced because there is always another available pool with higher fittingness factor.

Even though the observed behavior of the considered fittingness factor function ($F_{l,p}$=$f_1(U_{l,p})$) tracks well changes in interference levels, it may be ineffi-

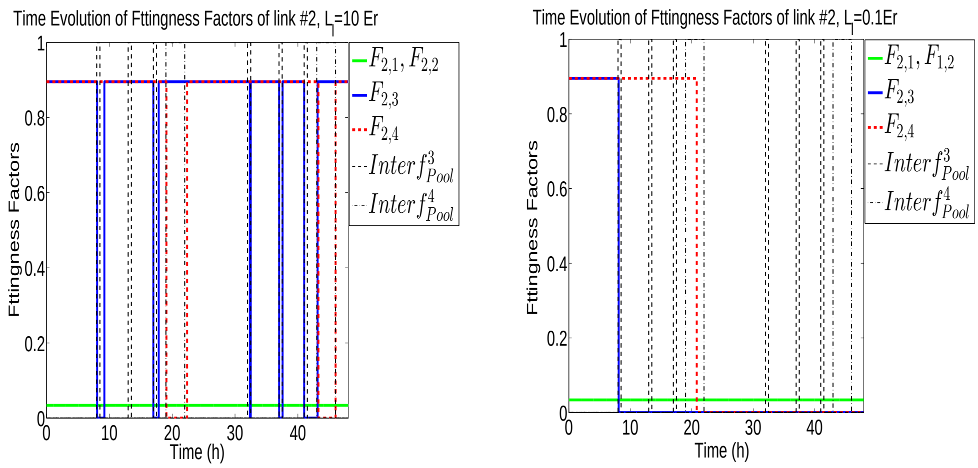

(a) (b)

Figure 4.3: Time evolution of fittingness factors for link $\#2$ for (a) High Traffic load (L_l=10 *Er*) and (b) Low Traffic load (L_l=0.1 *Er*)

cient in managing available spectral resources. To better illustrate this fact, let us consider for instance the low traffic load case for link $\#1$ in Figure 4.2(b). Before the interference increases at $t<8$ h, pools $\#3$ and $\#4$ are preferred since $F_{1,3}=F_{1,4}>F_{1,1}=F_{1,2}$. Correspondingly, low-data-rate sessions of link $\#1$ tend to be allocated pools $\#3$ and $\#4$ (that provide a bit rate of 1536 *Kbps*), although their required bit rate of 64 *Kbps* could also be achieved on pools $\#1$ and $\#2$ that provide only 512 *Kbps*. Such allocation will affect high-data-rate sessions of link $\#2$ that can be successfully served only when using pools $\#3$ and $\#4$, but will find these pools many times occupied by link $\#1$ sessions.

4.2.3 Performance evaluation

This section assesses the efficiency of the proposed fittingness factor-based SS in exploiting license-exempt bands.

Figure 4.4 illustrates a comparison between perceived dissatisfaction levels using fittingness factor functions $\#1$ and $\#2$ as far as link $\#2$ is concerned. The results for link $\#1$ are not presented because it is all the time satisfied (i.e., the bit

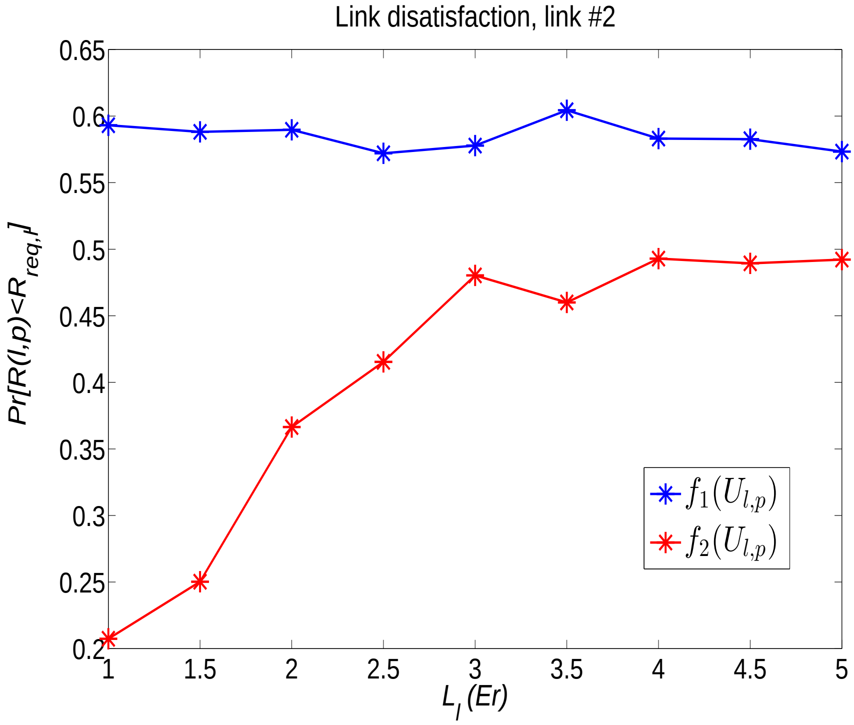

Figure 4.4: Link dissatisfaction of link #2

rate is always above the requirement of 64 *Kbps*) regardless of the allocated pool and its interference conditions.

The results show that function $f_2(U_{l,p})$ is outperforming $f_1(U_{l,p})$ for all traffic loads with a gain that reduces as traffic load increases. The observed reduction in the dissatisfaction level ranges from 65% for medium traffic load (i.e., L_1=L_2=1 *Er*) to 15% for high traffic load (i.e., L_1=L_2=5 *Er*). This is justified by the intuition behind $f_2(U_{l,p})$ that tries to assign just the required resources by a given link. As a matter of fact, $f_2(U_{l,p})$ tends to assign as much as possible pools #1 and #2 to link #1 because they can support the required throughput ($R(1,1)$=$R(1,2)$>$R_{req,1}$) with the minimum resources ($R(1,1)$<$R(1,3)$=$R(1,4)$). This tends to leave pools #3 and #4 available for link #2 sessions that would not be served adequately with pools #1 and #2.

This situation is clearly illustrated by Table 4.1 that gives the pool usage distribution of each link when both fittingness factor functions are used with L_1=L_2=1 *Er*. For $f_1(U_{l,p})$, link #1 uses pools #3 and #4 71% of the time, which forces

Table 4.1: Pool usage distribution for L_1=L_2=1 *Er*

	$f_1(U_{l,p})$				$f_2(U_{l,p})$			
	pool #1	pool #2	pool #3	pool #4	pool #1	pool #2	pool #3	pool #4
link #1	0.15	0.14	0.25	0.46	0.46	0.46	0.03	0.05
link #2	0.31	0.24	0.34	0.11	0.11	0.07	0.37	0.45

link #2 to access pools #1 and #2 during 55% of the time. This significantly increases the dissatisfaction level since $R(2,1)$=$R(2,2)$<$R_{req,2}$. As far as $f_2(U_{l,p})$ is concerned, link #1 uses pools #3 and #4 only 8% of the time, which keeps them mostly for link #2 usage (82% of the time). This reduces the dissatisfaction level since $R(2,3)$=$R(2,4)$>$R_{req,2}$.

4.3 Chapter summary

This chapter has addressed the particular case study of assisting open sharing of license-exempt bands. The fittingness factor concept has been considered to assess the suitability of these bands with respect to a set of heterogeneous CR requirements. In this respect, two formulations of the fittingness factor have been proposed and compared: a simple formulation that monotonically increases with the achievable bit rate ($f_1(U_{l,p})$) and a more intuitive formulation that reduces the value of the fittingness factor whenever the bit rate is much higher than CR application requirements ($f_2(U_{l,p})$). A greedy fittingness factor-based SS strategy has been considered to benchmark the usefulness of both formulations in a scenario with unexpected changes in interference levels.

The results have revealed that, for medium-to-high CR traffic loads, both fittingness factor formulations efficiently track changes in interference levels, and thus enable to select the most suitable bands for CR usage. A comparative study of the corresponding SS performance has indicated that $f_2(U_{l,p})$ outperforms $f_1(U_{l,p})$ with a gain that depends on traffic loads of CR applications. For low-to-medium traffic loads, $f_2(U_{l,p})$ performs a much more efficient usage of spectrum bands by assigning the most valuable bands (i.e., offering higher achievable bit rates) to the neediest CR applications, resulting in a significant improvement in the dissatisfaction level compared to $f_1(U_{l,p})$ (gains up to 65%). As traffic loads increases, spectrum resources become occupied most of the time, which gradually marginalizes the impact of the intelligent assignments performed by $f_2(U_{l,p})$.

5. Integrated Algorithmic Solution: Exploiting Temporal and Frequency Dimensions for Supporting Spectrum Management

Motivated by the usefulness of exploiting proper characterizations of spectrum pools at the time and frequency dimensions shown in Chapters 3 and 4, respectively, this chapter proposes an integrated strategy that exploits both dimensions to assist spectrum management in CRNs. In this respect, a set of SS criteria are proposed to efficiently exploit the set of fittingness factor statistics introduced in Section 2.2.1.3, and the SS, SM and CA functionalities are implemented accordingly. Then, different variants of the proposed strategy are compared to assess the relevance of several choices of implementation. Based on the obtained results, the performance of the best variant is assessed with respect to other strategies from both the cost and benefit perspectives.

5.1 Proposed SS criteria

This section proposes two fittingness-factor SS criteria that extend the greedy criterion proposed in Section 4.1. The first extension introduces a set of preferences in using the different spectrum pools, while the second exploits the temporal variability of observed fittingness factor values.

5.1.1 Greedy criterion

To meet CR application requirements at link establishment, the greedy criterion proposed in Section 4.1 is modified as follows:

$$p^*_{greedy}(l) = \arg \max_{p \in Av\_Pools} \left(\pi_{l,p} \cdot \hat{F}_{l,p} \right) \tag{5.1}$$

where $0 \leq \pi_{l,p} \leq 1$ is a preference factor to account for the fact that spectrum pools may correspond to bands controlled by different regulatory bodies, and thus have different preferences for utilization.

5.1.2 Proactive criterion

To jointly consider the suitability levels estimated by the KM at link establishment ($\hat{F}_{l,p}$) and the changes that may arise in these suitability levels along link session duration, the following proactive criterion is proposed:

$$p^*_{proactive}(l) = \arg \max_{p \in Av\_Pools} \left(g(\hat{F}_{l,p}) \right) \tag{5.2}$$

where the function $g(\hat{F}_{l,p})$ is defined as follows:

$$g(\hat{F}_{l,p}) = \begin{cases} \pi_{l,p} \left(1 + \frac{1}{T_{req,l}} \sum_{k=1}^{T_{req,l}} P^{l,p}_{H,H}(\Delta k_{l,p} + k, \delta_{l,p}) \right) & \text{if } \hat{F}_{l,p} \text{ is HIGH} \\ 0 & \text{if } \hat{F}_{l,p} \text{ is LOW} \end{cases} \tag{5.3}$$

If the estimate $\hat{F}_{l,p}$ is HIGH, $g(\hat{F}_{l,p})$ is constructed as the multiplication of two factors. The first one is the preference factor $\pi_{l,p}$ to reflect the potential prioritization of some pools. The second one sums probabilities of observing a HIGH

Algorithm 5.1 Fittingness factor-based SS

1: **if** link l establishment request **then**
2: **if** $Av\_Pools=\emptyset$ **then**
3: Reject request;
4: **else**
5: Send $INFO\_REQ(link\ l,\ all\ pools)$ to the KM;
6: Get $INFO\_RSP(\{\hat{F}_{l,p}\}_{1\leq p\leq P})$ from the KM;
7: Select the best pool $p^*(l)$ as follows:

$$p^*(l)=\begin{cases} p^*_{greedy}(l) \\ p^*_{proactive}(l) \end{cases};$$

8: **end if**
9: **end if**

$F_{l,p}$ value at link establishment and till the end of link session duration $T_{req,l}$, given that that the last measurement of $F_{l,p}$ stored in the KD was obtained $\Delta k_{l,p}$ time units before link establishment. Note that the first term resulting from the multiplication equals $\pi_{l,p}$, thus giving more priority to higher preference factors ($\pi_{l,p}$) versus higher $P^{l,p}_{H,H}$ values. In the very specific case of multiple pools fulfilling the maximization, the pool with the highest $\hat{F}_{l,p}$ value is selected.

Based on the proposed SS criteria, all SS, SM and CA functionalities are implemented in the following.

5.2 Proposed algorithms

5.2.1 Spectrum selection

The proposed fittingness factor-based SS algorithm is described in Algorithm 5.1. It is executed every time the start of a new CR application requires the establishment of a radio link to support communication. The request for establishing a link l is rejected if the set of available pools is empty (line 3). Otherwise, an estimation of $F_{l,p}$ values is obtained from the KM through the exchange of the the *INFO_-REQ(link l, all pools)* and *INFO_RSP*($\{\hat{F}_{l,p}\}_{1\leq p\leq P}$) messages shown in Figure 2.4 (line 5 and 6). Based on provided $\hat{F}_{l,p}$ values, the best spectrum $p^*(l)$ is selected following either the greedy or proactive criteria proposed in Section 5.1 (line 7).

Algorithm 5.2 Fittingness factor-based SM

1: **if** (link l^* release) OR (Change in any active F_{l,p^*}) **then**
2: Send $INFO\_REQ(all\ links,\ all\ pools)$ to the KM;
3: Get $INFO\_RSP(\{\hat{F}_{l,p}\}_{1\le L\le l,1\le p\le P})$ from the KM;
4: $new\_Assigned \leftarrow \emptyset$;
5: Sort $Active\_Links$ in the decreasing order of $R_{req,l}$;
6: **for** l=1 $\rightarrow |Active\_Links|$ **do**
7: Select the best pool $p^*(l)$ as follows:

$$p^*(l)=\begin{cases} p^*_{greedy}(l) \\ p^*_{proactive}(l) \end{cases};$$

8: **if** (($\hat{F}_{l,p^*(l)}$ is LOW) AND ($\hat{F}_{l,new\_p^*(l)}$ is HIGH)) OR
9: ((($\hat{F}_{l,p^*(l)}-\delta_{l,p})(\hat{F}_{l,new\_p^*(l)}-\delta_{l,p})$>0) AND ($\pi_{l,new\_p^*(l)}>\pi_{l,p^*(l)}$)) OR
10: ($p^*(l)\in new\_Assigned$) **then**
11: $p^*(l) \leftarrow new\_p^*(l)$;
12: $new\_Assigned \leftarrow new\_Assigned \bigcup \{new\_p^*(l)\}$;
13: **else**
14: $new\_Assigned \leftarrow new\_Assigned \bigcup \{p^*(l)\}$;
15: **end if**
16: **end for**
17: $Assigned \leftarrow new\_Assigned$;
18: **end if**

5.2.2 Spectrum mobility

To further adjust CR behavior to changes in suitability of spectrum resources, the SM functionality is executed whenever better pools can be found for some applications. SM is considered on a global perspective jointly optimizing all assignments in order to improve the overall pool usage efficiency.

As detailed by Algorithm 5.2, the proposed fittingness factor-based SM algorithm first gets the current $\hat{F}_{l,p}$ estimates from the KM through the exchange of *INFO_REQ(all links, all pools)* and *INFO_RSP(*$\{\hat{F}_{l,p}\}_{1\le l\le L,1\le p\le P}$*)* messages shown in Figure 2.5. Then, it explores the list of currently active links (*Active_-Links*) in the decreasing order of required throughputs ($R_{req,l}$) to prioritize the neediest links. The reconfiguration decision for each active link is based on a comparison between the in use pool ($p^*(l)$) and the currently best pool according to one of the proposed criteria in Section 5.1 ($new\_p^*(l)$) (line 8). Specifically, if $\hat{F}_{l,p^*(l)}$

Algorithm 5.3 Event-triggered acquisition strategy

for p=1 $\rightarrow P$ **do**
    Compute $current\_F_{l,p}$ according to (2.10) or (2.11) ;
    if (($current\_F_{l,p}$ is LOW) AND ($rep\_F_{l,p}$ is HIGH)) OR
        (($current\_F_{l,p}$ is HIGH) AND ($rep\_F_{l,p}$ is LOW)) **then**
        $rep\_F_{l,p} \leftarrow current\_F_{l,p}$;
        Generate $Meas\_Report(rep\_F_{l,p})$;
    end if
end for

is LOW and $\hat{F}_{l,new\_p^*(l)}$ is HIGH, an SpHO from $p^*(l)$ to $new\_p^*(l)$ is performed because $new\_p^*(l)$ fits better link l. The same SpHO should be performed if both $\hat{F}_{l,p^*(l)}$ and $\hat{F}_{l,new\_p^*(l)}$ are either LOW or HIGH and $new\_p^*(l)$ has higher preference than $p^*(l)$ ($\pi_{l,new\_p^*(l)} > \pi_{l,p^*(l)}$) (line 9). Finally, as reflected in the condition of line 10, the same SpHO should be performed if $p^*(l)$ is no longer available to link l after being reassigned to another link in the previous iterations of the loop of line 6. Once all active links have been explored, the list of assigned pools is updated to consider all SpHOs that need to be executed as the result of the algorithm (line 17).

5.2.3 Context awareness

In general, two types of acquisition strategies can be considered, namely a periodic strategy, in which the $Meas\_Report\_DL(rep\_F_{l^*,p^*})$ and $Meas\_Report(rep\_F_{l^*,p^*})$ messages shown in Figure 2.6 are periodically sent to the KD or an event-triggered strategy, in which measurements reports are generated only when some relevant conditions are met. If the radio environment changes frequently, a simple periodic acquisition strategy can be used. Conversely, in less varying environments, an event-based acquisition strategy is preferred to avoid unnecessary signaling loads between CA modules. This section proposes the use of the event-triggered acquisition strategy described by Algorithm 5.3. In this case, measurement reports are generated only if the currently measured $F_{l,p}$ value ($current\_F_{l,p}$) is LOW and the last reported $F_{l,p}$ value ($rep\_F_{l,p}$) was HIGH or vice versa. As it will be shown later in Section 5.3.5.4, this strategy provides better performance compared to the periodic strategy.

5.3 Evaluation study

This section aims at getting an insight into the effectiveness of the proposed framework in assisting in the spectrum management decision-making process. First, a preliminary analysis of several combinations of fittingness factor functions and SS criteria is conducted. Based on the obtained results, a detailed assessment of the best configuration is performed.

5.3.1 Simulation model

L=2 radio links are considered with independent traffic loads for each link, λ_l^L being the arrival rate over the l-th link that is varied during simulations. Link #1 is associated with low-data-rate sessions ($R_{req,1}$=64 *Kbps* and $T_{req,1}$=2 *min*), while link #2 is associated with high-data-rate sessions ($R_{req,2}$=1 *Mbps* and $T_{req,2}$=20 *min*).

Performance is evaluated using a system-level simulator operating in steps of 1 *s* under the following assumptions:

- The radio environment is modeled as a set of P=4 spectrum pools. The available bandwidth at each pool is BW_1=BW_2=0.4 *MHz* and BW_3=BW_4=1.2 *MHz*.

- A simple interference model that captures the most relevant features affecting SS has been retained. A heterogeneous interference situation is considered, in which the sum of the noise and interference power spectral density I_p experienced in each pool $p\in\{1,\ldots,P\}$ follows a two-state discrete time Markov chain jumping between a state of low interference $I_0(p)$ and a state of high interference $I_1(p)$ with transition probabilities $P_{01}(p)$ (i.e., the probability of moving from state I_0 to I_1 in one simulation step) and $P_{10}(p)$ (i.e., the probability of moving from state I_1 to I_0), as described by Figure 5.1(a).

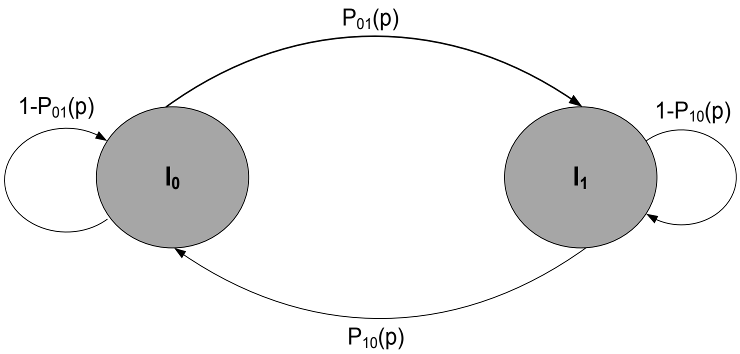

(a)

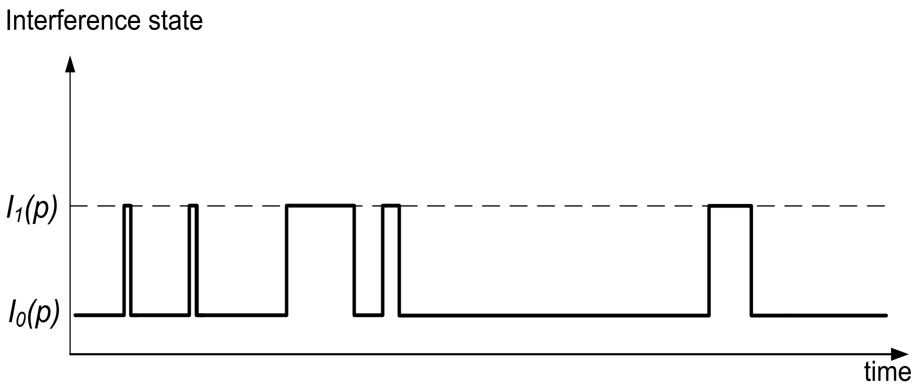

(b)

Figure 5.1: Evolution of the interference PSD (a) Markov chain and (b) example of temporal interference evolution

An example of the temporal evolution of $I(p)$ in a given pool p is shown in Figure 5.1(b).

- Based on these probabilities, the average durations of the $I_0(p)$ and $I_1(p)$ states are, respectively, given by:

$$\overline{I_0(p)} = \frac{1}{P_{01}(p)} \tag{5.4}$$

$$\overline{I_1(p)} = \frac{1}{P_{10}(p)} \tag{5.5}$$

- The interference I_p evolves independently in each pool, and this evolution is independent of the traffic load of radio links. Furthermore, no mutual interference effects between different pools exist.

5.3.2 Benchmarking

To assess the influence of the different components of the proposed framework, the following variants will be compared:

- *SS*: This approach uses the fittingness factor-based SS algorithm proposed in Section 5.2.1 supported by only the KD (i.e., the decision-making entity of Figure 2.2 is assumed to bypass the KM and retrieve only the last measured $F_{l,p}$ value from the KD).

- *SS+KM*: This approach considers the fittingness factor-based SS algorithm supported by the KM module. No SM support is considered. In comparison to *SS*, the use of KM will allow for a better capability to track changes in interference conditions due to the consideration of the temporal properties of $F_{l,p}$ statistics in addition to last measured values.

- *SS+SM*: This approach considers the fittingness factor-based SS algorithm supported by the KD (i.e., using only the last measured $F_{l,p}$) and SM modules. As a difference from *SS*, the inclusion of SM will allow performing pool reallocations to active links whenever better pools can be found.

- *SS+KM+SM*: This approach is the complete strategy that implements the fittingness factor-based SS algorithm supported by both the KM and SM functionalities. Therefore, this strategy incorporates the track-change benefits of KM together with the reallocation flexibility associated with SM.

Apart from the considered variants, the following reference schemes are introduced for benchmarking purposes:

- *Rand*: This scheme implements only the SS module of Figure 2.2 and performs a random selection among available pools. Neither SM nor KM modules are used.

- *Optim*: This scheme is an upper bound theoretical reference. In each simulation step, the procedure assigns, at a given time instant k, the combination of pools and active links that maximizes the total instantaneous throughput with the highest preference factors as follows:

$$\max_{\sum_{l \in Active\_Links(k)} \pi_{l,p^*(l)}} \left(\max \left(\sum_{l \in Active\_Links(k)} \min(R_{req,l}, R(l, p^*(l), k)) \right) \right) \quad (5.6)$$

  where $Active\_Links(k)$ and $R(l, p^*(l), k)$ denote the list of active links and measured bit rate $R(l, p^*(l))$ at time k, respectively.

  The inner maximization determines combinations of pools and active links that maximize the total throughput, while the outer maximization selects among these the combination that maximizes the sum of preference factors. Note that this theoretical scheme requires to continuously sent actual $R(l, p^*(l), k)$ values to the decision-making entity through measurement reports.

5.3.3 Performance indicators

To assess the performance of the proposed strategy, the following indicators are considered:

- The total dissatisfaction probability defined as

$$Dissf = \frac{\sum_k Nb\_Dissatisfied\_Links(k)}{\sum_k Nb\_Active\_Links(k)} \quad (5.7)$$

  where *Nb_Active_Links(k)* and *Nb_Dissatisfied_Links(k)* denote the number of active and dissatisfied links (i.e., those experiencing a bit rate $R(l, p, k)$ below the requirement $R_{req,l}$) at a given time instant k, respectively.

- The total signaling overhead in the radio interface experienced on average per link session given by

$$Overhead = \frac{1}{Nb\_Succ\_Estab}(Nb\_Estab\_Req \cdot \overline{Estab} + Nb\_Succ\_Estab \cdot \overline{Release} + Nb\_SpHO \cdot \overline{SpHO} + Nb\_Rep \cdot \overline{Rep}) \tag{5.8}$$

where *Nb_Estab_Req*, *Nb_Succ_Estab*, *Nb_SpHO*, and *Nb_Rep* denote the number of link establishment requests, successful link establishments, executed SpHOs, and measurement reports generated by CA modules during simulation duration, respectively. The corresponding costs for establishing a link session, releasing it, performing an SpHO, and generating a measurement report are set to $\overline{Estab}=266$ *Bytes*, $\overline{Release}=64$ *Bytes*, $\overline{SpHO}=167$ *Bytes* and $\overline{Rep}=43$ *Bytes*, respectively, following the message formats given in [71].

- The SpHO signaling introduced by either *SS+SM* or *SS+KM+SM* evaluated in terms of the number of SpHOs performed per link session (*Nb. SpHOs/session*).
- The overall SpHO rate per second (*Nb. SpHOs/s*).
- The amount of measurement reports sent from CA modules to the KD in Figure 2.6 evaluated in terms of the number of reported bits per second (*report signaling*).

5.3.4 Preliminary analysis

To reduce degrees of freedom of the proposed strategy, this section initially assesses performance when different combinations of fittingness factor functions and SS criteria are used. Enlightened by the obtained results, a detailed assessment of the best combination will be performed in Section 5.3.5.

5.3.4.1 Assumptions

The simulation model presented in Section 5.3.1 is considered. Pools $\#1$ and $\#2$ are assumed to be always in the state $I_0(p)$, while pools $\#3$ and $\#4$ alternate between $I_0(p)$ and $I_1(p)$ randomly with transition probabilities of $P_{01}(3)$=$3.7{\cdot}10^{-5}$ and $P_{10}(3)$=$55.5{\cdot}10^{-5}$ for pool $\#3$ and $P_{01}(4)$=$55.5{\cdot}10^{-5}$ and $P_{10}(4)$=$8.33{\cdot}10^{-3}$ for pool $\#4$. Based on these probabilities, the average durations of the high interference state for pools $\#3$ and $\#4$ are $\overline{I_1(3)}$=0.5 *h* and $\overline{I_1(4)}$=2 *min*, respectively, while the average durations of the low interference state for pools $\#3$ and $\#4$ are $\overline{I_0(3)}$=7.5 *h* and $\overline{I_0(4)}$=0.5 *h*, respectively. The average achievable bit rate by one link l in pools $\#1$ and $\#2$ is $R(l,1)$=$R(l,2)$=128 *Kbps*, while for pools $\#3$ and $\#4$, the average achievable bit rate alternates between $R(l,3)$=$R(l,4)$=1536 *Kbps* for the $I_0(p)$ state and $R(l,3)$=$R(l,4)$=96 *Kbps* for the $I_1(p)$ state.

Performance is obtained with a system-level simulator operating with steps of 1 *s* during a simulation time of $1,000$ *days*. The other simulation parameters are ξ=5, K=1, $\delta_{1,p}$=0.2, $\delta_{2,p}$=0.8, Thr_LOW=0.9 and Thr_HIGH=0.1.

5.3.4.2 Relevance of fittingness factor functions

This section conducts a comparative study between the proposed fittingness factor functions in Section 2.2.1.2. For the sake of simplicity, only *SS+KM* and *SS+KM+SM* variants are initially considered and compared to the reference *Rand* and *Optim* schemes assuming the greedy criterion introduced in Section 5.1.1.

Figure 5.2(a) plots the dissatisfaction probability of link $\#2$ (i.e., the most demanding in terms of required bit rate) as a function of the total offered traffic load in bits per second (bps) defined as

$$\textit{Offered Traffic (bps)}=\sum_{l} L_l{\cdot}R_{req,l} \tag{5.9}$$

where L_l is the offered traffic load to link l given by (3.10).

The results for link $\#1$ are not presented since it is all the time satisfied (i.e., the bit rate is always above the requirement of 64 *Kbps*). Figure 5.2(b) plots the fraction of time that link $\#2$ uses pools $\#3$ or $\#4$. When using these pools in the

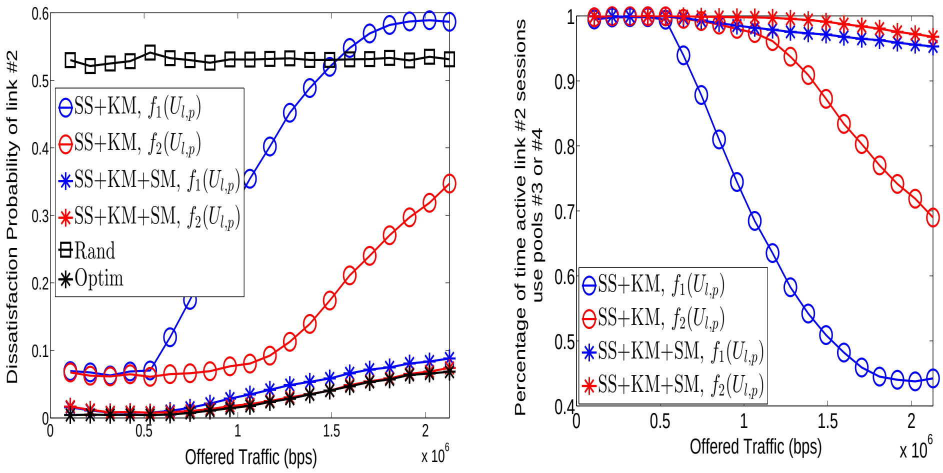

(a) (b)

Figure 5.2: SS performance comparison for link $\#2$ in terms of (a) Dissatisfaction probability and (b) Fraction of time that link $\#2$ uses pools $\#3$ or $\#4$

low interference state, link $\#2$ will be satisfied. In turn, link $\#2$ will be dissatisfied whenever it is allocated pools $\#1$ or $\#2$ or pools $\#3$ or $\#4$ in the high interference state.

As seen in Figure 5.2(a), for low traffic loads below 0.6 *Mbps*, a very important reduction of the dissatisfaction probability compared to *Rand* is observed for both variants when either $f_1(U_{l,p})$ or $f_2(U_{l,p})$ is used. This reduction is justified by the capability of the KM to identify changes in interference conditions of the different pools. Therefore, the most suitable pools are allocated to established radio links, and as a result, the dissatisfaction probability improves. The similar performance of $f_1(U_{l,p})$ and $f_2(U_{l,p})$ can be justified by the fact that, for this low traffic load, at least one of pools $\#3$ and $\#4$ is often available for link $\#2$, even if function $f_1(U_{l,p})$ tends to allocate these pools to link $\#1$. This is reflected in Figure 5.2(b), where it can be seen that the usage fraction of pools $\#3$ or $\#4$ by link $\#2$ is close to 1 for both fittingness factor functions.

When load increases above 0.6 *Mbps*, performance degrades more significantly with $f_1(U_{l,p})$ than with $f_2(U_{l,p})$. This is because $f_1(U_{l,p})$ tends to allocate pools $\#3$ and $\#4$ to link $\#1$ sessions, which forces link $\#2$ sessions to use pools $\#1$ and $\#2$ that are not able to provide the required bit rate. On the contrary, $f_2(U_{l,p})$

prioritizes pools #1 and #2 for link #1 sessions, and thus pools #3 and #4 tend to be more available for link #2 usage, resulting in a much lower dissatisfaction probability. As a result, it can observed in Figure 5.2(b) that the usage fraction of pools #3 and #4 by the most demanding link #2 is much higher with $f_2(U_{l,p})$ than with $f_1(U_{l,p})$.

With respect to the behavior of SM for each of the considered fittingness factor functions, for low loads, its use leads to small improvements for both functions (see the comparison in Figure 5.2(a) between *SS+KM* and *SS+KM+SM*). The reason for this marginal gain is that, for such low loads, it occurs very rarely that a link is not allocated the pool with the highest fittingness factor because of being occupied by another link. On the contrary, when the traffic load increases, the introduction of SM leads to a significant performance gain particularly when $f_1(U_{l,p})$ is used. The reason for this gain is that, whenever link #2 sessions are assigned to pools #1 or #2 due to unavailability of pools #3 and #4, the SM algorithm succeeds in reconfiguring these sessions to use pools #3 and #4 after they got released. Unavailability of pools #3 and #4 for link #2 usage occurs mainly due to the high traffic load in case of $f_2(U_{l,p})$, but also due to the inefficient allocation of these pools to link #1 sessions in case of $f_1(U_{l,p})$. Correspondingly, it can be observed that the difference in dissatisfaction probability between $f_1(U_{l,p})$ and $f_2(U_{l,p})$ becomes smaller when strategy *SS+KM+SM* is considered because the inappropriate allocations made by the function $f_1(U_{l,p})$ can be compensated by the reassignments performed by SM. This comes at the expense of an increase in signaling requirements in terms of executed SpHOs. This is shown in Figure 5.3 that plots the number of SpHOs performed per link session when *SS+KM+SM* is used with both fittingness factor functions. Note in particular that there is a very important reduction in the number of required SpHOs for link #2 when the function $f_2(U_{l,p})$ is used (at the expense of a slight increase in the SpHOs performed by link #1).

Another relevant observation in Figure 5.2(a) is that the proposed *SS+KM+SM* strategy with $f_2(U_{l,p})$ performs very closely to the upper-bound optimal scheme for all load conditions, thanks to the support of the KM and SM components. The gain observed by *SS+KM+SM* with respect to *Rand* (measured as the reduction in the dissatisfaction probability) ranges from 85% to 100%. Note that a slight degradation is observed for *SS+KM+SM* when $f_1(U_{l,p})$ is used. This is due to the

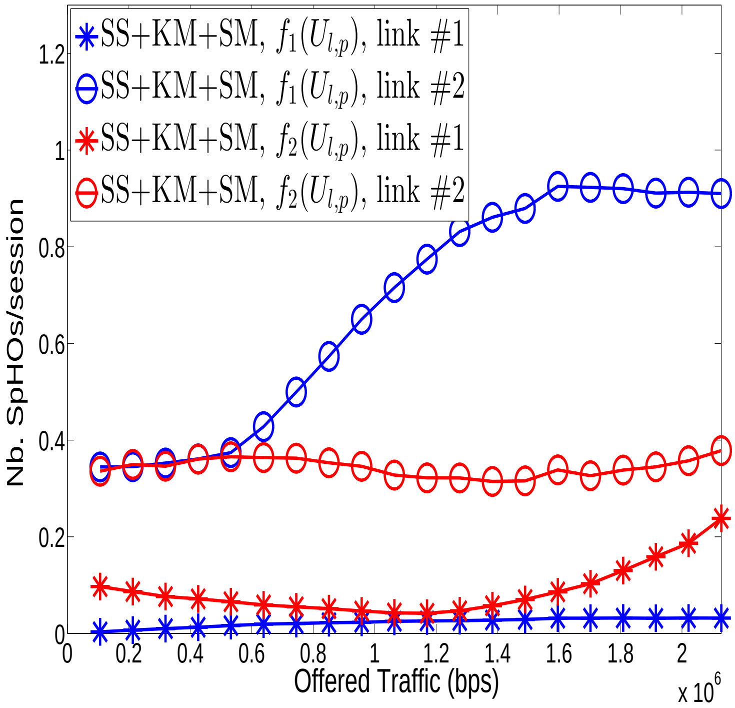

Figure 5.3: Average number of SpHOs/session

higher number of SM executions caused by inefficient allocation of pools. As a matter of fact, whenever link #2 sessions are inefficiently assigned pools #1 or #2, some time is spent before SM is triggered to reconfigure these sessions to use pools #3 or #4 instead, which slightly increases the dissatisfaction probability.

Enlightened by the above analysis, it can be concluded that the function $f_2(U_{l,p})$ performs much more efficient resource allocation compared to $f_1(U_{l,p})$, which results in a better dissatisfaction probability and less SpHO signaling requirements.

5.3.4.3 Relevance of SS criteria

To evaluate the impact of the decision-making criterion on the obtained performance, this section makes a comparison between the greedy and proactive criteria introduced in Section 5.1. Enlightened by the results obtained in Section 5.3.4.2,

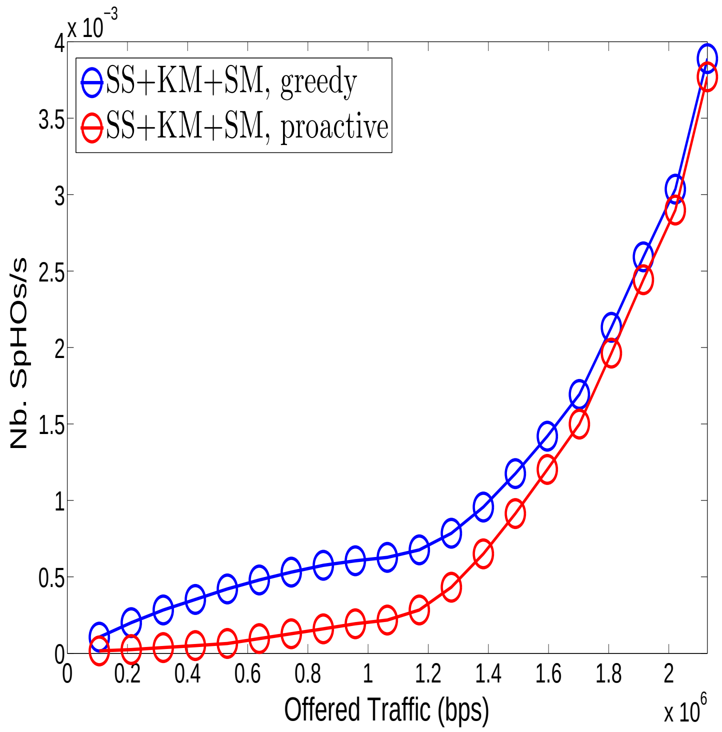

Figure 5.4: Impact of the decision-making criterion

only the function $f_2(U_{l,p})$ is considered for both criteria, together with the strategy *SS+KM+SM*.

Figure 5.4 plots the overall SpHO rate per second for both the greedy and proactive criteria as a function of the total offered traffic load. It is worth mentioning that the performance in terms of dissatisfaction probability reveals very similar performance for both criteria with the same result shown in Figure 5.2(a) when *SS+KM+SM* is used with $f_2(U_{l,p})$.

The results indicate that, from low-to-medium traffic loads, the proactive criterion strongly outperforms the greedy criterion. This is because, among pools $\#3$ or $\#4$, the proactive criterion tends to prioritize pool $\#3$ exhibiting much longer durations of the HIGH state (7.5 *h* for pool $\#3$ versus 0.5 *h* for pool $\#4$). Therefore, it becomes less likely to experience a state change from $I_0(p)$ to $I_1(p)$ during link session, which considerably reduces the number of executed SpHOs. As the traffic load increases, pools $\#3$ and $\#4$ become occupied most of the time, which marginalizes the effect of giving priority to pool $\#3$.

5.3.5 Proposed strategy

Enlightened by the preliminary analysis conducted in Section 5.3.4, the best variant *SS+KM+SM* combining $f_2(U_{l,p})$ with the proactive SS criterion is assessed in this section from both the cost and benefit perspectives.

5.3.5.1 Assumptions

The general simulation model presented in Section 5.3.1 is considered. Pools $\#1$ and $\#2$ are assumed to be always in the state $I_0(p)$, while pools $\#3$ and $\#4$ alternate between $I_0(p)$ and $I_1(p)$ randomly with transition probabilities of $P_{01}(3)$=3.7·10^{-5} and $P_{10}(3)$=55.5·10^{-5} for pool $\#3$ and $P_{01}(4)$=1.32·10^{-5} and $P_{10}(4)$=9.25·10^{-5} for pool $\#4$. Based on these probabilities, the average durations of the low interference state for pools $\#3$ and $\#4$ are $\overline{I_0(3)}$=7.5 *h* and $\overline{I_0(4)}$=21 *h*, respectively, while the average durations of the high interference state for pools $\#3$ and $\#4$ are $\overline{I_1(3)}$=0.5 *h* and $\overline{I_1(4)}$=3 *h*, respectively. The average achievable bit rate by one link l in pools $\#1$ and $\#2$ is $R(l,1)$=$R(l,2)$=512 *Kbps*, while for pools $\#3$ and $\#4$, the average achievable bit rate alternates between $R(l,3)$=$R(l,4)$=1536 *Kbps* for the $I_0(p)$ state and $R(l,3)$=$R(l,4)$=96 *Kbps* for the $I_1(p)$ state. It is assumed for the sake of simplicity that all pools have the same preference factor ($\pi_{l,p}$).

The system is observed during a simulation time of $1,000$ *days* operating in steps of 1 *s*. The other simulation parameters are ξ=5, K=1, $\delta_{1,p}$=0.2, $\delta_{2,p}$=0.9, Thr_LOW=0.9 and Thr_HIGH=0.1.

5.3.5.2 Performance evaluation

This section presents the performance evaluation of the different schemes introduced in Section 5.3.2. The goal of this analysis is two-fold: (1) to identify which of the functional elements of the proposed architecture have the most significant impact on performance depending on system operation conditions and (2) to benchmark the performance of the proposed spectrum management strategy with respect to the reference *Rand* and *Optim* schemes. For all schemes, the event-triggered acquisition strategy described in Algorithm 5.3 is considered.

Figure 5.5(a) plots the total dissatisfaction probability (*Dissf*) defined in Section 5.3.3 as a function of the total offered traffic load in bps. For the sake of simplicity, equal traffic loads are considered for both links (i.e., L_1=L_2). Note that because link $\#1$ is always satisfied regardless of the assigned pool, *Dissf* depends on link $\#2$ only. For a better understanding of the obtained results, Figure 5.5(b) plots the fraction of time that link $\#2$ uses pools $\#3$ or $\#4$ under the consideration that link $\#2$ will be satisfied only when using these pools during the low interference state, while it will be dissatisfied whenever it is allocated pools $\#1$ or $\#2$ or pools $\#3$ or $\#4$ during the high interference state.

As seen in Figure 5.5(a), for low traffic loads below 0.6 *Mbps*, the introduction of KM leads to a very important reduction of the dissatisfaction probability. The reason is that, whenever interference increases in pools $\#3$ and $\#4$ (i.e., they move to state I_1), the corresponding measured value of $F_{l,p}$ will be LOW. As a result, strategies *SS* and *SS+SM* that just keep this measured $F_{l,p}$ value will decide in the future to allocate only pools $\#1$ and $\#2$, which offer a lower bit rate. Then, the network will not be able to realize the situation when pools $\#3$ and $\#4$ move again to the low-interference state I_0 and become adequate for the link $\#2$ (see in Figure 5.5(b) that the fraction of time that these pools are allocated to link $\#2$ is approximately 0.2 for strategies not exploiting KM). On the contrary, the use of the KM component considers the temporal properties of $F_{l,p}$ statistics to disregard the last measured $F_{l,p}$ value and use an estimated value instead whenever a certain amount of time has passed since this last measure was taken (see conditions of lines 5 and 11 in Algorithm 2.1). Correspondingly, sometime after the interference increase, the network will allocate again pools $\#3$ and $\#4$ to link $\#2$, thus being able to identify if they have re-entered the low-interference state. Note in Figure 5.5(b) that the fraction of time that link $\#2$ uses pools $\#3$ or $\#4$ is close to 1 for strategies making use of KM, thus resulting in a better dissatisfaction probability.

In summary, for low loads, the KM allows a better exploration of the different pools to identify changes in their interference conditions, and as a result, the dissatisfaction probability improves. When load increases above 0.6 *Mbps*, pools $\#1$ and $\#2$ will tend to be occupied by link $\#1$ sessions most of the time, which

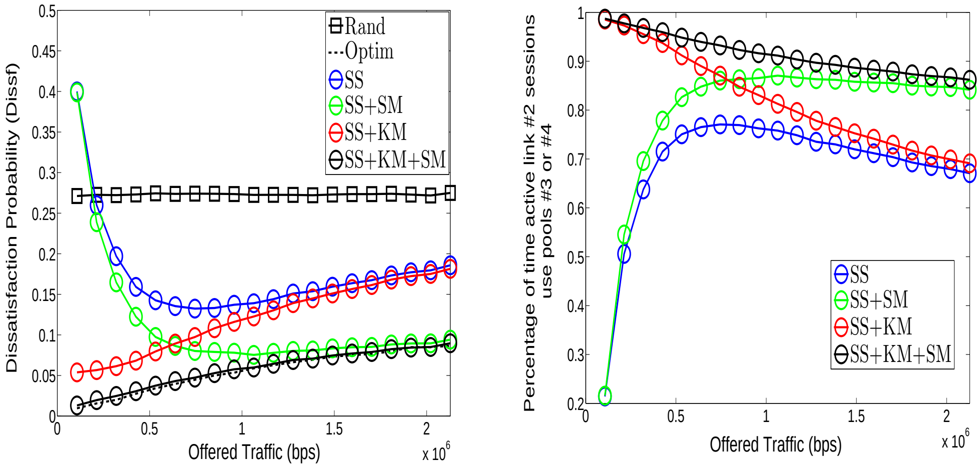

(a) (b)

Figure 5.5: Performance evaluation of the selected *SS+KM+SM* variant in terms of (a) Total dissatisfaction probability and (b) Usage fraction of pools #3 or #4 by link #2

forces the system to assign pools #3 and #4 to link #2 sessions even with reduced $F_{l,p}$ values. In this case, interference reductions in pools #3 and #4 are detected without the use of KM. This is reflected in Figure 5.5(a) where, for high loads, *SS* and *SS+KM* performances are equivalent, and the same occurs for *SS+SM* and *SS+KM+SM* performances.

With respect to the role of SM, for low loads, its use leads to small improvements (see the comparison in Figure 5.5(a) between *SS* and *SS+SM* or *SS+KM* and *SS+KM+SM*). The reason for this small gain is that, for low loads, it occurs very rarely that a link is not allocated to the pool with the highest fittingness factor because of being occupied by another link. Consequently, there is no need to perform an SpHO towards a better pool except when the interference level increases in the allocated pool, which justifies the small improvement observed when comparing *SS+KM* and *SS+KM+SM*. On the contrary, when load increases, the preferred pool becomes often occupied by another link, and thus a pool offering a lower bit rate is allocated. In this case, the execution of SM after the release of the link occupying the preferred pool will lead to improved performance. Note that, in Figure 5.5(b), link #2 is allocated most of the time pools #3 or #4 with *SS+KM+SM*, thus leading to the significant reduction in dissatisfaction probability achieved by *SS+KM+SM* with respect to *SS+KM* in Figure 5.5(a) for high loads.

The gain observed by *SS+KM+SM* with respect to the *Rand* scheme (measured as the dissatisfaction probability reduction) ranges from 70% to 100% (see Figure 5.5(a)). The proposed strategy performs very similarly to the upper-bound optimal scheme in terms of the dissatisfaction probability for all traffic load conditions, mainly due to the support of the KM and SM components for relatively low and high loads, respectively. Nevertheless, the slight improvement introduced by the upper-bound scheme comes at a much higher cost in terms of signaling overhead, as will be shown in the next section.

5.3.5.3 Associated signaling cost at the radio interface

To assess the signaling cost introduced by the proposed strategy, this section makes an analysis of the impact of SM reconfigurations on the radio interface. The impact is evaluated in terms of the signaling overhead (*Overhead*) and amount of SpHO signaling (*Nb. SpHOs/session*) introduced in Section 5.3.3.

Figure 5.6(a) plots the signaling overhead introduced by *SS+KM*, *SS+KM+SM*, and *Optim* as a function of the total offered traffic load in bps defined in (5.9) with a vertical axis in logarithmic scale for improved visualization. Figure 5.6(b) plots the corresponding amount of SpHO signaling *SS+KM+SM* is introducing for each of the two possible triggers of SM (i.e., a link release or change in $F_{l,p}$).

The results show that the overhead introduced by both *SS+KM+SM* and *SS+KM* is much smaller than that of the reference scheme *Optim* (Figure 5.6(a)). This significant reduction is because *Optim* requires to continuously report actual $R(l,p)$ values to the decision-making entity, which strongly increases the amount of report signaling per session, particularly for low traffic loads. In contrast, the additional overhead introduced by the proposed strategy (*SS+KM+SM*) compared to *SS+KM* is below 10% for even a very high traffic load due to the low number of SpHOs incurred by *SS+KM+SM* (see in Figure 5.6(b) that the average number of executed SpHOs is below 0.28 for all considered traffic loads). The analysis of the amount of SpHO signaling associated with each trigger in Figure 5.6(b) reveals that, for very low traffic loads, a non-negligible fraction of performed SpHOs

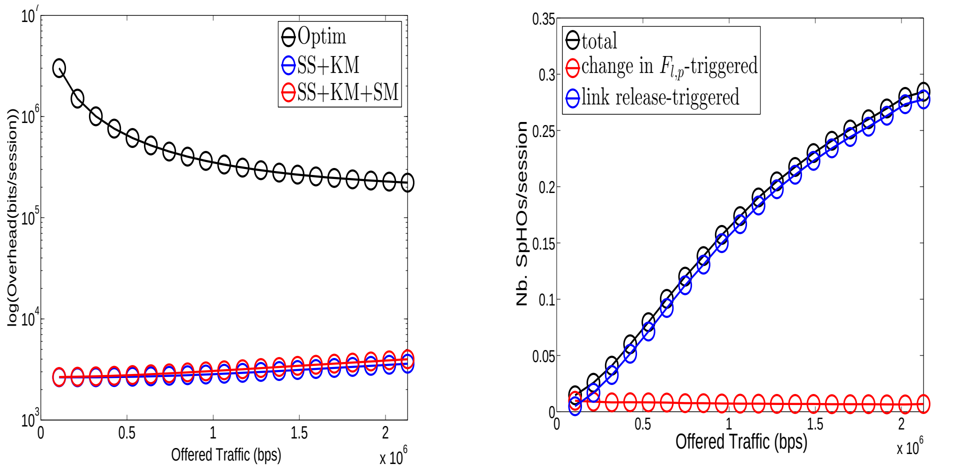

(a) (b)

Figure 5.6: Signaling cost at the radio interface in terms of (a) *Overhead* (bits/session) and (b) number of SpHOs/session with *SS+KM+SM*.

are triggered by changes in $F_{l,p}$ values because at such loads, links are typically assigned their preferred pools (i.e., pools $\#1$ or $\#2$ to link $\#1$ and $\#3$ or $\#4$ to link $\#2$). As the traffic load increases, the trigger of SM by link releases becomes more relevant with more SpHO executions. The increase in the number of executed SpHO is justified by the fact that, at this high traffic load, a link is more likely to find its preferred pool occupied by another link at link establishment.

5.3.5.4 Impact of the acquisition strategy

To assess relevance of the acquisition strategy, a joint analysis of its impact on system performance and signaling cost is conducted. Performance and cost are evaluated in terms of the total dissatisfaction probability (*Dissf*) and number of measurement reports generated by CA modules (*report signaling*), respectively.

Figure 5.7(a) plots the total dissatisfaction probability (*Dissf*) as a function of the total offered traffic load when *SS+KM+SM* uses the event-triggered acquisition strategy described in Algorithm 5.3. A periodic acquisition strategy that sends measurements reports every $\Delta T(s)$ is also considered for comparison purposes.

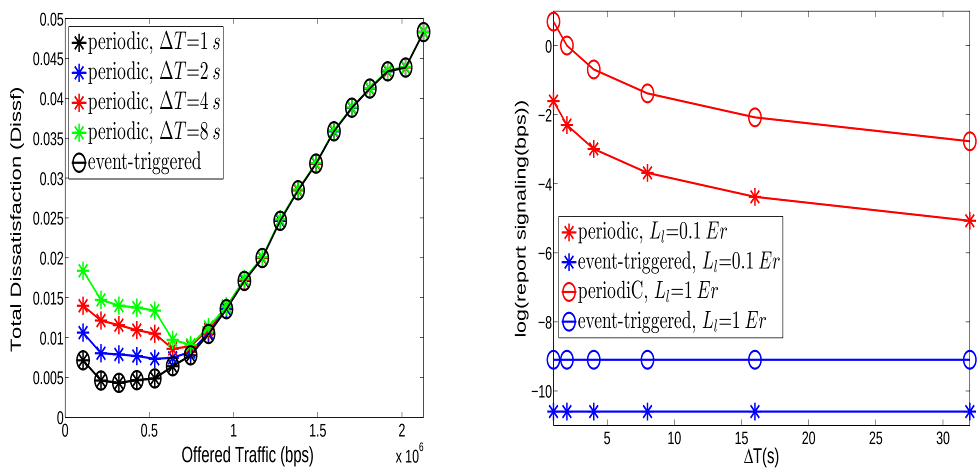

(a) (b)

Figure 5.7: Impact of the acquisition strategy of *SS+KM+SM* in terms of (a) dissatisfaction probability and (b) report signaling requirements.

The corresponding cost (*report signaling*) is presented in Figure 5.7(b) as a function of ΔT for different traffic loads with a vertical axis in logarithmic scale for improved visualization.

Regarding the periodic acquisition strategy, the results show that as ΔT increases, the dissatisfaction probability gets slightly worse at low loads but remains unchanged at high loads (Figure 5.7(a)). This behavior is because at low traffic loads, a non-negligible fraction of performed SpHOs are triggered following a change in $F_{l,p}$ values, as previously observed in Figure 5.6(b). Consequently, if ΔT is long, these SpHOs are delayed or even missed, which increases the dissatisfaction probability. As the traffic load increases, SpHOs become primarily triggered by releases of link sessions, which marginalizes the effect of increasing ΔT on the dissatisfaction probability. In contrast, increasing ΔT significantly reduces the measurement reports signaling cost, particularly for high traffic loads (see Figure 5.7(b)).

In summary, the results reveal that the event-triggered acquisition strategy outperforms the periodic approach from both the dissatisfaction probability and signaling requirements perspectives, as observed in Figure 5.7(a) and Figure 5.7(b), respectively.

Enlightened by the obtained results, only the strategy *SS+KM+SM* with the event-based acquisition strategy will be considered in the following chapters.

5.4 Chapter summary

Drawing inspiration from the obtained results in previous chapters, this chapter has developed a more general strategy to support spectrum management in CRNs with a proper characterization of spectrum pools in both the time and frequency domains. Specifically, the proposed strategy relies on the $\hat{F}_{l,p}$ estimates provided by the KM to track the temporal variability of suitability of spectrum pools. Based on these estimates, two greedy and proactive SS criteria have been proposed to maximize the observed $F_{l,p}$ value at link establishment and likelihood of observing a HIGH $F_{l,p}$ value up to the end of link session, respectively. A preliminary study of several variants combining the KM, SS and SM functionalities with different SS criteria (greedy and proactive) and fittingness factor functions ($f_1(U_{l,p})$ and $f_2(U_{l,p})$) has been conducted. The results have indicated, on the one hand, that the function $f_2(U_{l,p})$ outperforms $f_1(U_{l,p})$ in terms of dissatisfaction probability especially when the SM functionality is not supported (gains up to 40%). On the other hand, the proactive criterion outperforms the greedy criterion for low-to-medium traffic loads of CR applications with gains up to 80%. When the traffic load increases, pools become occupied most of the time, which marginalizes the impact of prioritizing pools and makes performances of both SS criteria similar.

Enlightened by these results, a more detailed assessment of the best variant combining $f_2(U_{l,p})$ with a proactive SS has been performed. The results have revealed that, for low traffic loads, the KM enables to track changes in interference levels of unexplored pools, and thus introduces a significant reduction of the dissatisfaction probability compared to a random selection (*Rand*) (gains up to 90%). For high loads, the SM enables to reconfigure radio links to use the best pools, and thus introduces a significant improvement in terms of the dissatisfaction probability especially for high traffic loads (gains up to 65%). By combining both functionalities, the proposed strategy significantly outperforms *Rand* in terms of the dissatisfaction probability with gains ranging from 70% to 90%, and performs very similarly to the upper bound theoretical scheme (*Optim*).

An analysis of the associated signaling amount has indicated a reduced cost that argues in favor of the practicality of the proposed approach. On the one hand, the proposed strategy significantly reduces the amount of report signaling per session compared to *Optim*, particularly when an event-triggered acquisition strategy is used. On the other hand, the average number of SpHOs performed per session remains below 0.28 for all traffic loads. The analysis of the amount of SpHO signaling associated with each trigger has revealed that the amount of SpHO signaling is distributed differently depending on traffic loads of CR applications. For low traffic loads, a non-negligible fraction of performed SpHOs are triggered by changes in $F_{l,p}$ values. As traffic load increases, the trigger of SM by link releases becomes more relevant than by changes in $F_{l,p}$ values.

6. Improving Robustness of the Proposed Framework

The proposed framework and algorithmic solutions have been shown in previous chapters to significantly improve SS performance as long as the information stored in the KD is reliable. Nevertheless, such assumption may not hold, either initially when the KD is constructed (e.g., if only a partial convergence can be achieved in KD statistics), or during system operation (e.g., if a relevant change occur in the environment so that KD data become out-of-date). Therefore, this chapter proposes to extend, when needed, the proposed framework to improve robustness to both types of imperfection in KD data.

6.1 Robustness to partial convergence of statistics

To assess robustness to partial convergence of KD statistics, the convergence times needed for some of these statistics are firstly analyzed. Enlightened by this analysis, the impact on SS performance is secondly evaluated.

6.1.1 Convergence analysis

This section proposes to analyze the convergence behavior of KD statistics. Such analysis cannot rely on a single statistic because, for a given acquis-

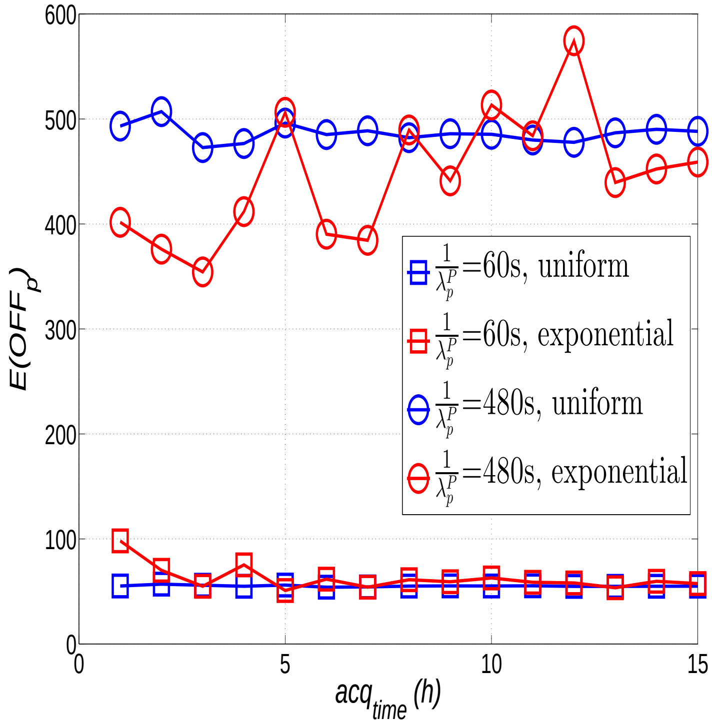

Figure 6.1: Convergence of $E(OFF_p)$

ition time acq_{time}, various convergence levels may be achieved for different orders of KD statistics. Therefore, it is proposed to consider both first-order (e.g., $E(OFF_p)$) and second-order statistics (e.g., $E(OFF_p/ON_p{\in}B_p^a)$). Given that the $E(OFF_p/ON_p{\in}B_p^a)$ statistic is bucket-dependent, the operating bucket configuration determined in Annex A is first selected. It corresponds to $N_B^{opr}{=}|B_p^{ON}|{=}|B_p^{OFF}|{=}31$ and $\tau^{opr}{=}0.1$

Figure 6.1 plots the time evolution of $E(OFF_p)$ for some selected values of the primary traffic arrival rate λ_p^P when OFF durations are distributed either uniformly or exponentially. It is first observed that $E(OFF_p)$ is much more stable for shorter OFF durations (i.e., $1/\lambda_p^P$ values). This is basically due to the fact that, for a given acq_{time}, as $1/\lambda_p^P$ gets longer, the range of possible outcomes of OFF_p gets wider with less OFF_p samples. With respect to convergence speed, $E(OFF_p)$ is relatively stable after $acq_{time}{=}2$ *h* for all selected values of $1/\lambda_p^P$ as far as uniform distributions are considered. However, it fluctuates much more for exponential distributions, particularly for long $1/\lambda_p^P$ values. This distinct behavior is due to the higher variability of exponential distributions, which makes random OFF outcomes deviate much from their corresponding means.

Next, the more challenging convergence of the conditional mean $E(OFF_p/ON_p{\in}B_p^a)$ is considered. In this case, estimation accuracy depends, not only on acq_{time}, but also on the number of possible combinations of successively observed ON/OFF buckets. To better illustrate this dependence, fully-dependent time series (i.e., q=1), whose ON/OFF mapping of (3.5) results in only N_B^{opr} out of the N_B^{opr2} possible combinations, are considered. As a matter of fact, $\forall a{\in}\{1,\ldots,|B_p^{ON}|\}$ and $\forall b{\in}\{1,\ldots,|B_p^{OFF}|\}$, the theoretical $CP^p_{OFF,ON}(B_p^b,B_p^a)$ is given in this case by:

$$CP^p_{OFF,ON}(B_p^b,B_p^a) = \begin{cases} 1 & \text{if } a=b, \\ 0 & \text{otherwise.} \end{cases} \tag{6.1}$$

Introducing $CP^p_{OFF,ON}(B_p^b,B_p^a)$ into (2.8), the obtained theoretical expected value $E(OFF_p/ON_p{\in}B_p^a){=}\hat{B}_p^a$ will be used as the convergence reference. Figure 6.2 illustrates the convergence evolution of $E(OFF_p/ON_p{\in}B_p^a)$ towards these theoretical values for an increasing acq_{time}, where $a{\in}\{6,14\}$ for uniform distributions and $a{\in}\{15,30\}$ for exponential distributions. Several values of the arrival rate λ_p^P are considered with a duty cycle DC_p=0.5.

The results show that $E(OFF_p/ON_p{\in}B_p^a)$ converges more slowly than $E(OFF_p)$ with different speeds for the considered distributions. Considering for instance acq_{time}=4 h, all observed $E(OFF_p/ON_p{\in}B_p^a)$ deviate within 5% of their theoretical values for the uniform case. As far as exponential distributions are considered, $E(OFF_p/ON_p{\in}B_p^a)$ values are deviating in some cases with more than 10% of their theoretical values even after long values of acq_{time}. This is basically due to the higher variability of exponential distributions, which makes the exploration of successive ON/OFF bucket combinations slower. Furthermore, the bucket that contains a specific ON/OFF outcome depends on the corresponding sample mean (i.e., $E(OFF_p)$ or $E(ON_p)$) that adjusts the bucket width. Considering for instance OFF outcomes, the previously observed fluctuations of $E(OFF_p)$, particularly for long $1/\lambda_p^P$ values, rearrange the distribution of OFF outcomes between buckets, which may make some of them empty (i.e., without any outcome).

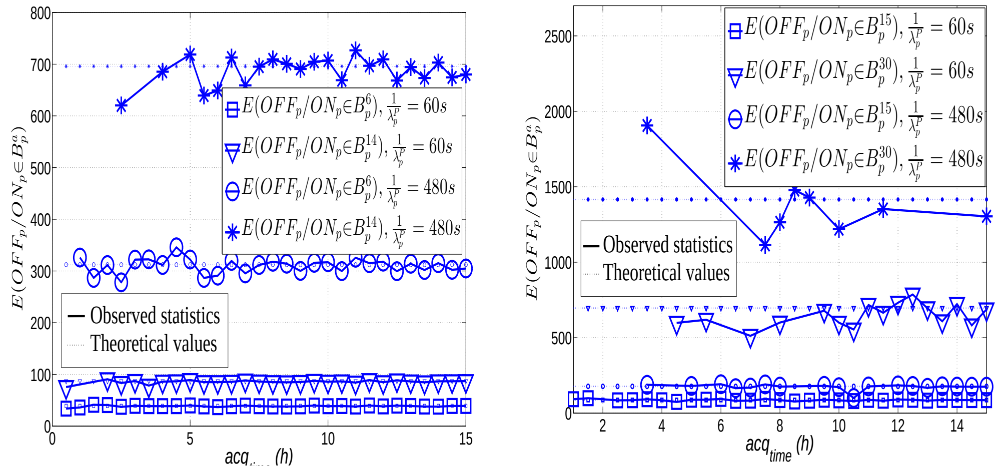

(a) (b)

Figure 6.2: Convergence of $E(OFF_p/ON_p \in B_p^a)$ for some selected values of B_p^a for (a) Uniform distributions and (b) Exponential distributions

6.1.2 Impact on SS performance

To evaluate the impact of the level of convergence achieved in KD statistics on SS performance, the single-application scenario described in Table 3.1 is considered. Specifically, acquisition time (acq_{time}) has been gradually decreased while checking the corresponding impact on the performance previously obtained in Section 3.2.4.1.

Considering the worst case of exponential distributions with $T_{req,1}$=24 s, Figure 6.3 plots performances of $Crit_1$ and $Crit_2$ for fully-dependent data (i.e., q=1). The key observed fact is that SS performance converges much faster than the corresponding KD statistics. As a matter of fact, starting from acq_{time}=3 h, both SS criteria tend to stabilize in spite of the previously observed fluctuations of $E(OFF_p)$ and $E(OFF_p/ON_p \in B_p^a)$ for comparable acq_{time} values. It has been checked and omitted for the sake of brevity that, for lower randomness levels (i.e., uniform distributions), performance tends to stabilize much faster (i.e., acq_{time} of few tens of seconds). This better stability is justified by the fact that even though increasing acq_{time} always improves the estimation accuracy of remaining OFF dur-

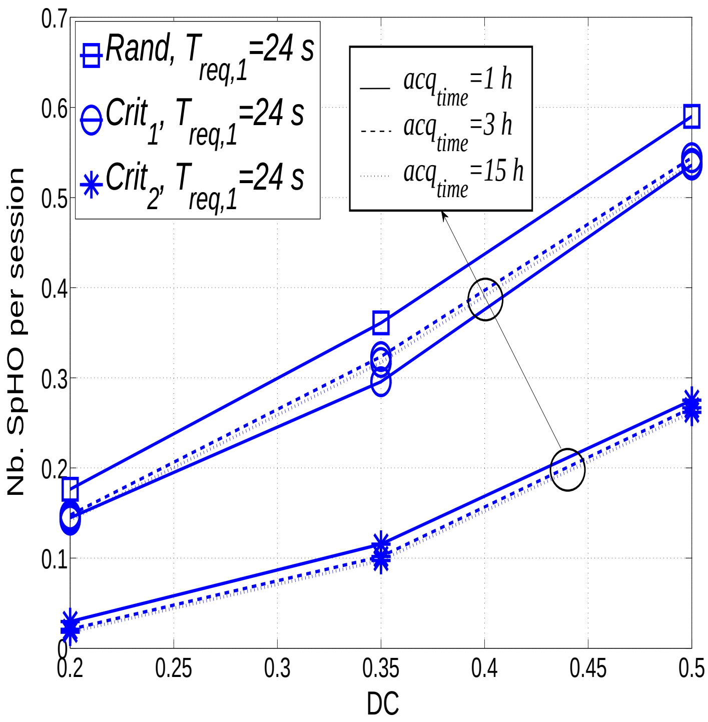

Figure 6.3: Performance sensitivity to acq_{time}, fully-dependent exponential data

ations, introduced gains are usually smaller than the differences observed between OFF durations of spectrum pools, which keeps the selected pool by SS criteria unchanged.

The conducted study show that the proposed framework exhibits good robustness to partial convergence in KD statistics, which defends its practicality.

6.2 Robustness to unknown changes in the scenario

This section proposes to extend the proposed framework to improve robustness in non-stationary environments. The proposed extension is firstly described together with its interactions with the existing modules. Relevance of the extended framework is secondly assessed in front of unexpected changes in the environment.

6.2.1 Reliability tester

To detect relevant changes in KD statistics when operating in non-stationary environments, the functional architecture proposed in Chapter 2 is extended as described in Figure 6.4. The proposed extension strengthens the knowledge management domain with a Reliability Tester (RT) to monitor reliability of KD data. In this respect, whenever a relevant change is detected, KD statistics are regenerated under the new conditions.

In this respect, the RT detects relevant changes by monitoring the pools used by active link sessions. A change is judged as relevant if it has a significant impact on the perceived performance by the end-user evaluated in terms of a set of M KPIs (Key performance Indicators) (e.g., the achievable bit rate $R(l,p)$, the number of SpHOs).

Specifically, the RT procedure computes first, for all $m\in\{1,\ldots,M\}$, an initial estimate of the m-th KPI (denoted as KPI_m) based on its observed sample mean over the established link sessions (let $\overline{KPI_m}$ denote this initial mean estimate). Then, the RT gradually increases the sample window size (denoted as S) as new link sessions are established and updates the observed sample mean ($\overline{KPI_m}$), sample variance ($\overline{\sigma_m}$) and γ confidence interval $\left[\overline{KPI}_{m,min},\overline{KPI}_{m,max}\right]$ defined as the interval that fulfills the following relationship:

$$Prob\left[KPI_m\in\left[\overline{KPI}_{m,min},\overline{KPI}_{m,max}\right]\right]=\gamma \tag{6.2}$$

Assuming large-sample conditions (typically in the order of $S>30$), $\overline{KPI}_{m,min}$ and $\overline{KPI}_{m,max}$ are given by:

$$\overline{KPI}_{m,min}=\overline{KPI}_m-z_{(1-\gamma)/2}\frac{\overline{\sigma_m}}{\sqrt{S}} \tag{6.3}$$

$$\overline{KPI}_{m,max}=\overline{KPI}_m+z_{(1-\gamma)/2}\frac{\overline{\sigma_m}}{\sqrt{S}} \tag{6.4}$$

where $z_{(1-\gamma)/2}=\phi^{-1}(1-\frac{1-\gamma}{2})$ and $\phi(.)$ denotes the cumulative normal distribution function.

Note that as the sample size window S increases, $\overline{KPI}_m$ tends to converge and the interval $\left[\overline{KPI}_{m,min},\overline{KPI}_{m,max}\right]$ gets narrower.

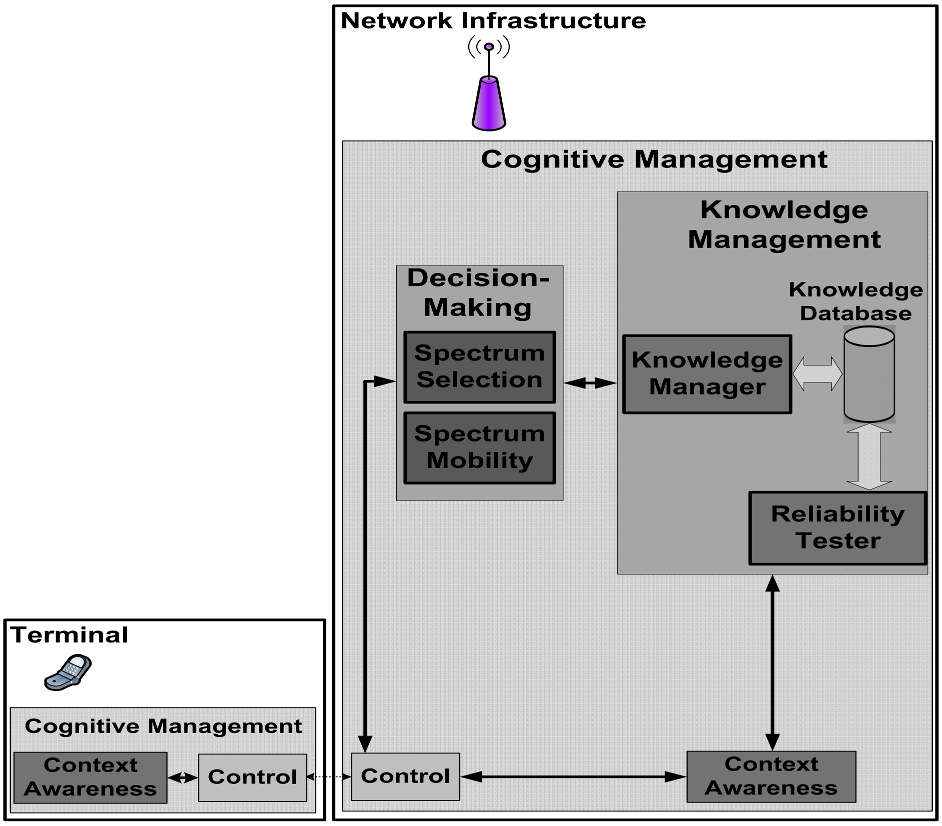

Figure 6.4: Proposed extension for non-stationary environments

To achieve a good level of convergence in the initial estimate of KPI_m, the window size S is progressively increased until the width of the γ confidence interval becomes smaller than a fraction $0<\rho<1$ of the sample mean ($\overline{KPI_m}$), that is:

$$\overline{KPI}_{m,max} - \overline{KPI}_{m,min} < \rho \cdot \overline{KPI_m} \tag{6.5}$$

Note that decreasing ρ would always improve convergence reliability, but would result in much more time before the condition in (6.5) is met. Therefore, the smallest value of ρ that would achieve an acceptable level of convergence in each KPI_m can be used in practice. For instance, for the scenario and set of KPIs considered in Section 6.2.2.1, it has been checked that all considered KPIs are achieving a good level of convergence around ρ=0.1.

After meeting the stopping rule of (6.5), $\overline{KPI_m}$ becomes the initial estimate and the current value S of the window size is kept.

Then, the RT starts a procedure of monitoring possible changes in the average value of KPI_m based on the statistical technique known in the literature as binary hypothesis testing [72]. Specifically, a null hypothesis (H_0) is introduced to claim that there is no difference between the initial average value ($\overline{KPI_m}$) and a new average value continuously updated based on a moving window of the same size S. Let $\widehat{KPI_m}$ denote this new average value, $\widehat{\sigma_m}$ be its sample variance and $\left[\widehat{KPI}_{m,min},\widehat{KPI}_{m,max}\right]$ be the corresponding confidence interval. As long as H_0 holds, KD statistics are assumed to be valid. On the contrary, an alternative hypothesis (H_1) claims that there is a difference between the initial and new average values, and thus KD statistics are no longer valid.

Nevertheless, the difference that may be observed between the two average values $\overline{KPI_m}$ and $\widehat{KPI_m}$ does not always imply invalidity of KD statistics but may be just the result of the pure chance of the experiment. Therefore, the hypothesis testing procedure should ensure with a certain probability that only those differences caused by an actual change in the scenario (e.g., appearance of a new external interferer or change in the position of the transmitter and/or receiver of a given link) are detected. This means, on the one hand, that the probability of selecting H_1 when H_0 actually holds (the so-called Type I error in hypothesis testing terminology [72]) should be kept below a maximum level α. On the other hand, the probability of selecting H_0 when H_1 actually holds (the so-called type II error) should also be kept below a maximum level β.

In general, different detection strategies may be followed to strike a balance between Type I and II errors. More specifically, it has been shown in [73] that the detection strategy should be designed based on the standardized difference (D_m) between $\overline{KPI_m}$ and $\widehat{KPI_m}$ and the ratio of the largest to smallest sample variance (k_m), defined as

$$D_m = \frac{|\overline{KPI_m} - \widehat{KPI_m}|}{\sqrt{\overline{KPI_m}^2 + \widehat{KPI_m}^2}} \tag{6.6}$$

$$k_m = \frac{max(\overline{\sigma_m}, \widehat{\sigma_m})}{min(\overline{\sigma_m}, \widehat{\sigma_m})} \tag{6.7}$$

For the scenario considered in Section 6.2.2.1, it has been checked that, on the one hand, the considered changes typically result in high values of the standardized difference D_m. On the other hand, the ratio of sample variances k_m is typically close to 1 because both $\overline{KPI_m}$ and $\widehat{KPI_m}$ are determined based on the same window size S. Under these conditions (high D_m and low k_m), the overlap decision method, that selects H_0 when the confidence intervals of the two average values overlap and H_1 otherwise, has been shown in [73] to exhibit a very low Type I error and an acceptable Type II error. Consequently, it has been retained in this paper. The reader is referred to Appendix C for a detailed analysis of Type I and II errors.

Algorithm 6.1 describes the general RT procedure for detecting changes. After testing for changes in each of the converged KPIs in lines 5-11, obtained hypothesis testing results are combined to decide about reliability of the whole KD data according to the procedure described in lines 13-17. Specifically, if H_1 is selected for at least one of the considered KPIs, the combined test selects H_1 (line 14).

Note that the procedure described in lines 13-17 is adequate to detect changes that occur in pools that are used with some regularity by active links. However, it is not valid to detect changes occurring in pools that are never assigned. To overcome this issue, when H_0 is selected, the procedure described in lines 18-30 is carried out for each pool that remains unused by any of the considered links for more than a certain period of time named T_Inact. Specifically, a total of N forced measurements are taken to obtain the value of the actual $F_{l,p}$ state that is compared against the estimate $\hat{F}_{l,p}$ determined by the KM to test for possible changes (line 25) and select H_1 in case of change (line 26).

The algorithm is concluded by regenerating KD data (line 32) if H_1 is selected following a change in converged KPIs (line 7) or inactive pools (line 26). Then, the RT sets S to zero and loops back to the sequential analysis procedure described in the beginning of the section to recalculate all initial estimates $\{\overline{KPI_m}\}_{1\leq m\leq M}$ under the new conditions (line 33). In this case, the KM will continue using old KD statistics until the new statistics become available.

It is worth mentioning that the combination of tests of the different KPIs (as done in lines 13-17) increases in general the Type I error as more tests are combined [74]. To avoid useless generation of KD data, it is proposed to upper-bound the number of KPIs that may be combined to guarantee some Type I error for the whole test (α_{max}) based on the conservative Bonferroni correction [74]:

$$M_{max}=\left\lfloor\frac{\alpha_{max}}{Type\_I_{indiv}}\right\rfloor \tag{6.8}$$

Algorithm 6.1 The RT procedure of detecting changes

for $m = 1 \to M$ **do**
  if condition in (6.5) holds for KPI_m **then** % Checking convergence of KPIs
    $Converge(KPI_m) = TRUE$
  end if
  if $Converge(KPI_m) = TRUE$ **then** % Individual Tests for converged KPIs
    if $\left[\overline{KPI}_{m,min}, \overline{KPI}_{m,max}\right] \bigcap \left[\widehat{KPI}_{m,min}, \widehat{KPI}_{m,max}\right] = \emptyset$ **then**
      Select H_1;
    else
      Select H_0;
    end if
  end if
end for
if H_1 is selected for at least one KPI_m **then** % Multiple Tests for detecting changes
  Select H_1;
else
  Select H_0;
end if
if (H_0 is selected) AND ($\Delta k_{l,p} > T\_Inact$) **then** % Detecting changes in inactive pools
  for $n = 1 \to N$ **do**
    Force a measurement of $F_{l,p}$;
    if $F_{l,p} \neq \hat{F}_{l,p}$ **then**
      $count{+}{+}$;
    end if
  end for
  if $count = N$ **then**
    Select H_1;
  else
    Select H_0;
  end if
end if
if H_1 is selected **then** % Perform required updates if a change is detected
  Regenerate KD statistics;
  Recalculate $\{\overline{KPI_m}\}_{1 \leq m \leq M}$;
end if

where $\lfloor . \rfloor$ and $Type\_I_{indiv}$ denote the floor function and the Type I error of each individual test, respectively.

For instance, by setting α_{max}=0.05, k_m=1, D_m=5, and γ=0.95, (6.8) yields M_{max}=8.

Note that M_{max} provides an upper bound on the number KPIs that may be combined associated with the maximum tolerable Type I error (α_{max}). Nevertheless, much smaller Type I errors may be obtained in practice. From the one hand, the considered conservative Bonferroni correction assumes the worst case of independent individual tests to guarantee the target α_{max}. This means, whenever tests are dependent, smaller Type I errors are in general observed. On the other hand, by properly selecting the KPIs that are most likely to be altered following the considered changes, it may be enough to combine M<M_{max} KPIs to detect changes with the corresponding decrease in the Type I error. For instance, for the scenario considered in Section 6.2.2.1, by using only M=4<M_{max} dependent KPIs, the considered change has been detected with a much smaller Type I error compared to the target α_{max}. General strategies for optimizing the set of combined KPIs are out of the scope of this dissertation.

Finally, it is worth pointing out that the parameters N and T_Inact that are used by the procedure of lines 18-30 should be properly set to efficiently detect changes in inactive pools. On the hand, T_Inact should be longer than the inter-assignment time of pools to the different links for the considered scenario. On the other hand, N should strike a balance between speeding up the detection procedure (i.e., small N) and minimizing the number of Type I errors (i.e., wrongly select H_1 in line 26) due to the imperfection of the KM in estimating $F_{l,p}$ values (i.e., high N). In practice, N should be set to a slightly higher value than the maximum number of consecutive errors that may be made by the KM. In this paper, by setting N=200 and T_Inact=10 *h*, we were able to quickly detect the considered change in inactive pools ($Change$ #2 defined in Section 7.2) without any Type I error.

Table 6.1: Interference conditions of spectrum pools around the considered change

pool	Before the change				After the change			
	I_0		I_1		I_0		I_1	
	Duration (*h*)	$R(l,p)$ (*Kbps*)	Duration (*min*)	$R(l,p)$ (*Kbps*)	Duration (*h*)	$R(l,p)$ (*Kbps*)	Duration (*min*)	$R(l,p)$ (*Kbps*)
1	∞	512	-	-	7.5	1536	30	96
2	∞	512	-	-	∞	512	-	-
3	7.5	1536	30	96	∞	512	-	-
4	0.5	1536	2	96	0.5	1536	2	96

6.2.2 Robustness analysis

To assess the effectiveness of the proposed RT to improve robustness in non-stationary environments, this section firstly conducts an analysis of its capability to detect changes, and secondly assesses the corresponding impact on SS performance.

6.2.2.1 Assumptions

The simulation model of Section 5.3.1 is considered. To assess robustness in front of changes in interference conditions of the different pools, the simulation is assumed to start with some specific statistical patterns of the interference PSD $I(p)$ for the different pools. Then, at a certain point of time, interference patterns are altered in some pools. Table 6.1 specifies durations of the two possible states of $I(p)$ together with the corresponding achievable bit rates before and after the change. Note that, after the change, interference conditions of pools $\#1$ and $\#3$ are swapped.

To assess the impact of RT support on SS performance, the following variants are compared:

- *SS*: This approach makes use of the SS, KM and SM algorithms, but does not include the RT to detect possible changes and regenerate KD statistics in case.

- *SS+RT*: This is the complete approach that includes the SS, KM, SM and RT functionalities.

Finally, the procedure of detecting changes described in Section 6.2.1 is performed by monitoring the following 2 KPIs observed for each link l (which yields a total of M=$2L$=4 KPIs):

- The average dissatisfaction probability, $Dissf(l)$.
- The average number of SpHOs performed per session, $SpHO(l)$.

The system is observed till establishing $65,000$ sessions for each link. The change in interference conditions occurs for all simulations after establishing $22,000$ sessions for each link. The other simulation parameters are ξ=5, K=1, $\delta_{1,p}$=0.2, $\delta_{2,p}$=0.9, ρ=0.1, α_{max}=0.05, k_m=1, D_m=5, γ=0.95, T_Inact=10 *h*, and N=200.

6.2.2.2 The RT capability to detect changes

This section evaluates the capability of the RT to detect relevant changes in the radio and interference conditions of the different spectrum pools.

Figure 6.5(a) plots the temporal evolution of the initial RT estimate of the number of SpHOs/session for link #2 ($\overline{SpHO(2)}$) with the corresponding confidence interval shown in dashed lines for a traffic load of L_l=1 *Er* for $l \in \{1, 2\}$. The time evolution on the x-axis is shown in terms of the number of established link #2 sessions according to the generation process described in Section 5.3.1. Note that only $SpHO(2)$ is considered because this is the KPI for which H_1 is selected by the RT after the change occurs.

The results show that $\overline{SpHO(2)}$ tends to converge as more link #2 sessions are established. Specifically, the stopping rule of (6.5) is met after establishing around $3,700$ sessions. At this point of time, the initial $\overline{SpHO(2)}$ estimate and its confidence interval are frozen, and the RT starts to watch the second moving-average estimate ($\widehat{SpHO(2)}$).

Figure 6.5(b) plots the temporal evolution of $\widehat{SpHO(2)}$ and its corresponding confidence interval around the considered change. The initial $\overline{SpHO(2)}$ estimate

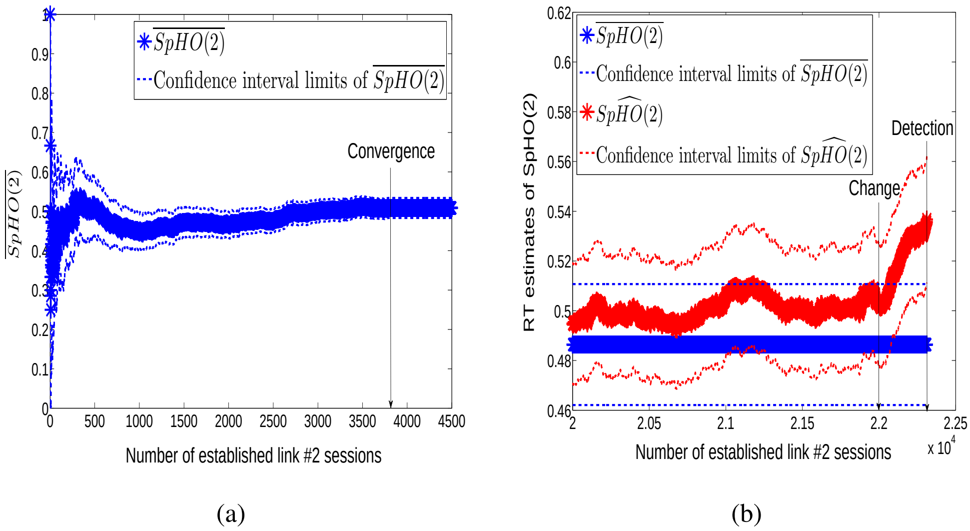

Figure 6.5: Evolution of RT estimates of $SpHO(2)$: (a) initially and (b) around the considered change.

is also shown for comparison purposes. The results show that, before the change occurs, the moving average estimate $\widehat{SpHO(2)}$ oscillates close to $\overline{SpHO(2)}$ due to the intrinsic randomness of the radio environment. Nevertheless, the RT disregards these oscillations and selects H_0 because confidence intervals of the two estimates are still overlapping. After the change occurs, $\widehat{SpHO(2)}$ starts to deviate much from $\overline{SpHO(2)}$ till their confidence intervals no longer overlap. At this moment, H_1 is selected for $SpHO(2)$ and the considered change is detected by the RT. It is worth mentioning that only one wrong change (Type I error) is detected during the whole simulation, which corresponds to Type I error$=1.6{\cdot}10^{-5}$. This much smaller value compared to α_{max} is because, on the one hand, only $M{=}4{<}M_{max}{=}8$ KPIs have been used. On the other hand, the individual tests associated with the considered KPIs are dependent since the considered change in interference conditions has a joint impact on all KPIs. Therefore, a much better performance can be achieved with respect to the conservative Bonferroni correction as previously explained Section 6.2.1.

In summary, the RT probabilistic detector, based on hypothesis testing, enables to properly filter those changes related to the intrinsic randomness of the radio environment and efficiently detect relevant changes in the scenario.

6.2.2.3 Performance evaluation

This section evaluates the performance of the proposed strategy in front of changes in interference conditions under which KD statistics were generated.

Figure 6.6(a) shows the online evolution of the average number of SpHOs performed per link $\#2$ session ($SpHO(2)$). A traffic load of L_l=1 *Er* is initially considered for both links. To analyze the impact of RT, both variants *SS* and *SS+RT* defined in Section 6.2.2.1 are considered. The corresponding dissatisfaction probability ($Dissf(2)$) is not shown because it is exhibiting a similar behavior.

The results show that, after the change in interference conditions occurs, the use of the RT functionality results in a significant reduction of the number of performed SpHOs (Figure 6.6(a)). At the end of the simulation, the observed reduction is of about 40$\%$. The reason for this improvement is that, before the change, both strategies are mainly assigning pools $\#1$ and $\#2$ to link $\#1$ and pools $\#3$ and $\#4$ to link $\#2$. After the change, the strategy *SS* without any support from the RT still relies on the out-of-date KD statistics previously generated, so it continues to exclude pool $\#1$ and assign pool $\#3$ to link $\#2$ sessions. This turns out to be a wrong decision because, according to the new conditions after the change, pool $\#1$ should be assigned instead of pool $\#3$ that becomes, from now on, unable to support the bit rate requirements of link $\#2$. Correspondingly, much more frequent SpHOs are required to change pool $\#3$ whenever it is assigned. On the contrary, when RT is used (*SS+RT*), new KD statistics are generated after detecting the change. As a consequence, $\hat{F}_{l,p}$ estimates provided by the KM prevent *SS+RT* from further assigning pool $\#3$ to link $\#2$ in the future. Instead, pool $\#1$, which allows a much higher bit rate, is assigned to link $\#2$ sessions. This results in a significant gain in the number of performed SpHOs (Figure 6.6(a)). Note that the performance achieved with RT after the change remains approximately the same as before the change. This equal performance is because the change shown in Table 6.1 does not change the overall set of pools but just swaps interference patterns of pools $\#1$ and $\#3$. Consequently, if KD statistics are properly updated after the change, the strategy *SS+RT* should be able to find the proper combination of pools and active links that keeps the same performance that existed before the change.

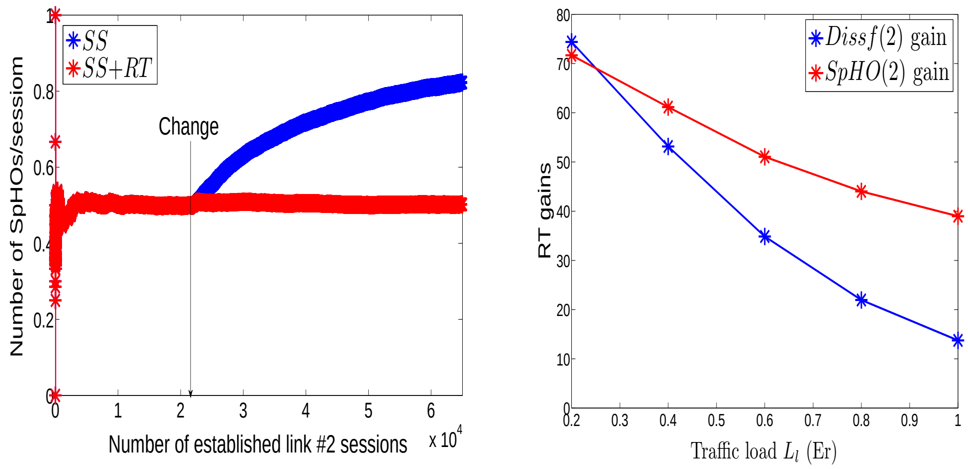

(a) (b)

Figure 6.6: Analysis of robustness for link #2 performance in terms of (a) Number of SpHOs/session and (b) Impact of traffic load on RT gains

Next, the impact of the traffic load of CR applications is analyzed. RT gains are defined as the percentages of reduction in the number of performed SpHOs and dissatisfaction probability of link #2, respectively, when using *SS+RT* with respect to *SS*. Figure 6.6(b) plots RT gains observed at the end of the simulation (i.e., after establishing $65,000$ sessions) for different traffic loads.

The results show that, for low traffic loads, the RT is introducing significant gains (around 75%) in terms of both $SpHO(2)$ and $Dissf(2)$. This improvement is because, after the change, *SS+RT* is able to disregard pool #3 and assign instead pool #1 to link #2 based on the new KD statistics as previously explained. As the traffic load increases, RT gains gradually decrease to reach 40% and 15% in terms of $SpHO(2)$ and $Dissf(2)$, respectively. This reduction is because, as more link sessions are established, spectrum pools become used most of the time, which marginalizes the impact of the wrong assignments that may be performed by *SS* based on old KD statistics.

6.3 Chapter summary

This chapter has called into question reliability of KD data by introducing two sources of uncertainty, namely imperfection of the acquisition process and non-stationarity of the environment.

An assessment of robustness to the former source has revealed that, for a given acquisition time (acq_{time}), the level of convergence achieved in KD statistics strongly depends on the order of KD statistics and level of primary activity variability. For low randomness levels (i.e., uniform distributions), first-order statistics (e.g., $E(OFF_p)$) achieve good convergence levels around acq_{time}=2 *h*, while second-order statistics (e.g., $E(OFF_p/ON_p{\in}B_p^a)$) deviate with less than 5% of their theoretical values starting from acq_{time}=4 *h*. For high randomness levels (i.e., exponential distributions), only partial levels of convergence can be achieved by all statistics after even long values of acq_{time}. An analysis of the corresponding impact on performance has revealed that SS performance converges much faster than the corresponding KD statistics: it stabilizes for acq_{time} of few tens of seconds and few hours for low and high randomness levels, respectively. This faster convergence is because, even with a rough estimation of remaining OFF durations, the best pools can be correctly selected due to the large differences observed between OFF durations of spectrum pools.

To improve robustness to the latter source of uncertainty, the framework has been extended with a RT that detects relevant changes in the environment based on hypothesis testing, and updates KD statistics accordingly. The proposed RT is able to disregard most of changes due to the intrinsic randomness of the radio environment and efficiently detect actual changes in the scenario. Thanks to the RT support, the proposed spectrum management strategy exhibits substantial robustness when the environment becomes non-stationary, obtaining performance improvements of up to 75% with respect to the reference case that does not make use of the RT.

7. Applicability Example: The Future Digital Home

To evaluate the practicality of the proposed framework, the realistic Digital Home (DH) environment introduced in [75] is considered. The DH environment offers new opportunities to improve efficiency through provisioning new management services. The future DH is expected to consist of not only computing devices with communication capabilities (e.g., desktop PCs, laptops and the like), but also consumer electronics (e.g., TV sets with wireless interfaces, digital media servers, camcorders, game consoles, home security and automation systems), as well as more traditional appliances (e.g., washing machines and fridges) equipped with communication interfaces to enable, for example, remote control and monitoring. The provisioning of wireless management services in the DH requires an efficient exploitation of all possible sources of available spectrum resources, such as license-exempt ISM bands and Ultra High Frequency (UHF) bands (i.e., TV white spaces) through e.g., the ECMA-392 radio networking standard [76] and also the exploitation of licensed spectrum (e.g., spectrum licensed to a mobile network operator providing management services in the DH) as a mechanism for enhancing QoS provision to some DH connections.

7.1 Considered environment

The considered indoor environment is a single floor of dimensions $16.8\ m \times 30.4\ m$ organized in six different rooms, where a set of radio links need to be established from co-located transmitters to DH node receivers that may be located anywhere in the floor plan shown in Figure 7.1(a).

The following $P=3$ candidate spectrum pools are considered:

- Pool $\#1$: $BW_1=20$ *MHz* bandwidth in the 2.4 GHz ISM license-exempt band;
- Pool $\#2$: $BW_2=16$ *MHz* bandwidth in the 600 MHz TV White Space (TVWS) band that can be operated opportunistically;
- Pool $\#3$: $BW_3=20$ *MHz* bandwidth in a 2.6 GHz licensed band of the Mobile Network Operator (MNO) serving as the DH management service provider.

The radio and interference conditions experienced in each of these pools are described as follows:

- Radio propagation path losses are modeled using the COST 231 indoor propagation model [77] that is given by:

$$PL(dB) = L_0 + 20 \log f(Mhz) + 10\sigma_p \log d(m) + N_w \cdot L_w \tag{7.1}$$

  where $L_o=-27.55$ *dB*, σ_p is the propagation coefficient at distance $d(m)$, N_w is the number of traversed walls between transmitter/receiver and L_w is the attenuation of one wall dependent on its material and width. Based on the measurements performed in [75], the propagation model can be properly tuned to the considered indoor environment by setting $\sigma_p=2.6$ and $L_w=5.1$ *dB*.

- The transmitted power is assumed to be 20 *dBm* in all pools.

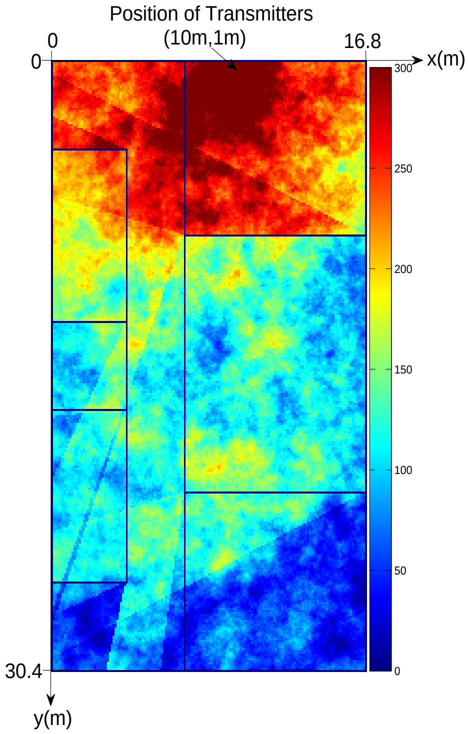

(a)

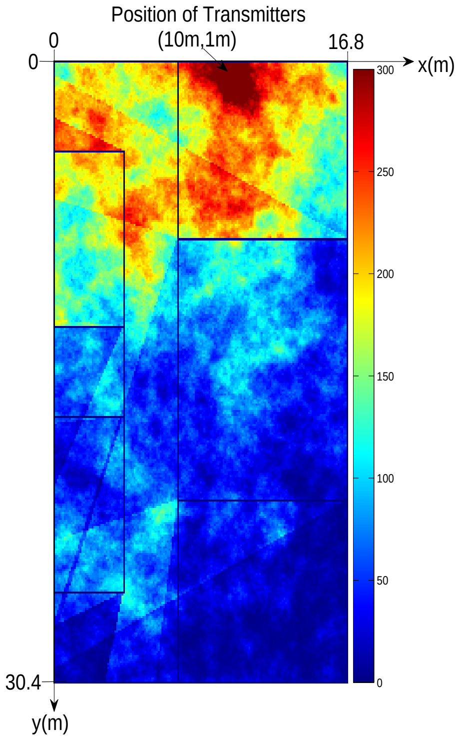

(b)

Figure 7.1: Achievable bit rates (Mbit/s) with pool #1 in (a) the low interference state I_0 and (b) the high interference state I_1

- A heterogeneous interference situation is considered in which the sum of the noise and interference PSD $I(p)$ experienced in each pool $p \in \{1, \ldots, P\}$ follows the two- state discrete time Markov chain described in Section 5.3.1. Furthermore, it is assumed that the external interference evolution is not affected by the established links within the DH and the associated decisions of the SS framework.

- In our specific case, it is assumed that pools #1 and #2 alternate between $I_0(p)$ and $I_1(p)$ randomly with transition probabilities of $P_{10}(1){=}55.5{\cdot}10^{-5}$ and $P_{01}(1){=}3.7{\cdot}10^{-5}$ for pool #1 and $P_{10}(2){=}833.33{\cdot}10^{-5}$ and $P_{01}{=}55.5{\cdot}10^{-5}(2)$ for pool #2. Based on these probabilities, the average durations of the low interference state for pools #1 and #2 are $\overline{I_0(1)}{=}7.5\,h$ and $\overline{I_0(2)}{=}0.5\,h$, respectively, while the average dur-

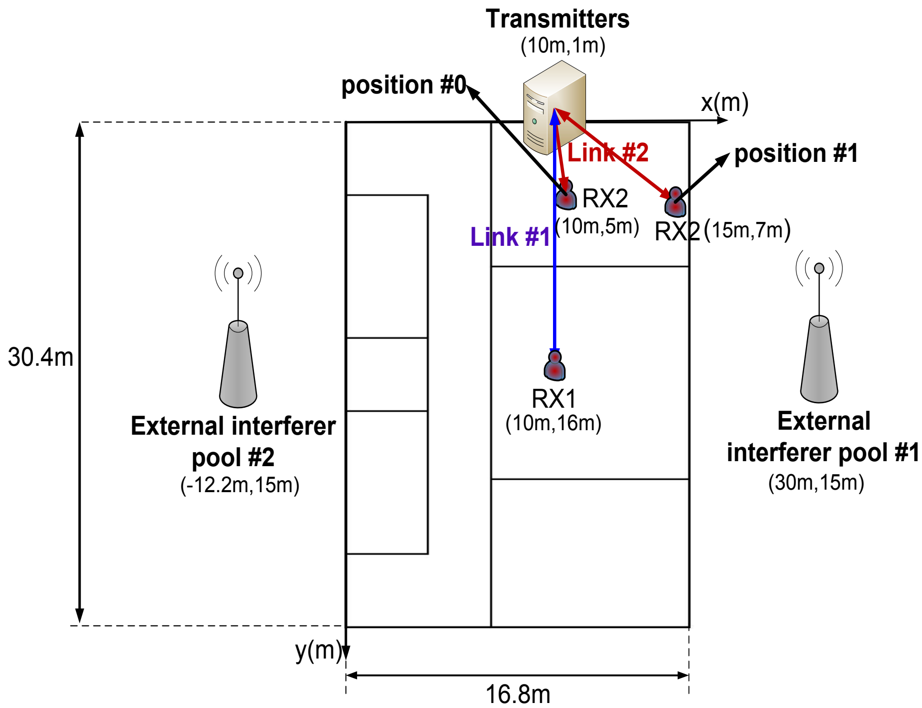

Figure 7.2: Positions of the different links

ations of the high interference state for pools #1 and #2 are $\overline{I_1(1)}$=0.5 *h* and $\overline{I_1(2)}$=2 *min*, respectively. In turn, pool #3, which relies on the MNO interference control mechanisms, is assumed to be always free of interference.

- External interferers of pools #1 and #2 are assumed to transmit with power P=10 *dBm* and P=20 *dBm* in the low and high interference states, respectively. They are located at coordinates (30 *m*, 15 *m*) and (−12.2 *m*, 15 *m*), respectively (see Figure 7.2).

The proposed model captures well richness of the considered DH environment and the diverse radio and interference conditions that may be experienced within it. As illustrative example, Figure 7.1(a) and Figure 7.1(b) represent a spatial map of the Shannon-bound achievable bit rates (Mbit/s) using pool #1 in the low and high interference states, respectively. The map clearly illustrates the extent to which interference conditions affect the achievable bit rates in each position within the DH environment.

Table 7.1: Average achievable bit rates (Mbps)

	pool #1		pool #2		pool #3
	State I_0	State I_1	State I_0	State I_1	State I_0
Link #1	88.8	32.5	106.6	55.45	229.3
Link #2 (position #0)	228	161.9	244.2	191.2	361.7
Link #2 (position #1)	157.7	92.4	239.8	187.2	285.6

Performance is evaluated considering L=2 radio links placed in the positions shown in Figure 7.2 under the following assumptions:

- The link #1 receiver is situated in a fixed position, while the link #2 receiver may jump between positions #0 and #1 indicated in Figure 7.2. Link #1 is associated with low-data-rate sessions ($R_{req,1}$=20 *Mbps* and $T_{req,1}$=2 *min*), while link #2 is associated with high-data-rate sessions ($R_{req,2}$=200 *Mbps* and $T_{req,2}$=20 *min*).
- The l-th link generates sessions with constant duration $T_{req,l}$ and inactivity periods exponentially distributed with average $1/\lambda_l^L$ for each link $l \in \{1, 2\}$.
- To smooth short-term variability of interference conditions, $R(l, p)$ values experienced within each of the $I_0(p)$ and $I_1(p)$ states are averaged. The average bit rates achievable in the different pools are presented in Table 7.1.
- Preference factors are set to $\pi_{l,1}$=$\pi_{l,2}$=0.9 and $\pi_{l,3}$=0.1, $l \in \{1, 2\}$ to reflect the will of the DH communications manager to limit the use of the MNO band by exploiting as much as possible either the ISM or TVWS bands.

The system is observed in steps of 1 *s* till establishing $65,000$ sessions for each link. The first fittingness factor function of (2.10) is considered with ξ=5, $\delta_{1,p}$=0.5, Thr_LOW=0.9 and Thr_HIGH=0.1. The other simulation parameters are ρ=0.25, α_{max}=0.05, k_m=1, D_m=5, γ=0.95, T_Inact=10 *h*, and N=200.

7.2 Model of non-stationary conditions

To assess robustness to changes in radio and interference conditions of the different spectrum pools, it is assumed that the position of the link #2 receiver may jump during system operation between the two positions indicated in Figure 7.2 according to one of the following changes:

- *Change #1*: the link #2 receiver is initially placed in position #0, and then moved to position #1.
- *Change #2*: the link #2 receiver placed in position #1 is moved back to position #0.

Unlike position #0, where both LOW and HIGH $F_{l,p}$ values are observed by link #2 using pool #1 in the high and low interference states, respectively, position #1 is so close to the external interferer of pool #1 that only LOW values are observed regardless of the interference state.

7.3 Performance indicators

To assess performance of the proposed strategy, the following KPIs are considered:

- $Dissf(l,p)$: Dissatisfaction probability of link l in using pool p, defined as

$$Dissf(l,p) = Prob\left[R(l,p) < R_{req,l}\right] \tag{7.2}$$

- $Usage(l,p)$: Fraction of time for which pool p is used by link l sessions.
- $Regret(l,p)$: Regret of link l in using pool p to capture the fulfillment of pool preference constraints. It is defined as the probability that there exists another available pool p' able to equally fulfill the bit rate requirements of link l with higher preference than pool p, weighted by $Usage(l,p)$, that is:

$$Regret(l,p) = Usage(l,p) \cdot Prob[\exists p' \in Av\_Pools/(R(l,p') > R_{req,l}) \\ AND(R(l,p) > R_{req,l}) AND(\pi_{l,p'} > \pi_{l,p})] \tag{7.3}$$

- $Global\_Eff$: Global system efficiency defined as the weighted sum of the individual efficiencies of the different links weighted by their corresponding traffic loads in Er (L_l) that is:

$$Global\_Eff = \frac{\sum_{l \in \{1,\ldots,L\}} L_l \cdot Eff_l}{\sum_{l \in \{1,\ldots,L\}} L_l} \tag{7.4}$$

where $Eff(l)$ is the individual efficiency of link l operation that combines the degree of satisfaction and fulfillment of preference constraints, and is defined as

$$Eff(l) = \sum_{p \in \{1,\ldots,P\}} (1 - Dissf(l,p))\,(Usage(l,p) - Regret(l,p)) \qquad (7.5)$$

- *Nb. SpHOs/session*: The total number of SpHOs performed per link session.

Furthermore, the RT detection of changes described in Section 6.2.1 is performed based the following subset of KPIs observed for each link l:

- The average dissatisfaction probability, $Dissf(l)$.
- The average number of SpHOs performed per session, $SpHO(l)$.
- The average fraction of using pool #3, $Usage(l, 3)$.

7.4 Performance evaluation

This section conducts a performance evaluation study to (1) benchmark performance of the *SS+RT* strategy defined in Section 6.2.2.1 with respect to the reference *Rand* and *Optim* schemes defined in Section 5.3.2 and (2) assess the extent to which preference constraints in using the different bands are met by each scheme. For the sake of simplicity, the model of non-stationary conditions described in Section 7.2 is initially not considered. In this respect, it is assumed that link receivers are kept in the fixed positions shown in Figure 7.2 with link #2 in position #0, and that interference conditions remain stationary, which means that *SS+RT* is equivalent to *SS*.

Figure 7.3(a) plots the global efficiency ($Global\_Eff$) of the proposed *SS+RT* strategy and reference *Rand* and *Optim* schemes as a function of the total offered traffic load in bps defined in (5.9). For a better analysis of the impact of the different factors influencing $Global\_Eff$, Figure 7.3(b) and Figure 7.3(c) plot the dissatisfaction level of link #2 ($Dissf(2)$) and the regret of link #2 in using the least-preferred pool #3 ($Regret(2, 3)$), respectively. The results for link #1 are

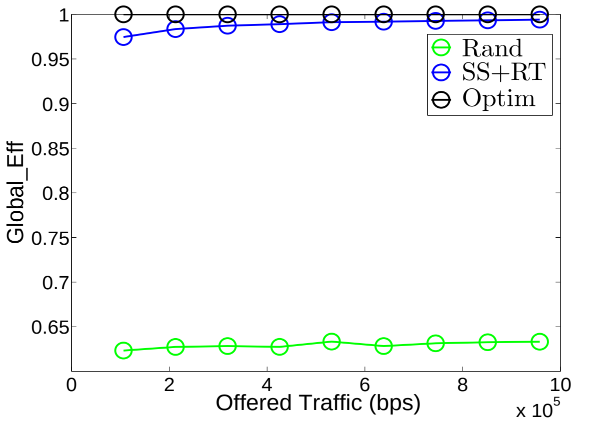

(a)

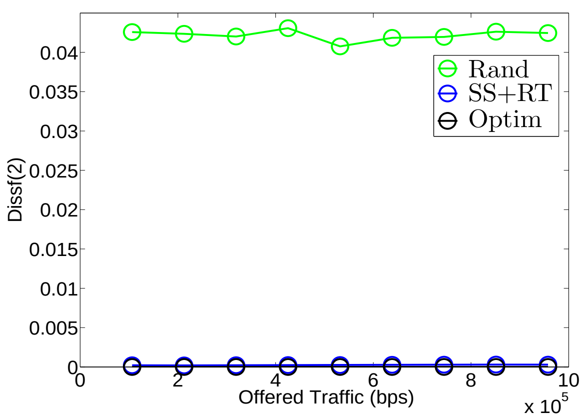

(b)

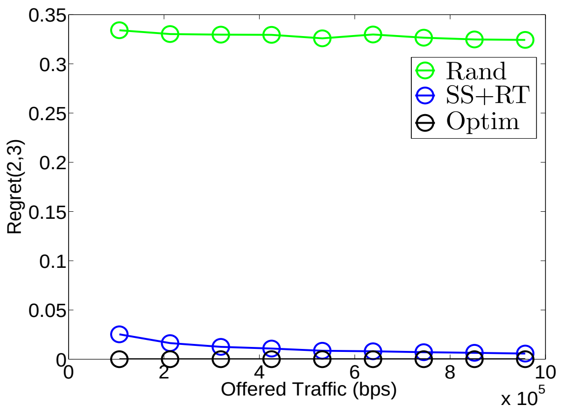

(c)

Figure 7.3: Performance analysis of *SS+RT* in terms (a) Global efficiency, (b) $Dissf(2)$ and (c) $Regret(2,3)$

not presented because it is always satisfied (i.e., the bit rate is always above the requirement of 20 *Mbps*) and it never uses pool #3.

The results in Figure 7.3(a) show that the proposed strategy (*SS+RT*) leads to a substantial increase of the global efficiency compared to *Rand* (gain up to 55%). This improvement is because, on the one hand, $\hat{F}_{l,p}$ estimates provided by the KM together with the SM support help to assign the most suitable pools for link #2 sessions, which reduces the risk of being dissatisfied as reflected in Figure 7.3(b). On the other hand, the prioritization of pools #1 and #2 tends to avoid using pool #3 as much as possible, which significantly improves the regret of using it (Figure 7.3(c)).

Moreover, the proposed *SS+RT* strategy performs very closely to the upper-bound optimal scheme in terms of the global efficiency for most of traffic loads, mainly thanks to the support of the KM and SM components. The small deviation observed for low traffic loads is mainly due to the slight loss in the regret of using pool #3 as observed in Figure 7.3(c).

7.5 Signaling cost

To further assess the proposed strategy in terms of the cost associated with the reconfigurations performed by the SM functionality, Figure 7.4 plots the average number of SpHOs per session (*Nb. SpHOs/session*) experienced by *SS+RT* for each of the two possible triggers of SM (i.e., a link release or change in $F_{l,p}$).

The results show that *Nb. SpHOs/session* is below 0.06 for all considered traffic loads. Compared to the previously observed result in Figure 5.6(b), there is a much higher fraction of SpHOs caused by changes in $F_{l,p}$ values than by link releases for even high traffic loads. This new distribution is because most of the average durations of the low and high interference states considered in Section 7.1 are comparable to durations of CR applications, which makes experiencing a change in $F_{l,p}$ during a given link session very likely. Furthermore, for the considered traffic conditions with at most two simultaneous active links, the probability of experiencing an SpHO due to a link release is small.

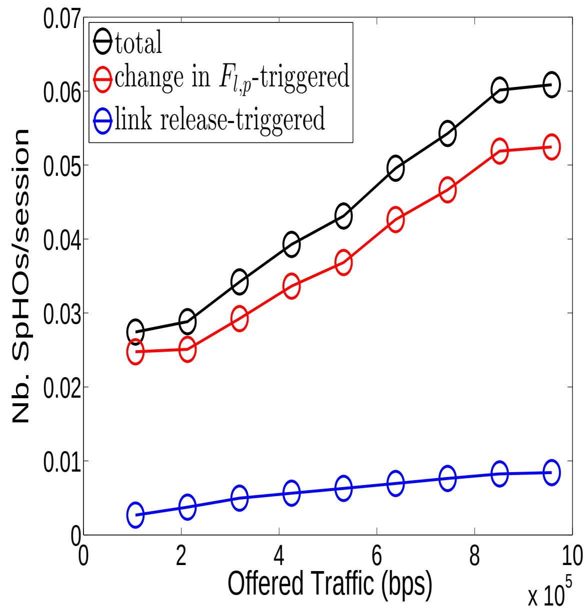

Figure 7.4: SpHO performance of *SS+RT*

7.6 Robustness analysis

This section evaluates robustness of the proposed strategy when the initial radio and interference conditions under which KD statistics were generated no longer hold. For that purpose, the two possible changes in the position of link #2 receiver described in Section 7.2 are introduced in two different simulations.

Let us consider first *Change #1*, in which the receiver is moved to a position with worse interference conditions for pool #1. Figure 7.5(a) shows the online evolution of the dissatisfaction level of link #2 ($Dissf(2)$). The time evolution on the x-axis is shown in terms of the number of established link #2 sessions according to the generation process described in Section 7.1 with the position change occurring after $9,750$ sessions. To analyze the impact of RT, both *SS* and *SS+RT* variants are compared. Only link #2 sessions are considered with L_2=0.9 *Er* for a better analysis of system reactivity because link #1 is always satisfied. Figure 7.5(b) and Figure 7.5(c) plot the corresponding number of SpHOs per session and regret in using pool #3, respectively.

The results show that, after *Change #1*, both *SS* and *SS+RT* exhibit worse

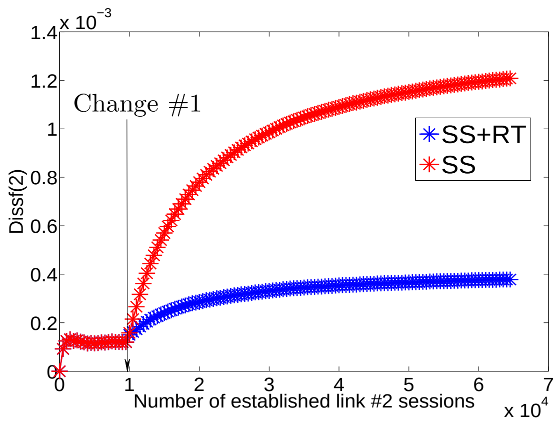

(a)

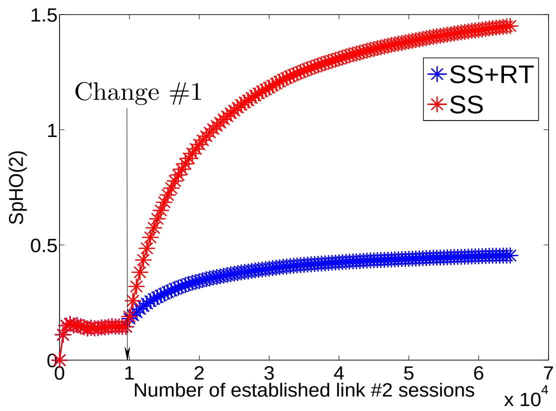

(b)

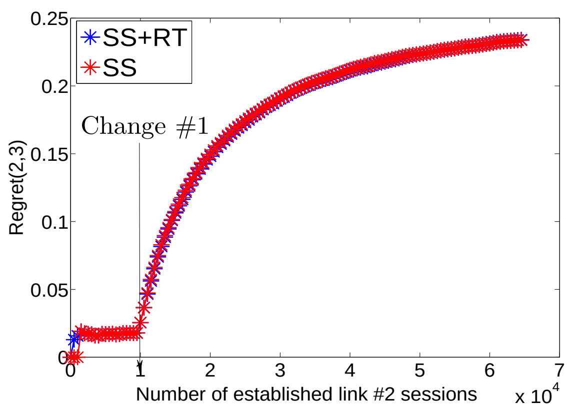

(c)

Figure 7.5: Online evolution of performance of link #2 with *Change #1* occurring after 9,750 sessions in terms of (a) *Dissf(2)*, (b) *Nb.SpHOs/session* and (c) *Regret(2,3)*.

performance in terms of $Dissf(2)$ and *Nb. SpHOs/session*. As a matter of fact, as the number of established sessions increases, both KPIs tend to converge to larger values than those obtained prior to the change. The observed degradation is because after the change, the new position $\#1$ is too close to the external interferer of pool $\#1$, thus making it useless regardless of its interference conditions (i.e., providing always a LOW $F_{l,p}$ value). Nevertheless, the use of the RT functionality (*SS+RT*) results in much smaller degradation. The reason for this better robustness is that, after the position change, the strategy *SS* without any support from the RT still relies on the out-of-date KD statistics previously generated in position $\#0$, so it may decide in some cases to assign pool $\#1$ to link $\#2$ sessions. However, this turns out to be a wrong allocation because, in the new position $\#1$, pool $\#1$ has always a LOW $F_{l,p}$ value. Correspondingly, this degrades the dissatisfaction probability (see Figure 7.5(a)). In addition, much more frequent SpHOs are required to change pool $\#1$ whenever it is assigned (Figure 7.5(b)). On the contrary, when RT is used (*SS+RT*), new KD statistics are generated in position $\#1$ after detecting $Change\ \#1$. As a consequence, the estimate $\hat{F}_{l,p}$ of pool $\#1$ is always set to a LOW value, and pool $\#1$ is never assigned in the future to link $\#2$ sessions. This penalization of pool $\#1$ results a significant gain in terms of both the dissatisfaction probability (Figure 7.5(a)) and number of performed SpHOs (Figure 7.5(b)).

Note that, in Figure 7.5(c), the regret of using pool $\#3$ performs similarly for both strategies before and after the change. Before the change, either pool $\#1$ or $\#2$ can be allocated because both alternate between LOW and HIGH fittingness factor values. This marginalizes the risk of unnecessarily using the less preferred pool $\#3$ because it is not likely to wrongly set $\hat{F}_{l,p}$ of pools $\#1$ and $\#2$ to a LOW value, which would lead to an unnecessary assignment of pool $\#3$. Then, after the change, the use of pool $\#1$ is excluded by both strategies (at first assignment by *SS+RT* or after initially assigning it and executing an SpHO by *SS*). As a consequence, whenever the estimate $\hat{F}_{l,p}$ of pool $\#2$ is wrongly set to a LOW value, pool $\#3$ will be unnecessarily assigned with the corresponding increase in the regret that can be observed in Figure 7.5(c) after the change.

Focusing now on $Change\ \#2$, Figure 7.6(a) shows the online evolution of the dissatisfaction probability of link $\#2$ with the position change occurring after

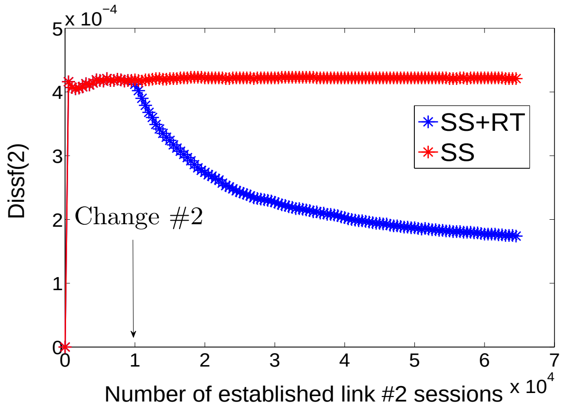

(a)

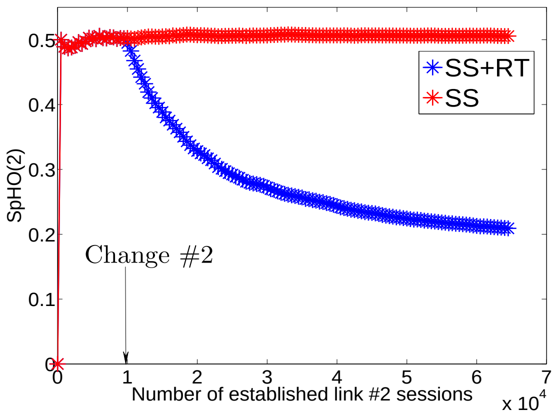

(b)

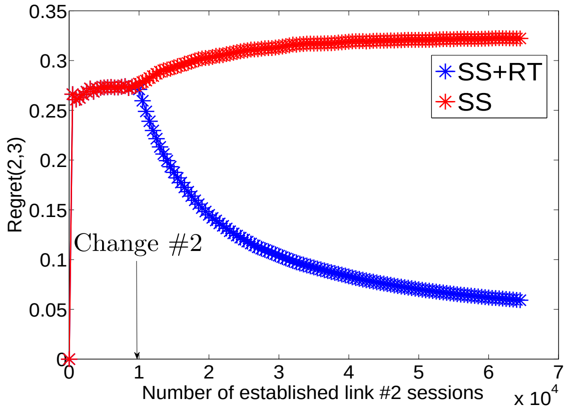

(c)

Figure 7.6: Online evolution of performance of link #2 with *Change #2* occurring after 9,750 sessions in terms of (a) $Dissf(2)$, (b) $Nb.SpHOs/session$ and (c) $Regret(2,3)$.

$9,750$ sessions. The number of SpHOs per session and regret in using pool $\#3$ are plot in Figure 7.6(b) and Figure 7.6(c), respectively.

The results indicate that after $Change\ \#2$, the use of the RT functionality results in a significant reduction of both the dissatisfaction probability (Figure 7.6(a)) and number of performed SpHOs (Figure 7.6(b)). This improvement is because pool $\#1$, which is initially not used in position $\#1$, becomes often the most suitable pool for link $\#2$ after $Change\ \#2$. This change in the interference conditions of the unused pool $\#1$ is detected by the RT based on the procedure described in lines 18-30 of Algorithm 6.1 and new KD statistics are regenerated in the new position. On the contrary, when the RT is not supported (*SS*), $Change\ \#2$ has no impact on the observed dissatisfaction level (Figure 7.6(a)) and number of SpHOs (Figure 7.6(b)) because link $\#2$ continues to exclude pool $\#1$ based on old KD statistics. In contrast to *SS+RT*, this behavior results in penalizing the regret of using pool $\#3$ whenever this pool is assigned instead of pool $\#1$ (see Figure 7.6(c)).

7.7 Chapter summary

In this chapter, the proposed framework has been applied to efficiently exploit the heterogeneous sources of spectrum that may be available in a DH environment. The findings obtained in previous chapters based on simulations have been confirmed under the real world conditions experienced within the DH. In particular, the results have indicated that, under stationary conditions, the proposed spectrum management strategy significantly improves SS performance while complying with the set of constraints in using the different spectrum bands. Gains up to 55% have been observed in terms of global efficiency with respect to a pure random scheme. The introduced signaling cost in terms of *Nb. SpHOs/session* remains below 0.06 for all traffic loads of CR applications. When conditions become non-stationary due to user mobility within the DH environment, the RT is able to efficiently detect those movements and trigger an update procedure of KD data. Thanks to the RT support, the proposed spectrum management strategy exhibits significant robustness. Gains up to 70% and 65% are introduced in terms of the dissatisfaction probability and number of performed SpHOs, respectively, with respect to the strategy that does not support the RT functionality, thus showing the practicality of the proposed framework in such realistic environments

8. Concluding Remarks and Future Directions

8.1 Conclusions

The Cognitive Radio (CR) paradigm has emerged to opportunistically access unused portions of spectrum in both time and space and perform the so-called Dynamic Spectrum Access (DSA). Nevertheless, the complexity of the resulting ecosystem in techno-economic and regulatory domains has delayed the massive deployment of Cognitive Radio Networks (CRNs) and limited their applications to very specific scenarios (e.g., TV white spaces) to date.

In order to contribute towards paving the way for the adoption of such disruptive technologies, this dissertation has constructed a generic cognitive management framework to support spectrum management in CRNs (Chapter 2). The proposed framework relies on a standalone knowledge-management domain to characterize spectrum resources at both the time and frequency dimensions out of the decision-making domain. Both domains have been implemented in various scenarios and case studies. In summary, the obtained results have confirmed the large possibilities cognitive management support would offer to CRNs, through proper adjustment depending on the specific working conditions of CRNs.

In this respect, the dissertation has first addressed two of the most promising CR applications, namely an OSA-type access to licensed bands and open sharing of license-exempt bands. With respect to the former case study (Chapter 3), the results have indicated that exploiting dependence structures that may exist between primary activity/inactivity durations significantly improves the reliability of estimating remaining inactivity durations particularly for high dependence levels and low variability levels. The improved reliability can result in a significant Spectrum Selection (SS) performance gain when the SS strategy is properly adjusted based on the specificities of the scenario in terms of primary dependence levels and traffic loads of CR applications. Therefore, a generic strategy has been developed to capture these dependencies and achieve approximately the best performance under various working conditions. With respect to the latter case study (Chapter 4), the results have revealed that a proper characterization of these bands in terms of fittingness factors enables to efficiently track changes in interference levels particularly for medium-to-high traffic loads of CR applications. An evaluation of SS performance, when different formulations of the fittingness factor are used, has revealed that the relevance of each formulation strongly depends on traffic loads of CR applications. For low traffic loads, a simple formulation that maximizes the achievable bit rate suffices to achieve good SS performance, while for higher traffic loads, a more intuitive formulation is required to efficiently exploit the various bands.

Drawing inspiration from these case studies, a more general strategy to support spectrum management in CRNs has been developed (Chapter 5). The proposed strategy relies on a Knowledge Management (KM) and Spectrum Mobility (SM) functionalities to support spectrum management under various working conditions. A comparative analysis of several variants of the proposed strategy with various choices of implementation has revealed that the relevance of each implementation choice strongly depends on the specific working conditions of the CRN. For instance, a proactive SS that gives priority to the expected-to-be suitable spectrum portions significantly improves performance for low-to-medium traffic load, but performs equally to a simple greedy strategy for high traffic loads. The KM enables to efficiently track changes in interference levels for low traffic loads, while its support is gradually marginalized as the traffic load increases. The SM functionality enables to frequently reconfigure radio links to use the best spectrum resources for high traffic loads, while for low traffic loads; there is no need to perform such reconfigurations. By combining all these functionalities, the proposed strategy has been shown to perform very closely to the upper bound theoretical scheme in terms of the CR dissatisfaction level for all CR traffic loads. The analysis of the corresponding signaling cost at the radio interface has revealed that an event-based approach enables to significantly reduce measurement report signaling and perform very few spectrum handovers, thus keeping the total signaling overhead acceptable.

To assess sensitivity to unreliable KD data, various sources of uncertainty have been introduced (Chapter 6). The results have indicated that robustness of the proposed framework strongly depends on the type of introduced uncertainty, and it is not always needed to invest on additional cognitive management functionalities. Specifically, when the KD acquisition process can only achieve partial convergence levels in KD data, the proposed spectrum management strategy exhibits substantial robustness and often selects the best spectrum portions. Nevertheless, when radio and interference conditions become non-stationary, SS performance degrades significantly, making the extension of the proposed framework a must. Therefore, a Reliability Tester (RT) has been proposed to detect, based on hypothesis testing, relevant changes in the environment and trigger, when needed, an update procedure of KD data. The results have shown that the proposed RT is able to disregard most of changes due to the intrinsic randomness of the radio environment and efficiently detect actual changes in the scenario. Thanks to the RT support, the spectrum management strategy exhibits substantial robustness when the environment becomes non-stationary, obtaining significant performance improvements with respect to the reference case that does not make use of the RT.

Finally, the key findings obtained along this dissertation have been validated in a realistic Digital Home (DH) environment (Chapter 7). The results have indicated that, under stationary conditions, the proposed spectrum management strategy significantly improves SS performance while complying with a set of constraints in using the different spectrum portions. The corresponding signaling cost remains limited for all traffic loads of CR applications. When conditions become non-stationary due to user mobility within the DH environment, the RT is able to efficiently detect these movements, and thus significantly improve spectrum management robustness. These results have confirmed the previous obtained key findings and shown the practicality of the proposed framework in such realistic environments.

8.2 Future directions

The research conducted in this dissertation has shown that proper cognitive management functionalities can be extremely beneficial to support spectrum management in CRNs. As part of future work, it is envisaged to extend the proposed proposed framework to exploit a characterization of spectrum resources in the spatial domain in addition to the considered time and frequency domains. This characterization would enable to capture dependencies that may exist between different spatial positions due to either the behavior of users in some particular regions (e.g., hotspots or highways) or some particular features of the spectrum allocation strategy (e.g., frequency plan or frequency hopping).

Another future direction is to exploit the proposed spectrum management strategy to assist the use cases recently proposed for operation in white space frequency bands, namely ad-hoc networking, backhaul link and multimedia broadcast multicast service. In this context, the proposed framework may be strengthened with additional functionalities to exploit the specificities of some of these use cases. For instance, the fittingness factor formulation will be extended to consider the complex requirements of multimedia applications. Furthermore, the applicability of the proposed framework to decentralized scenarios will be further developed, including the adaptation of decision making strategies.

Finally, it is envisaged to exploit the proposed framework to assess the value of exploiting cognitive management support in various contexts. Both qualitative and quantitative studies may be performed to exclude all the impractical options for a given scenario, and select the most relevant possibilities early in the design process of CRNs, which would significantly save design effort and time. In this respect, a multi-disciplinary approach would be particularly useful to first import concepts and methodologies from other relevant disciplines, such as cognitive science and belief theory, and then adapt them to the CRN context.

Appendices

A. Operating Bucket Configuration

To support high randomness variability, exponentially-distributed ON/OFF durations are initially considered. Given an exponential random variable X of mean λ_X, N_B of the buckets defined in Section 2.2.1.1 are considered. With respect to the conditional mean estimator, it is proposed to make exponential outcomes most likely fall in one of the first finite ($N_B{-}1$) buckets. The lowest limit of the last bucket, denoted as x_{max}, is determined such that $Prob[X{\leq}x]{<}0.05$. This implies that $1{-}F_X(x_{max}){<}0.05$, where F_X is the characteristic function of X defined as

$$F_X(x){=}Prob\,[X{\leq}x] = 1{-}e^{-\frac{1}{\lambda_X}\cdot x} \tag{A.1}$$

Solving (A.1) for x_{max}, we get $x_{max}{\approx}3{\cdot}\lambda_X$.

To introduce a reference point, fully-dependent primary activity time series (i.e., $q{=}1$) and the $Crit_2$ SS criterion proposed in Section 3.1.1 are considered. Furthermore, an ideal scenario where SS is based on perfect KD statistics is introduced. The corresponding upper-bound performance will be used as a reference for the evaluation of the convergence of $Crit_2$-based SS. Specifically, buckets are incrementally squeezed (by gradually decreasing τ) to determine the width, at which the observed behavior gets close to the ideal case. Note that for a given τ, the number of buckets N_B is given by:

$$N_B{=}\lceil\frac{x_{max}}{\tau{\cdot}\lambda_X}\rceil{+}1{=}\lceil\frac{3}{\tau}{+}1\rceil \tag{A.2}$$

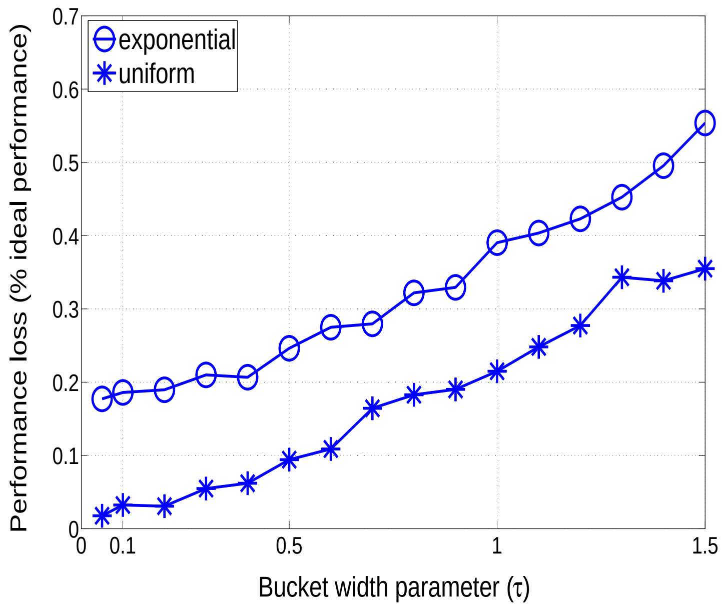

Figure A.1: Performance sensitivity to bucket configuration

where $\lceil . \rceil$ denotes the ceiling function.

Considering the case study of Table 3.1, Figure A.1 plots the SS performance loss with respect to the ideal case as a function of τ, where performance is measured in terms of the number of SpHOs per session for maximum traffic load conditions (DC=0.5 and $T_{req,1}$=24 s).

The results show that, starting from τ=1.5, decreasing τ with a step equal to 0.1 significantly reduces performance loss up to τ=0.1. It has been checked that a further reduction of τ below 0.1 does not significantly improve performance at the expense of an exponentially-increasing computational complexity. Therefore, it is proposed to use τ^{opr}=0.1, which corresponds to N_B^{opr}=0.1.

Next, the validity of the selected bucket configuration is analyzed for uniformly-distributed data. As illustrated by Figure A.1, for a given bucket length, the obtained behavior with uniform distributions is much closer to the ideal case. Specifically, at τ^{opr}=0.1, performance loss is below 3% (compared to 17% for the exponential case). This better performance is justified by the lower randomness variability of uniform distributions. Hence, the determined (τ^{opr},N_B^{opr}) would provide a reliable choice during performance evaluation phase.

B. Dependence levels of patterns of activity/inactivity durations

According to (3.5), OFF periods are generated according to a weighted sum whose weights are the probabilities q and $1-q$.

Considering for instance the case of uniform distributions, $CP^{p}_{OFF,ON}(B^b_p, B^a_p)$ is given by:

$$CP^{p}_{OFF,ON}(B^b_p, B^a_p) = q \cdot CP^{p}_{f(ON_p(j)),ON_p}(B^b_p, B^a_p) + (1-q) \cdot CP^{p}_{unif([OFF^{min}_p, OFF^{max}_p]),ON_p}(B^b_p, B^a_p) \tag{B.1}$$

where $CP^{p}_{f(ON_p(j)),ON_p}$ and $CP^{p}_{unif([OFF^{min}_p,OFF^{max}_p]),ON_p}$ denote the probability $CP^{p}_{OFF,ON}(B^b_p, B^a_p)$ when OFF durations are generated according to $f(ON_p(j))$ and $unif([OFF^{min}_p, OFF^{max}_p])$, respectively. It follows that the dependence indicator $\delta_{a,b}$ is also a weighted sum of dependence indicators of $CP^{p}_{f(ON_p(j)),ON_p}$ and $CP^{p}_{unif([OFF^{min}_p,OFF^{max}_p]),ON_p}$:

$$\delta_{a,b} = q \cdot \delta^{f(ON_p(j)),ON_p}_{a,b} + (1-q) \cdot \delta^{unif([OFF^{min}_p,OFF^{max}_p]),ON_p}_{a,b} \tag{B.2}$$

On one hand, from the mapping performed in (3.6), we obtain:

$$CP_{f(ON_p(j)),ON_p}(B^b_p, B^a_p) = \begin{cases} 1 & a=b, \\ o & \text{otherwise.} \end{cases} \tag{B.3}$$

Therefore, the corresponding dependence indicator is given by:

$$\delta_{a,b}^{f(ON_p(j)),ON_p}=\begin{cases}1 & a=b,\\ o & \text{otherwise.}\end{cases} \tag{B.4}$$

On the other hand, since $unif([OFF_p^{min}, OFF_p^{max}])$ is independent of ON_p durations, the following equality holds:

$$CP^p_{unif([OFF_p^{min},OFF_p^{max}]),ON_p}=pdf^p_{OFF}(B_p^b) \tag{B.5}$$

In this case, the corresponding dependence indicator is given by:

$$\delta_{a,b}^{unif([OFF_p^{min},OFF_p^{max}]),ON_p}=0 \tag{B.6}$$

Combining (B.1)- (B.6), the product $\delta_{a,b}\cdot CP_{OFF,ON}(B_p^b, B_p^a)$ is given by:

$$\delta_{a,b}\cdot CP_{OFF,ON}(B_p^b, B_p^a)=\begin{cases}q & a=b,\\ o & \text{otherwise.}\end{cases} \tag{B.7}$$

Applying the definition of DEP_p in (2.6), we obtain $DEP_p=q$.

C. Analysis of Type I and II errors of the overlap detection method

Asymptotic Type I and II errors of the overlap detection method are given by [73]:

$$Type\ I\ error = 2\phi(\frac{z_{(1-\gamma)/2}(1+k_m)}{\sqrt{1+k_m^2}}) \tag{C.1}$$

$$Type\ II\ error = 1-\phi(\frac{z_{(1-\gamma)/2}(1+k_m)}{\sqrt{1+k_m^2}}+D_m)-\phi(\frac{z_{(1-\gamma)/2}(1+k_m)}{\sqrt{1+k_m^2}}-D_m) \tag{C.2}$$

Figure C.1 plots Type I and II errors as a function of the ratio of sample variances k_m. Different values of D_m are considered for the Type II error.

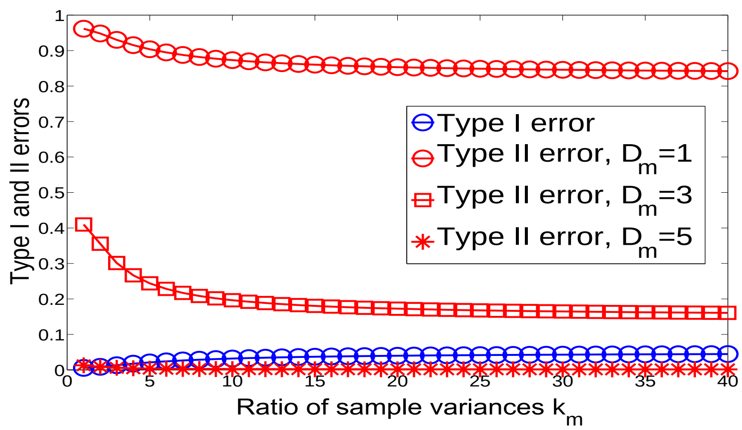

Figure C.1: Type I and II errors of the considered overlap detection method

It can be seen that for high D_m and low k_m values, the overlap detection method provides a very low Type I error (e.g, 0.0056 for k_m=1) and an acceptable Type II error (e.g, 0.013 for k_m=1 and D_m=5). Therefore, it provides a good option to detect relevant changes in the environment while minimizing the risk of useless generation of KD data.

Bibliography

[1] "Report of the spectrum efficiency working group," Federal Communications Commission (FCC), Spectrum Policy Task Force, Tech. Rep., Nov. 2002.

[2] "ET docket no. 03-322: Notice of proposed rule making and order," Federal Communications Commission (FCC), Tech. Rep., Dec. 2003.

[3] M. Wellens, J. Riihijärvi, and P. Mähönen, "Empirical time and frequency domain models of spectrum use," *Physical Communication*, vol. 2, no. 1-2, pp. 10–32, 2009.

[4] S. Yin, D. Chen, Q. Zhang, M. Liu, and S. Li, "Mining spectrum usage data: A large-scale spectrum measurement study," *Mobile Computing, IEEE Transactions on*, vol. 11, no. 6, pp. 1033–1046, 2012.

[5] J. Mitola III and G. Q. Maguire, Jr., "Cognitive radio: making software radios more personal," *Personal Communications, IEEE*, vol. 6, no. 4, pp. 13–18, Aug. 1999.

[6] J. Mitola III, "Cognitive radio — an integrated agent architecture for software defined radio," DTech thesis, Royal Institute of Technology (KTH), Kista, Sweden, May 2000.

[7] S. Haykin, "Cognitive radio: brain-empowered wireless communications," *Selected Areas in Communications, IEEE Journal on*, vol. 23, no. 2, pp. 201–220, Feb. 2005.

[8] Q. Zhao and B. Sadler, "A survey of dynamic spectrum access," *Signal Processing Magazine, IEEE*, vol. 24, no. 3, pp. 79–89, 2007.

[9] D. Hatfield and P. Weiser, "Property rights in spectrum: taking the next step," in *New Frontiers in Dynamic Spectrum Access Networks, 2005. DySPAN 2005. 2005 First IEEE International Symposium on*, 2005, pp. 43–55.

[10] L. Xu, R. Tönjes, T. Paila, W. Hansmann, M. Frank, and M. Albrecht, "DRiVE-ing to the internet: Dynamic radio for IP services in vehicular environments," in *Local Computer Networks, 2000. LCN 2000. Proceedings. 25th Annual IEEE Conference on*, 2000, pp. 281–289.

[11] P. Leaves, K. Moessner, R. Tafazolli, D. Grandblaise, D. Bourse, R. Tönjes, and M. Breveglieri, "Dynamic spectrum allocation in composite reconfigurable wireless networks," *Communications Magazine, IEEE*, vol. 42, no. 5, pp. 72–81, 2004.

[12] Y. Benkler, "Overcoming agoraphobia: Building the commons of the digitally networked environment," *Harvard Journal of Law and Technology*, vol. 11, no. 2, pp. 287–400, 1998.

[13] W. Lehr and J. Crowcroft, "Managing shared access to a spectrum commons," in *New Frontiers in Dynamic Spectrum Access Networks, 2005. DySPAN 2005. 2005 First IEEE International Symposium on*, 2005, pp. 420–444.

[14] C. Raman, R. Yates, and N. B. Mandayam, "Scheduling variable rate links via a spectrum server," in *New Frontiers in Dynamic Spectrum Access Networks, 2005. DySPAN 2005. 2005 First IEEE International Symposium on*, 2005, pp. 110–118.

[15] V. Brik, E. Rozner, S. Banerjee, and P. Bahl, "DSAP: a protocol for coordinated spectrum access," in *New Frontiers in Dynamic Spectrum Access Networks, 2005. DySPAN 2005. 2005 First IEEE International Symposium on*, 2005, pp. 611–614.

[16] R. Etkin, A. Parekh, and D. Tse, "Spectrum sharing for unlicensed bands," *Selected Areas in Communications, IEEE Journal on*, vol. 25, no. 3, pp. 517–528, 2007.

[17] J. Huang, R. Berry, and M. Honig, "Spectrum sharing with distributed interference compensation," in *New Frontiers in Dynamic Spectrum Access Networks, 2005. DySPAN 2005. 2005 First IEEE International Symposium on*, 2005, pp. 88–93.

[18] G. Hardin, "The tragedy of the commons," *Science (New York, N.Y.)*, vol. 162, no. 3859, pp. 1243–1248, Dec 1968.

[19] ——, "Extensions of 'the tragedy of the commons'," *Science*, vol. 280, no. 5364, p. 682, 1998.

[20] C. Santivanez, R. Ramanathan, C. Partridge, R. Krishnan, M. Condell, and S. Polit, "Opportunistic spectrum access: challenges, architecture, protocols," in *Proceedings of the 2nd annual international workshop on Wireless internet*, ser. WICON '06. New York, NY, USA: ACM, 2006.

[21] Q. Zhao and A. Swami, "A survey of dynamic spectrum access: Signal processing and networking perspectives," in *Acoustics, Speech and Signal Processing, 2007. ICASSP 2007. IEEE International Conference on*, vol. 4, 2007, pp. IV–1349–IV–1352.

[22] I. Akyildiz, W.-Y. Lee, M. C. Vuran, and S. Mohanty, "A survey on spectrum management in cognitive radio networks," *Communications Magazine, IEEE*, vol. 46, no. 4, pp. 40–48, 2008.

[23] Z. Youping, L. Bin, and J. H. Reed, "Network support - the radio environment map," in *Cognitive Radio Technology*, B. A. FETTE, Ed. Elsevier, 2006.

[24] Y. Zhao, J. Reed, S. Mao, and K. K. Bae, "Overhead analysis for radio environment map-enabled cognitive radio networks," in *Networking Technologies for Software Defined Radio Networks, 2006. SDR '06.1st IEEE Workshop on*, 2006, pp. 18–25.

[25] J. Riihijärvi, P. Mähönen, M. Petrova, and V. Kolar, "Enhancing cognitive radios with spatial statistics: From radio environment maps to topology engine," in *CROWNCOM '09*, june 2009, pp. 1–6.

[26] Y. Zhao, L. Morales, J. Gaeddert, K. K. Bae, J.-S. Um, and J. H. Reed, "Applying radio environment maps to cognitive wireless regional area networks," in *DySPAN 2007*, april 2007, pp. 115–118.

[27] Y. Zhao, D. Raymond, C. da Silva, J. Reed, and S. Midkiff, "Performance evaluation of radio environment map-enabled cognitive spectrum-sharing networks," in *Military Communications Conference, 2007. MILCOM 2007. IEEE*, 2007, pp. 1–7.

[28] P. Zhang, Y. Liu, Z. Feng, Q. Zhang, Q. Li, and D. Xu, "Intelligent and efficient development of wireless networks: A review of cognitive radio networks," *Chinese Science Bulletin*, vol. 57, no. 28-29, pp. 3662–3676, 2012.

[29] R. W. Thomas, D. H. Friend, L. A. Dasilva, and A. B. Mackenzie, "Cognitive networks: adaptation and learning to achieve end-to-end performance objectives," *Communications Magazine, IEEE*, vol. 44, no. 12, pp. 51 –57, Dec. 2006.

[30] J. Kephart and D. Chess, "The vision of autonomic computing," *Computer*, vol. 36, no. 1, pp. 41–50, Jan 2003.

[31] P. Demestichas, G. Dimitrakopoulos, J. Strassner, and D. Bourse, "Introducing reconfigurability and cognitive networks concepts in the wireless world," *Vehicular Technology Magazine, IEEE*, vol. 1, no. 2, pp. 32 –39, 2006.

[32] P. Demestichas, K. Tsagkaris, and V. Stavroulaki, "Cognitive management systems for supporting operators in the emerging Future Internet era," in *Personal, Indoor and Mobile Radio Communications Workshops (PIMRC Workshops), 2010 IEEE 21st International Symposium on*, Sept. 2010, pp. 21–25.

[33] E. Meshkova, Z. Wang, J. Nasreddine, D. Denkovski, C. Zhao, K. Rerkrai, T. Farnham, A. Ahmad, A. Gefflaut, L. Gavrilovska, and P. Mähönen, "Using cognitive radio principles for wireless resource management in home networking," in *Consumer Communications and Networking Conference (CCNC), 2011 IEEE*, Jan. 2011, pp. 669–673.

[34] D. Petromanolakis, Y. Kritikou, V. Stavroulaki, and P. Demestichas, "Context learning and configuration selection for cognitive device management," in *Vehicular Technology Conference, 2009. VTC Spring 2009. IEEE 69th*, 2009, pp. 1–5.

[35] G. Dimitrakopoulos, M. Logothetis, and P. Demestichas, "Performance evaluation of cognitive management functionality for emergency healthcare applications," in *Telecommunications (AICT), 2010 Sixth Advanced International Conference on*, 2010, pp. 445–451.

[36] Q. He, Z. Feng, Y. Wang, and P. Zhang, "Cross-layer parameters reconfiguration in cognitive radio networks using ant colony optimization," in *Personal Indoor and Mobile Radio Communications (PIMRC), 2012 IEEE 23rd International Symposium on*, 2012, pp. 631–635.

[37] Q. Zhang, Q. He, and P. Zhang, "Topology reconfiguration in cognitive radio networks using ant colony optimization," in *Vehicular Technology Conference (VTC Fall), 2012 IEEE*, 2012, pp. 1–5.

[38] The End-to-End-Efficiency (E3) project. [Online]. Available: https://www.ict-e3.eu/

[39] The ICT EU (Opportunistic Networks and Cognitive Management Systems for Efficient Application Provision in the Future InterneT) OneFIT Project. [Online]. Available: http://www.ict-onefit.eu/

[40] The Wireless World Research Forum (WWRF), WG6 (working group 6). [Online]. Available: http://www.wireless-worldresearch.org/

[41] IEEE Standard Coordinating Committee 41 (SCC41). [Online]. Available: http://grouper.ieee.org/groups/scc41/index.html/

[42] ETSI Technical Committee (TC) on Reconfigurable Radio Systems (RRS). [Online]. Available: http://www.etsi.org/WebSite/technologies/RRS.aspx

[43] E. Jung and X. Liu, "Opportunistic spectrum access in heterogeneous user environments," in *DySPAN 2008*, Oct. 2008, pp. 1'–11.

[44] X. Liu, B. Krishnamachari, and H. Liu, "Channel selection in multi-channel opportunistic spectrum access networks with perfect sensing," in *New Frontiers in Dynamic Spectrum, 2010 IEEE Symposium on*, 2010, pp. 1–8.

[45] D. Xu, E. Jung, and X. Liu, "Optimal bandwidth selection in multi-channel cognitive radio networks: How much is too much?" in *New Frontiers in Dynamic Spectrum Access Networks, 2008. DySPAN 2008. 3rd IEEE Symposium on*, Oct. 2008, pp. 1–11.

[46] D. Chen, Q. Zhang, and W. Jia, "Aggregation aware spectrum assignment in cognitive ad-hoc networks," in *Cognitive Radio Oriented Wireless Networks and Communications, 2008. CrownCom 2008. 3rd International Conference on*, May 2008, pp. 1–6.

[47] U. Berthold, F. Fu, M. van der Schaar, and F. Jondral, "Detection of spectral resources in cognitive radios using reinforcement learning," in *New Frontiers in Dynamic Spectrum Access Networks, 2008. DySPAN 2008. 3rd IEEE Symposium on*, oct. 2008, pp. 1 –5.

[48] K.-L. Yau, P. Komisarczuk, and P. Teal, "A context-aware and intelligent dynamic channel selection scheme for cognitive radio networks," in *Cognitive Radio Oriented Wireless Networks and Communications, 2009. CROWNCOM '09. 4th International Conference on*, june 2009, pp. 1 –6.

[49] Y. Teng, Y. Zhang, F. Niu, C. Dai, and M. Song, "Reinforcement learning based auction algorithm for dynamic spectrum access in cognitive radio networks," in *VTC 2010-Fall*, sep. 2010, pp. 1–5.

[50] E. Ozekin, F. Demirci, and F. Alagoz, "Self-evaluating reinforcement learning based spectrum management for cognitive ad hoc networks," in *Information Networking (ICOIN), 2013 International Conference on*, 2013, pp. 444–449.

[51] J. Vartiainen, M. Höyhtyä, J. Lehtomäki, and T. Bräysy, "Priority channel selection based on detection history database," in *crowncom, 2010*, June 2010, pp. 1–5.

[52] P. A. K. Acharya, S. Singh, and H. Zheng, "Reliable open spectrum communications through proactive spectrum access," in *PROC. OF TAPAS*, 2006.

[53] Y. Li, Y. Dong, H. Zhang, H. Zhao, H. Shi, and X. Zhao, "Qos provisioning spectrum decision algorithm based on predictions in cognitive radio networks," in *Wireless Communications Networking and Mobile Computing (WiCOM), 2010 6th International Conference on*, 2010, pp. 1–4.

[54] M. Höyhtyä, S. Pollin, and A. Mäandmmelä and, "Classification-based predictive channel selection for cognitive radios," in *Communications (ICC), 2010 IEEE International Conference on*, may 2010, pp. 1 –6.

[55] V. Mishra, L. C. Tong, and C. Syin, "Deterministic time pattern based channel selection in cognitive radio network," in *Information Networking (ICOIN), 2013 International Conference on*, 2013, pp. 169–174.

[56] Y. Zhang, "Spectrum handoff in cognitive radio networks: Opportunistic and negotiated situations," in *Communications, 2009. ICC '09. IEEE International Conference on*, June 2009, pp. 1–6.

[57] O. Jo, J. H. Park, and D.-H. Cho, "Qos provisioning spectrum management based on intelligent matching and reservation for cognitive radio system," in *Cognitive Radio Oriented Wireless Networks and Communications, 2007. CrownCom 2007. 2nd International Conference on*, Aug. 2007, pp. 530–534.

[58] D. Pacheco-Paramo, V. Pla, and J. Martinez-Bauset, "Optimal admission control in cognitive radio networks," in *Cognitive Radio Oriented Wireless Networks and Communications, 2009. CROWNCOM '09. 4th International Conference on*, June 2009, pp. 1–7.

[59] C.-W. Wang and L.-C. Wang, "Modeling and analysis for proactive-decision spectrum handoff in cognitive radio networks," in *Communications, 2009. ICC '09. IEEE International Conference on*, June 2009, pp. 1–6.

[60] R. Hincapie, L. Zhang, J. Tang, G. Xue, R. Wolff, and R. Bustamante, "Efficient recovery algorithms for wireless mesh networks with cognitive radios," in *Communications, 2009. ICC '09. IEEE International Conference on*, June 2009, pp. 1–5.

[61] C.-W. Wang and L.-C. Wang, "Analysis of reactive spectrum handoff in cognitive radio networks," *Selected Areas in Communications, IEEE Journal on*, vol. 30, no. 10, pp. 2016–2028, 2012.

[62] P. H. Chang, K. F. Chang, Y. C. Chen, and L. K. Ye, "Performance analysis of channel switching with various bandwidths in cognitive radio," in *The Twelfth International Conference on Networks (ICN)*, 2013, pp. 29–33.

[63] L. Giupponi and A. Perez-Neira, "Fuzzy-based spectrum handoff in cognitive radio networks," in *Cognitive Radio Oriented Wireless Networks and Communications, 2008. CrownCom 2008. 3rd International Conference on*, May 2008, pp. 1–6.

[64] O. Jo, H. H. Choi, and D.-H. Cho, "Seamless spectrum handover improving cell outage in cognitive radio systems," in *Cognitive Radio Oriented Wireless Networks and Communications, 2009. CROWNCOM '09. 4th International Conference on*, June 2009, pp. 1–6.

[65] "Reconfigurable Radio Systems, functional architecture for the management and control of reconfigurable radio systems," ETSI TR 102 682, 1.1.1, Tech. Rep., July 2009.

[66] One FIT Deliverable D2.2. (2011, February) Onefit functional and system architecture. [Online]. Available: http://www.ict-onefit.eu/

[67] "Reconfigurable Radio Systems (RRS); Feasibility Study on Control Channels for Cognitive Radio Systems," ETSI RRS 03, Tech. Rep. TR 102 684 V1.1.1, April 2012.

[68] V. Stavroulaki, K. Tsagkaris, P. Demestichas, J. Gebert, M. Mueck, A. Schmidt, R. Ferrus, O. Sallent, M. Filo, C. Mouton, and L. Rakotoharison, "Cognitive control channels: from concept to identification of implementation options," *Communications Magazine, IEEE*, vol. 50, no. 7, pp. 96–108, 2012.

[69] F. Bouali, O. Sallent, J. Pérez-Romero, and R. Agustí, "A framework based on a fittingness factor to enable efficient exploitation of spectrum opportunities in cognitive radio networks," in *Wireless Personal Multimedia Communications (WPMC), 2011 14th International Symposium on*, Oct. 2011, pp. 1–5.

[70] L. Badia, M. Lindström, J. Zander, and M. Zorzi, "Demand and pricing effects on the radio resource allocation of multimedia communication systems," in *GLOBECOM '03. IEEE*, vol. 7, Dec. 2003, pp. 4116–4121.

[71] One FIT Deliverable D3.3. (2012, June) Protocols, performance assessment and consolidation on interfaces for standardization. [Online]. Available: http://www.ict-onefit.eu/

[72] E. L. Lehmann and J. P. Romano, *Testing statistical hypotheses*, 3rd ed., ser. Springer Texts in Statistics. New York: Springer, 2005.

[73] N. Schenker and J. F. Gentleman, "On judging the significance of differences by examining the overlap between confidence intervals," *The American Statistician*, vol. 55, no. 3, pp. pp. 182–186, 2001.

[74] R. J. Simes, "An improved bonferroni procedure for multiple tests of significance," *Biometrika*, vol. 1, 1986.

[75] R. Ferrus, O. Sallent, J. Pérez-Romero, and R. Agustí, "A solution framework to provide management services for wireless communications in the digital home," *Communications Magazine, IEEE*, vol. 50, no. 11, pp. 132 –141, november 2012.

[76] ECMA, "MAC and PHY for operation in TV white space," Tech. Rep. ECMA-392, December 2009.

[77] COST, "Chapter 4, propagation prediction models," COST 231 Book, Tech. Rep. Final Report.

Declaration

I herewith declare that I have produced this work without the prohibited assistance of third parties and without making use of aids other than those specified; notions taken over directly or indirectly from other sources have been identified as such. This work has not previously been presented in identical or similar form to any examination board.

The dissertation work was conducted from 2009 to 2013 under the supervision of Dr. Oriol Sallent at Universitat Politècnica de Catalunya (UPC).

Barcelona,

This dissertation was finished writing in Barcelona on Tuesday 23rd July, 2013

This page is intentionally left blank